

A Computational Study of Substituted
2,2'-bithiophene as Building Blocks for
Organic Solar Cells

James Patrick Connell

MSc by Research

University of York

Chemistry

January 2022

Abstract

The ability of 2,2'-bithiophene to act as an electron donor in an organic solar cell can be influenced through the addition of substituents, the nature of which can result in differing impacts on the molecule's excitation energy.

The ground and excited state geometries of trans and cis 2,2'-bithiophene were investigated using the CC2 and ADC(2) ab initio methods. Adiabatic excitation energies were calculated from these geometries and compared to resonance-enhanced multiphoton ionization spectroscopy data in the literature, good agreement to which determined the basis set to be used when performing subsequent calculations on the substituted molecule.

OH, formyl, nitro, nitroso, OC(H)O, OC(CH₃)O, phenyl and dimethylamino substituents were chosen with the aim of influencing the excitation energy through both differing electronic and steric effects. Substitutions were made singly and doubly in five combinations of position and number of substituents. Ground and excited state geometries were calculated, and it was found that the CC2 and ADC(2) methods were unable to yield results for the formyl, nitro and nitroso substituents due to the multi-reference character of their ground states. The effect of the substituents on the bond lengths and dihedral angles of the thiophene rings compared to unsubstituted 2,2'-bithiophene was analysed before adiabatic excitation energies were calculated and the diethylamino and phenyl substituents found to cause the greatest decrease in excitation energy, almost regardless of substitution position.

A final series of calculations were performed on unsubstituted, OH and OC(H)O substituted oligomers of three and four repeat units and the reciprocal of the repeat units against adiabatic excitation energy plotted in order to extrapolate to the excitation energy of a theoretical substituted polythiophene of infinite length. The utility of performing this type of extrapolation with this few repeat units, due to constraints imposed by computational cost, was reviewed.

Contents

Abstract.....	2
Contents.....	3
List of Figures	5
List of Tables	6
Acknowledgements.....	11
Author's Declaration	12
1 Chapter 1: Introduction	13
1.1 Background and Operating Principles of Organic Solar Cells.....	13
1.2 Computational studies of substituted 2,2'-bithiophene.....	16
1.3 Computational Studies of Oligothiophenes.....	19
1.4 Overview of Thesis	20
2 Chapter 2: Computational Methods	21
2.1 The Schrödinger Equation.....	21
2.2 The Born-Oppenheimer Approximation	22
2.3 Hartree-Fock Theory	22
2.4 Second-Order Møller-Plesset Perturbation Theory	23
2.5 Coupled-Cluster Theory	24
2.6 Algebraic Diagrammatic Construction Scheme	26
2.7 Basis Sets.....	27
3 Chapter 3.....	29
3.1 Introduction	29
3.2 Computational Methods.....	29
3.3 Results and Discussion	30
3.3.1 Unsubstituted trans-2,2'-bithiophene	30
3.3.2 Unsubstituted cis-2,2'-bithiophene	32
3.3.3 Excitation Energies.....	34
3.4 Conclusion.....	35
4 Chapter 4.....	37
4.1 Introduction	37
4.2 Selection of Substituted Groups and Substitution Positions	37
4.3 Computational Methods.....	40
4.4 Substituted trans 2,2'-bithiophene Results and Discussion	41
4.4.1 OH substituted trans-2,2'-bithiophene.....	41
4.4.2 OC(H)O Substituted trans-2,2'-bithiophene	49
4.4.3 OC(CH ₃)O Substituted trans 2,2'-bithiophene	55

4.4.4	Phenyl Substituted trans-2,2'-bithiophene.....	61
4.4.5	Dimethylamino Substituted trans-2,2'-bithiophene.....	68
4.5	Substituted Cis-2,2'-bithiophene Results and Discussion.....	77
4.5.1	OH substituted cis-2,2'-bithiophene.....	77
4.5.2	OC(H)O Substituted cis 2,2'-bithiophene.....	79
4.5.3	OC(CH ₃)O Substituted cis-2,2-bithiophene.....	81
4.5.4	Phenyl Substituted cis-2,2-bithiophene.....	83
4.5.5	Dimethylamino Substituted cis-2,2-bithiophene.....	85
4.6	Conclusion.....	86
5	Chapter 5.....	90
5.1	Introduction.....	90
5.2	Linkage and Substitution Positions.....	90
5.3	Computational Methods.....	91
5.4	Results and Discussion.....	91
5.4.1	Geometries.....	91
5.4.2	Excitation Energies and Extrapolation.....	95
5.5	Conclusion.....	98
6	Chapter 6.....	99
6.1	Conclusion.....	99
6.2	Potential Areas of Further Study.....	100
7	Appendix.....	101
7.3	Chapter 3 Supplementary Material.....	101
7.4	Chapter 4 Supplementary Material.....	102
7.5	Chapter 5 Supplementary Material.....	129
	References.....	135

List of Figures

Figure 1.1 Schematic of bilayer vs. bulk heterojunction.....	14
Figure 1.2 Donor-Acceptor block schematic.....	14
Figure 1.3 Unsubstituted trans-2,2'-bithiophene	15
Figure 2.1 Comparison between Slater-Type Orbital STO and Gaussian-Type Orbital GTO	27
Figure 3.1 unsubstituted trans 2,2'-bithiophene.....	30
Figure 3.2 MOs of the ground state to S_1 excitation of trans 2,2'-bithiophene at the ADC(2)/aug-cc-pVDZ level.....	32
Figure 3.3 MOs of the ground state to S_1 excitation of cis 2,2'-bithiophene at the ADC(2)/aug-cc-pVDZ level.....	34
Figure 4.1 Structures of the selected substituents using 3 substituted trans-2,2'-bithiophene as an example.....	38
Figure 4.2 Diagram of substitution locations.....	40
Figure 4.3 MOs involved in S_1 excitation of OH substituted trans 2,2'-bithiophene.....	47
Figure 4.4 MOs involved in S_1 excitation of OC(H)O substituted trans 2,2'-bithiophene.....	53
Figure 4.5 MOs involved in S_1 excitation of OC(CH ₃)O substituted trans 2,2'-bithiophene	59
Figure 4.6 MOs involved in S_1 excitation of phenyl substituted trans 2,2'-bithiophene	66
Figure 4.7 MOs involved in S_1 excitation of singly dimethylamino substituted trans 2,2'-bithiophene.....	74
Figure 4.8 MOs involved in S_1 excitation of doubly dimethylamino substituted trans 2,2'-bithiophene.....	75
Figure 5.1 OH substituted tetrathiophene.....	90
Figure 5.2 Geometry change of OC(H)O substituted terthiophene.....	95
Figure 5.3 Geometry change of OC(H)O substituted tetrathiophene on excitation	95
Figure 5.4 Extrapolation to an infinite length of the adiabatic excitation energy of unsubstituted, OH and OC(H)O substituted oligomers at the CC2/aug-cc-pVDZ level	97
Figure 7.1 MOs involved in S_1 excitation of OH substituted cis 2,2'-bithiophene	117
Figure 7.2 MOs involved in S_1 excitation of OC(H)O substituted cis 2,2'-bithiophene.....	118
Figure 7.3 MOs involved in S_1 excitation of OC(CH ₃)O substituted cis 2,2'-bithiophene	119
Figure 7.4 MOs involved in S_1 excitation of phenyl substituted cis 2,2'-bithiophene	120
Figure 7.5 MOs involved in S_1 excitation of singly dimethylamino substituted cis 2,2'-bithiophene.....	121
Figure 7.6 MOs involved in S_1 excitation of doubly dimethylamino substituted cis 2,2'-bithiophene.....	122

List of Tables

Table 3.1: Selected bond lengths and dihedral angle of unsubstituted trans-2,2'-bithiophene	31
Table 3.2: Changes in selected bond lengths and dihedral angle of trans 2,2'-bithiophene on excitation	31
Table 3.3 Selected bond lengths and dihedral angle of unsubstituted cis-2,2'-bithiophene	33
Table 3.4 Changes in selected bond lengths and dihedral angle of cis 2,2'-bithiophene on excitation	33
Table 3.5 Adiabatic excitation energies of trans 2,2'-bithiophene	34
Table 3.6 Adiabatic excitation energies of cis 2,2'-bithiophene	35
Table 4.1 Selected bond lengths and dihedral angle of the OH substituted BP ground state geometry at the MP2 level	41
Table 4.2 Selected bond lengths and dihedral angle of the OH substituted BP ground state geometry at the CC2 level	42
Table 4.3 Selected bond lengths and dihedral angle of the OH substituted BP excited state geometry at the ADC(2) level	43
Table 4.4 Selected bond lengths and dihedral angle of the OH substituted BP excited state geometry at the CC2 level	43
Table 4.5 Changes in selected bond lengths and dihedral angle of OH substituted BP on excitation at the ADC(2) level	44
Table 4.6 Changes in selected bond lengths and dihedral angle of OH substituted BP on excitation at the CC2 level	45
Table 4.7 Changes in selected bond lengths and dihedral angles of OH substituents on excitation	45
Table 4.8 Adiabatic Excitation energies of OH substituted trans 2,2'-bithiophene	48
Table 4.9 Selected bond lengths and dihedral angle of the OC(H)O substituted BP ground state geometry at the MP2 level	49
Table 4.10 Selected bond lengths and dihedral angle of the OC(H)O substituted BP ground state geometry at the CC2 level	49
Table 4.11 Selected bond lengths and dihedral angle of the OC(H)O substituted BP excited state geometry at the ADC(2) level	50
Table 4.12 Selected bond lengths and dihedral angle of the OC(H)O substituted BP excited state geometry at the CC2 level	50

Table 4.13 Changes in selected bond lengths and dihedral angle of OC(H)O substituted BP on excitation at the ADC(2) level	51
Table 4.14 Changes in selected bond lengths and dihedral angle of OC(H)O substituted BP on excitation at the CC2 level	51
Table 4.15 Changes in selected bond lengths and dihedral angles of OC(H)O substituents on excitation	52
Table 4.16 Adiabatic Excitation energies of OC(H)O substituted trans 2,2'-bithiophene	54
Table 4.17 Selected bond lengths and dihedral angle of the OC(CH ₃)O substituted BP ground state geometry at the MP2 level	55
Table 4.18 Selected bond lengths and dihedral angle of the OC(CH ₃)O substituted BP ground state geometry at the CC2 level.....	55
Table 4.19 Selected bond lengths and dihedral angle of the OC(CH ₃)O substituted BP excited state geometry at the ADC(2) level.....	56
Table 4.20 Selected bond lengths and dihedral angle of the OC(CH ₃)O substituted BP excited state geometry at the CC2 level.....	56
Table 4.21 Changes in selected bond lengths and dihedral angles of OC(CH ₃)O substituents on excitation	57
Table 4.22 Adiabatic Excitation energies of OC(CH ₃)O substituted trans 2,2'-bithiophene.....	60
Table 4.23 Selected bond lengths and dihedral angle of the phenyl substituted BP ground state geometry at the MP2 level	61
Table 4.24 Selected bond lengths and dihedral angle of the phenyl substituted BP ground state geometry at the CC2 level.....	61
Table 4.25 Selected bond lengths and dihedral angle of the phenyl substituted BP excited state geometry at the ADC(2) level.....	62
Table 4.26 Selected bond lengths and dihedral angle of the phenyl substituted BP excited state geometry at the CC2 level.....	62
Table 4.27 Changes in selected bond lengths and dihedral angle of phenyl substituted BP on excitation at the ADC(2) level	64
Table 4.28 Changes in selected bond lengths and dihedral angle of phenyl substituted BP on excitation at the CC2 level	64
Table 4.29 Changes in dihedral angles of phenyl substituents on excitation.....	65
Table 4.30 Adiabatic Excitation energies of phenyl substituted trans 2,2'-bithiophene.....	67
Table 4.31 Selected bond lengths and dihedral angle of the dimethylamino substituted BP ground state geometry at the MP2 level.....	68
Table 4.32 Selected bond lengths and dihedral angle of the dimethylamino substituted BP ground state geometry at the CC2 level	68

Table 4.33 Selected bond lengths and dihedral angle of the dimethylamino substituted BP excited state geometry at the ADC(2) level	69
Table 4.34 Selected bond lengths and dihedral angle of the dimethylamino substituted BP excited state geometry at the CC2 level	69
Table 4.35 Changes in selected bond lengths and dihedral angle of dimethylamino substituted BP on excitation at the ADC(2) level	71
Table 4.36 Changes in selected bond lengths and dihedral angle of dimethylamino substituted BP on excitation at the CC2 level	71
Table 4.37 Changes in selected bond lengths of dimethylamino substituents on excitation	72
Table 4.38 Table 4.39 Changes in dihedral angles of dimethylamino substituent methyl groups on excitation	72
Table 4.40 Adiabatic Excitation energies of dimethylamino substituted trans 2,2'-bithiophene	76
Table 4.41 Thiophene ring and substituent dihedral angles of OH substituted cis-2,2'-bithiophene.....	77
Table 4.42 Adiabatic Excitation energies of OH substituted cis 2,2'-bithiophene.....	78
Table 4.43 Thiophene ring and substituent dihedral angles of OC(H)O substituted cis-2,2'-bithiophene.....	79
Table 4.44 Adiabatic Excitation energies of OC(H)O substituted cis 2,2'-bithiophene	80
Table 4.45 Thiophene ring and substituent dihedral angles of OC(CH ₃)O substituted cis-2,2'-bithiophene.....	81
Table 4.46 Adiabatic Excitation energies of OC(CH ₃)O substituted cis 2,2'-bithiophene	82
Table 4.47 Thiophene ring and substituent dihedral angles of phenyl substituted cis-2,2'-bithiophene.....	83
Table 4.48 Adiabatic Excitation energies of phenyl substituted cis 2,2'-bithiophene.....	84
Table 4.49 Thiophene ring and substituent dihedral angles of dimethylamino substituted cis-2,2'-bithiophene	85
Table 4.50 Adiabatic Excitation energies of dimethylamino substituted cis 2,2'-bithiophene ..	86
Table 4.51 Ranking of the change in adiabatic excitation energies of substituted compared to unsubstituted trans 2,2'-bithiophene	88
Table 4.52 Ranking of the change in adiabatic excitation energies of substituted compared to unsubstituted cis 2,2'-bithiophene	89
Table 5.1 Dihedral angles of unsubstituted and substituted terthiophene	92
Table 5.2 Dihedral angles of unsubstituted and substituted tetrathiophene	93
Table 5.3 Dihedral angles of OH and OC(H)O substituents	94
Table 5.4 Adiabatic excitation energies of unsubstituted and substituted terthiophene.....	95

Table 5.5	Adiabatic excitation energies of unsubstituted and substituted tetrathiophene	96
Table 7.1	Contributors to the S_1 excitation of trans 2,2'-bithiophene	101
Table 7.2	Contributors to the S_1 excitation of cis 2,2'-bithiophene.....	101
Table 7.3	Contributors to the S_1 excitation of OH substituted trans 2,2'-bithiophene	102
Table 7.4	Contributors to the S_1 excitation of OC(H)O substituted trans 2,2'-bithiophene	103
Table 7.5	Contributors to the S_1 excitation of OC(CH ₃)O substituted trans 2,2'-bithiophene..	104
Table 7.6	Contributors to the S_1 excitation of phenyl substituted trans 2,2'-bithiophene	105
Table 7.7	Contributors to the S_1 excitation of singly dimethylamino substituted trans 2,2'- bithiophene.....	106
Table 7.8	Contributors to the S_1 excitation of doubly dimethylamino substituted trans 2,2'- bithiophene.....	107
Table 7.9	Changes in selected bond lengths and dihedral angle of OC(CH ₃)O substituted BP on excitation at the ADC(2) level	108
Table 7.10	Changes in selected bond lengths and dihedral angle of OC(CH ₃)O substituted BP on excitation at the CC2 level	108
Table 7.11	Selected bond lengths of substituents of phenyl substituted trans 2,2'-bithiophene at ADC(2) level	108
Table 7.12	Selected bond lengths of substituents of phenyl substituted trans 2,2'-bithiophene at CC2 level.....	109
Table 7.13	Selected bond lengths of the OH substituted cis BP ground state geometry.....	109
Table 7.14	Selected bond lengths of the OH substituted cis BP excited state geometry.....	109
Table 7.15	Selected bond lengths of the OC(H)O substituted cis BP ground state geometry..	110
Table 7.16	Selected bond lengths of the OC(H)O substituted cis BP excited state geometry .	110
Table 7.17	Selected bond lengths of the OC(CH ₃)O substituted cis BP ground state geometry	111
Table 7.18	Selected bond lengths of the OC(CH ₃)O substituted cis BP excited state geometry	111
Table 7.19	Selected bond lengths of the phenyl substituted cis BP ground state geometry...	112
Table 7.20	Selected bond lengths of the phenyl substituted cis BP excited state geometry...	112
Table 7.21	Selected bond lengths of the dimethylamino substituted cis BP ground state geometry.....	113
Table 7.22	Selected bond lengths of the dimethylamino substituted cis BP excited state geometry.....	113
Table 7.23	OH substituted cis 2,2'-bithiophene selected substituent bond length changes on excitation	114

Table 7.24 OC(H)O substituted cis 2,2'-bithiophene selected substituent bond length changes on excitation	114
Table 7.25 OC(CH ₃)O substituted cis 2,2'-bithiophene selected substituent bond length changes on excitation	115
Table 7.26 phenyl substituted cis 2,2'-bithiophene selected substituent bond length changes on excitation at the ADC(2) level	115
Table 7.27 phenyl substituted cis 2,2'-bithiophene selected substituent bond length changes on excitation at the CC2 level	115
Table 7.28 Dimethylamino substituted cis 2,2'-bithiophene selected substituent bond length changes on	116
Table 7.29 Contributors to the S ₁ excitation of OH substituted cis 2,2'-bithiophene	123
Table 7.30 Contributors to the S ₁ excitation of OC(H)O substituted cis 2,2'-bithiophene	124
Table 7.31 Contributors to the S ₁ excitation of OC(CH ₃)O substituted cis 2,2'-bithiophene....	125
Table 7.32 Contributors to the S ₁ excitation of phenyl substituted cis 2,2'-bithiophene	126
Table 7.33 Contributors to the S ₁ excitation of singly dimethylamino substituted cis 2,2'-bithiophene.....	127
Table 7.34 Contributors to the S ₁ excitation of doubly dimethylamino substituted cis 2,2'-bithiophene.....	128
Table 7.35 Selected bond lengths of unsubstituted and substituted terthiophene ground state geometries at the MP2 level.....	129
Table 7.36 Selected bond lengths of unsubstituted and substituted terthiophene ground state geometries at the CC2 level.....	129
Table 7.37 Selected bond lengths of unsubstituted and substituted terthiophene excited state geometries at the ADC(2) level.....	130
Table 7.38 Selected bond lengths of unsubstituted and substituted terthiophene excited state geometries at the CC2 level.....	130
Table 7.39 Selected bond lengths of unsubstituted and substituted tetrathiophene ground state geometries at the ADC(2) level.....	131
Table 7.40 Selected bond lengths of unsubstituted and substituted tetrathiophene ground state geometries at the CC2 level.....	132
Table 7.41 Selected bond lengths of unsubstituted and substituted tetrathiophene excited state geometries at the ADC(2) level.....	133
Table 7.42 Selected bond lengths of unsubstituted and substituted tetrathiophene excited state geometries at the CC2 level.....	134
Table 7.43 Selected bond length changes on excitation of oligomer substituents.....	134

Acknowledgements

This project was undertaken on the Viking Cluster, which is a high performance compute facility provided by the University of York. I am grateful for computational support from the University of York High Performance Computing service, Viking and the Research Computing team.

I would also like to thank Dr Conor Rankine and Eleanor Burrow for their advice and support.

Author's Declaration

I hereby certify that this thesis is a presentation of original work and I am the sole author. This work has not previously been presented for an award at this, or any other, University. All sources are acknowledged as References.

1 Chapter 1: Introduction

1.1 Background and Operating Principles of Organic Solar Cells

An organic photovoltaic (OPV) is a solar cell in which the energy from incident light is absorbed by an organic semiconducting layer, usually a polymer as these will possess the high degree of conjugation necessary for their HOMO-LUMO band gap to be small enough that visible light is able to excite an electron from the HOMO to the LUMO. A conjugated organic system consists of alternating carbon single and double bonds. The double bonds contain a σ -bond and a π -bond, and as the π -electrons are much more mobile than the σ -electrons they are able to move from site to site between carbon atoms due to mutual overlap of the π -orbitals, causing the wavefunctions to delocalise along the entire length of conjugation.¹

This absorbing organic semi-conducting layer is sandwiched between two different electrodes, one of which must be at least semi-transparent.² When an electron in the absorbing layer is excited it leaves behind a positive hole and the two are attracted to one another as they possess opposite charges, forming a quasiparticle known as an exciton. In order for the electron to be freed up to do work in the external circuit of the OPV the exciton must undergo dissociation. In an inorganic solar cell this dissociation would typically occur at room temperature, as the high dielectric constant of the material would mean that the attraction between the electron and hole, known as the exciton binding energy, E_b , is small enough that it can be overcome by thermal energy at this temperature.³

Conversely, organic semiconductors have low dielectric constants and therefore larger values of E_b , meaning that thermal energy alone cannot cause exciton dissociation. To overcome this, OPVs contain two organic semiconductors with offset HOMO-LUMO band gaps; one known as the 'donor' which will absorb the photon energy and 'donate' the resultant excited electron from its LUMO to the LUMO of the 'acceptor', leaving behind the hole on the donor. This donor-acceptor form for the organic layer, known as a heterojunction, originally took the form of a

bilayer structure and was proposed by Tang in 1986⁴, before being further developed into a mixture of two phase-segregated semiconductors by Halls et al in order to overcome the low exciton diffusion range of the bilayer structure.⁵ This phase segregated mixture is known as a 'dispersed' or 'bulk' heterojunction.²

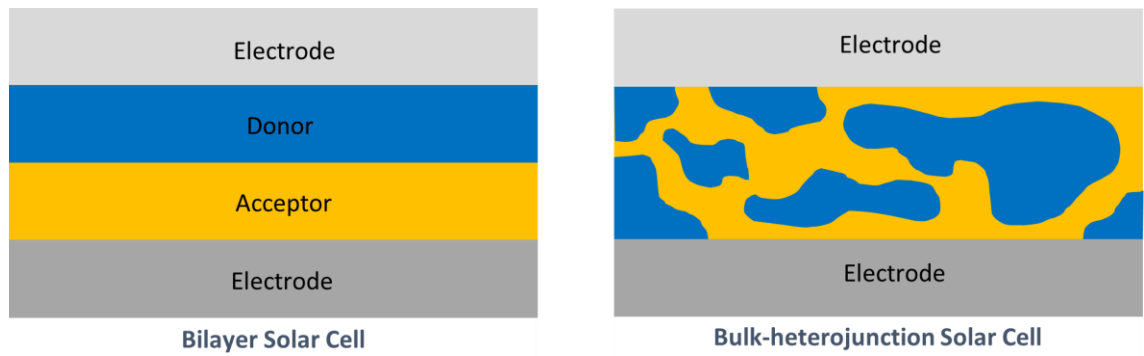


Figure 1.1 Schematic of bilayer vs. bulk heterojunction

Figure 1.1 shows a diagram illustrating the difference between the two different types of heterojunction.

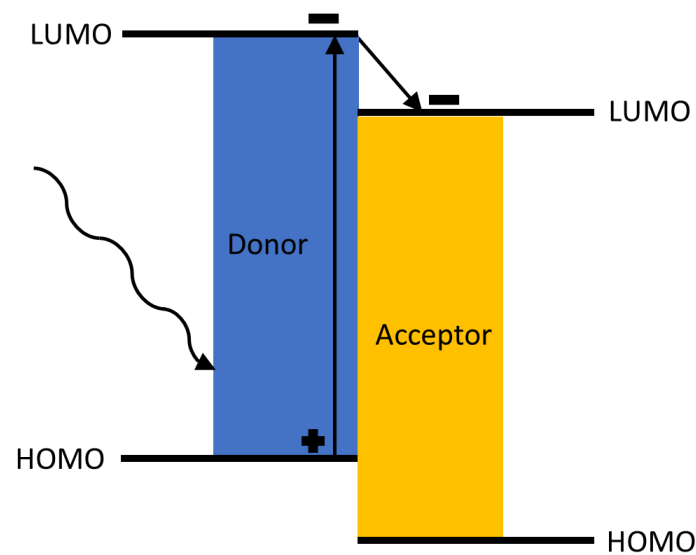


Figure 1.2 Donor-Acceptor block schematic

The donor-acceptor process is shown in Figure 1.2. Even after this process the electron and hole will still be attracted to each other but as the distance between them increases the attraction decreases until it can eventually be overcome by thermal energy and dissociation occurs. The electron and hole then diffuse to the relevant electrodes through interfacial layers, where they are then collected and do work in the external circuit of the cell to produce a current.

Fullerenes⁶ are very efficient electron acceptors and many OPV electron acceptors are fullerene derivatives such as PCBM-60¹ and Bis-PCBM⁷, however non-fullerene acceptors are also being investigated as new and more efficient alternative^{8,9}. Some donors include MEH-PPV¹⁰, PEOPT and PEDOT¹¹. An important consideration when selecting the electron donor for an OPV is that if the energy of the incident photon exceeds the HOMO-LUMO band gap then this excess energy is typically lost as heat in a process known as thermalization, which is a significant loss mechanism in all solar cells, and especially OPVs.¹² 2,2'-bithiophene, the molecule of interest for this thesis, and its polymeric form serve the roles of the electron donor in the OPV; the structure of unsubstituted 2,2'-bithiophene is shown in figure 1.2. The atoms are labelled following the convention that will be used throughout this thesis going forward.

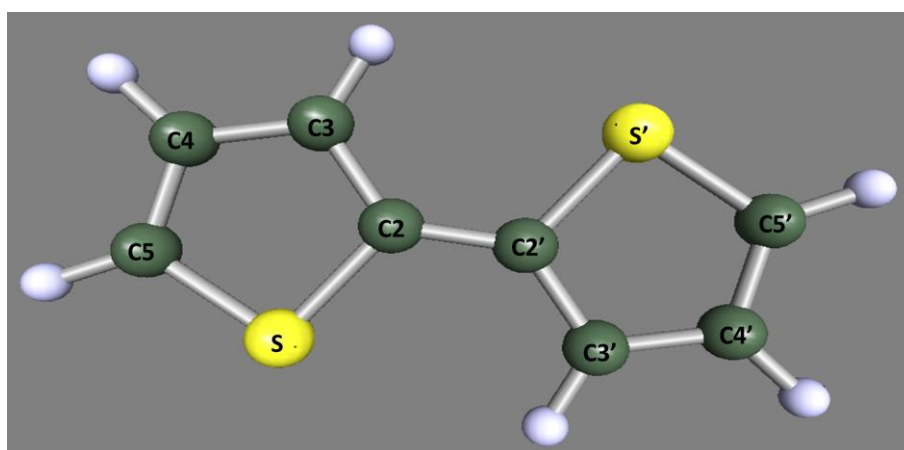


Figure 1.3 Unsubstituted *trans*-2,2'-bithiophene

1.2 Computational studies of substituted 2,2'-bithiophene

The addition of substituted groups allows for the tailoring of the properties of electron donors in OPVs, and the near infinite variability of organic compounds is considered a key advantage on OPVs.⁶ Whilst primarily serving to alter the HOMO-LUMO band gap and therefore the ease of excitation of the donor by incident light, the addition of substituted groups can also serve to avoid unwanted aggregation by introducing steric hinderance¹³, improving backbone planarity to increases charge carrier transport^{14, 15} and influencing the solubility of the polymer.¹⁶

Computational chemistry allows for the analysis of many molecular properties including geometries, HOMO-LUMO band gaps, the appearance of molecular orbitals, vibrational modes and the verification of a structure as belonging to a transition state, and various types of spectra. There are two main computational modelling approaches when conducting theoretical investigations; the first of which involves the use of Density Functional Theory (DFT). DFT uses functionals of the electron density, which is itself a function of time and space, to determine the properties of a many-electron system, and time-dependant density function theory (TD-DFT) can be used in the investigation of excitations. A major advantage of both DFT and TD-DFT is their high computational efficiency, allowing for the study of larger systems.¹⁷ The second type of approach involves the use of post Hartree-Fock (HF) methods such as nth-Order Moller-Plesset Perturbation (MPn) theory and Coupled-Cluster (CC) theory, that introduce approximations to allow the Schrodinger equation for a system involving more than two particles equation to be solved and the many-body wavefunction obtained, from which information about the properties of the system being studied can be gained. All computational chemistry calculations require the use of basis sets; one-particle functions used to build the molecular orbitals that define the space in which the calculations are solved.

There have been several computational studies on substituted 2,2'-bithiophene relating to their role as donors in organic solar cells, using both post Hartree-Fock *ab initio* methods and density functional theory (DFT), many of which are performed on substituted 2,2'-bithiophenes that

have been simultaneously experimentally synthesised.^{8, 13, 14, 18-20} A wide variety of substituted groups have been investigated including ester groups^{13, 21, 22}, alkyl groups^{13, 15}, aryl groups¹⁸, halogens^{13, 14}, alkoxy groups^{15, 19, 23}, carboxylic acid groups¹⁶ and various acceptor groups including nitrile and nitro groups¹⁵, and amino groups²³. Substitutions are usually made at the C3 and C4 positions, as thiophene typically undergoes linear polymerisation, with linkages between the C2 and C5' positions.

Swaroop et al conducted a theoretical investigation into aryl-substituted bithiophene that they had synthesised.¹⁸ Substitutions made at the C4 position and the ground state geometries were optimised at the M062X/6-31G(d) level, with subsequent frequency calculations to confirm these optimised structures to the lowest energy conformations. TD-DFT was then used to optimise the S_1 excited state geometry at the B3LYP/6-31G(d) level and the vertical emission energies from S_1 to S_0 at the B3LYP/6-311+G(d,p) level calculated. A single point TD-DFT calculation was also performed at the B3LYP/6-311+F(d,p) level to obtain simulated UV-Vis spectra. Ichiro Imae et al similarly performed ground state DFT optimisations and corresponding frequency calculations on n-butoxy substituted bithiophene. In this case substitutions were made doubly at both the C3/C3' and C4/C4' positions and calculations were made at the B3LYP/6-21G(d) level.¹⁹ Andicsová-Eckstein et al used computational chemistry to further investigate three substituted bithiophenes that they had synthesized.¹³ In each of the three substituted bithiophenes C(O)OCH₃ was substituted at the C5 position; CH₃ and C₁₂H₂₅ were substituted at C3 positions in select cases, and Cl at position C5' in selected cases. Ground state geometry optimisations were performed at the B3LYP/6-31G(d) level, before TD-DFT simulations of excitations were performed using the PBE0, B3LYP, CAMB3LYP, TPSSH and M062X functionals and the 6-31G(d) basis set, with the TPSSH/6-31G(d) level HOMO-LUMO band gap being presented in the paper. TD-DFT calculations at M062X and CAMB3LYP levels were used to evaluate the optical absorption spectra.

In addition to using computational chemistry to further investigate and develop on results obtained from physically conducted experiments, such as the previously mentioned syntheses,

there have also been purely theoretical studies of substituted bithiophenes. Tzu-Jen Lin and Shiang-Tai Lin investigated the effect of a range of substituents; methoxy (-OCH₃), amino (NH₂), cyano (CN), formyl (CHO), nitro (NO₂) groups, and methyl and ethyl groups used to represent conjugated polymers with alkyl side chains, on the torsional potential of bithiophene.¹⁵ Methyl and ethyl groups were doubly substituted at the C3,C3', C3,C4' and C4,C4' positions, whilst the other substituted groups were only singly substituted at the C3 position. Ground state geometry optimisations were performed at the B3LYP/6-311+G(2df,p) level, followed by a series of single point energy calculations on these optimised geometries using the B3LYP, wB97x, wB97xd, M062X functionals and the MP2 method with the 6-311+G(2df,p) basis set, and CCSD(T), which provided a high accuracy but also very high computational cost coupled-cluster method²⁴, with the cc-pVTZ basis set.

Casanovas et al investigated the structural and electronic effects of substituting carboxylic acid, again making substitutions at the C4/4', C3/4' and C3/3' positions to model tail-to-tail, tail-to-head and head-to-head linkages.¹⁶ Geometry optimisation calculations, with associated frequency calculations to characterise as the equilibrium geometries, were performed using the B3PW91 functional and the 6-31+G(d,p) basis set. Examination of the change in electronic properties on extension of the polymer chain was also investigated by performing similar geometry optimisations on substituted oligothiophenes up to seven rings with different types of linkages. M. Pomerantz performed multiple investigations on C(O)OCH₃ and C(O)N(H)CH₃ substituted bithiophene in order to investigate the change in planarity on substitution.^{21, 22} Geometry optimisation calculations were performed and as with the previously mentioned investigation substitutions were made at the C3/3', C3/C4' and C4/4' positions.

It can be seen that the vast majority of computational investigations on substituted bithiophenes are conducted using DFT functionals, with only the occasional calculation being performed using a post-HF method such as MP2. This can likely be attributed to the relatively large size of the molecule, especially when substituted, and the subsequent high computational cost of performing calculations that are not DFT. Through the use of the Viking Cluster the opportunity

to perform these types of calculations has been presented, using methods typically regarded as having a higher computational cost.

1.3 Computational Studies of Oligothiophenes

There have also been investigations into the excited states of thiophene oligomers; both substituted and unsubstituted. De Oliveira et al investigated the HOMO-LUMO band gaps of OMe and NO₂ substituted oligothiophenes of up to six repeat units in length, where the substitutions were made at the terminal C3 positions of the chains.²³ Geometry optimisations were performed at the HF/6-31G* level followed by single point calculations using the B3LYP, BLYP and SVWN functionals all with the 6-31G* basis set, and also at the MP2/6-31G* level. Della Sala et al studied the excitation spectra of terthiophene and terthiophene-S,S-dioxide; the ground state geometries were first optimised using the B3LYP functional and the 6-311G** basis set before a subsequent TD-DFT calculation at the same level was performed to find the first six excitation energies for each molecule.²⁵ Rubio et al conducted a similar study into the excited states of terthiophene and tetrathiophene. In that study ground state geometries were optimised using MP2 and the 6-31G* basis set before the geometries of the lowest singlet and triplet states were optimised using the multireference CASSCF method and the cc-pVDZ basis set, and the electronic states were computed by CASPT2, another multireference method.²⁶

Multireference methods become necessary when the system cannot be described well by a single determinant, as the mean-field approach used by Hartree-Fock can result in important information being neglected, but are generally avoided outside of these cases due to their high computational cost.²⁷

1.4 Overview of Thesis

The aim of this thesis is to investigate the effect of the addition of various substituents, chosen with the aim of providing a range of electronic and steric effects, on to 2,2'-bithiophene both singly and doubly substituted at different positions on the molecule, on the adiabatic excitation energy and geometry changes experienced on excitation using ab initio techniques.

Chapter 2 presents the computational methods used throughout this thesis. Chapter 3 describes the results of ground and excited state geometry optimisation calculations on unsubstituted trans- and cis- 2,2'-bithiophene. Chapter 4 presents the results of ground and excited state calculations on substituted trans- and cis-2,2'-bithiophene. Chapter 5 presents the results of ground and excited state geometry optimisations on unsubstituted and selected substituted oligomers of thiophene of up to four repeat units and examines an extrapolation to obtain the excitation energy of theoretical polymers of infinite repeat units.

2 Chapter 2: Computational Methods

2.1 The Schrödinger Equation

The Schrödinger equation is a partial differential eigenvalue equation, which can be solved to yield eigenvalues representing observables associated with the Hamiltonian operator, H , and a set of eigenfunctions, or wavefunctions, Ψ , and is shown as equation 2.1.

$$H\Psi = E\Psi \quad (2.1)$$

A wavefunction is a probability amplitude, which, when squared, yields the probability of finding a particle constrained by the potential described by the Hamiltonian, at each point in space.²⁸ For a many-body system, one that contains more than a single particle, the Hamiltonian can be broken down into kinetic and potential energy terms as shown in equation 2.2.

$$H = T + V \quad (2.2)$$

T is the kinetic energy of the particles and V is the potential energy of the particle pairs. In terms of molecules this can be further separated as five terms; a kinetic energy term for the nuclei (T_N) and a kinetic energy term for the electrons (T_e), and a potential energy term arising from repulsion between the nuclei (V_{NN}), a potential energy term arising from attraction between the nuclei and the electrons (V_{Ne}), and a potential energy term arising from repulsion between the electrons (V_{ee}), as shown in equation 2.3; the Hamiltonian of a diatomic molecule.

$$H = T_N + T_e + V_{NN} + V_{Ne} + V_{ee} \quad (2.3)$$

For a molecule containing N electrons and M nuclei, equation 2.3 can be rewritten as

$$\begin{aligned} = & -\sum_{A=1}^M \frac{\hbar^2}{2m_A} \nabla_A^2 - \sum_{i=1}^N \frac{\hbar^2}{2m_e} \nabla_i^2 + \sum_{A=1}^M \sum_{B=A+1}^M \frac{Z_A Z_B e^2}{4\pi\epsilon_0 R_{AB}} - \sum_{A=1}^M \sum_{i=1}^N \frac{Z_A e^2}{4\pi\epsilon_0 r_{iA}} \\ & + \sum_{i=1}^N \sum_{j=i+1}^N \frac{e^2}{4\pi\epsilon_0 r_{ij}} \quad (2.4) \end{aligned}$$

In atomic units this can be simplified as

$$H = - \sum_{A=1}^M \frac{1}{2m_A} \nabla_A^2 - \sum_{i=1}^N \frac{1}{2} \nabla_i^2 + \sum_{A=1}^M \sum_{B=A+1}^M \frac{Z_A Z_B}{R_{AB}} - \sum_{A=1}^M \sum_{i=1}^N \frac{Z_A}{r_{iA}} + \sum_{i=1}^N \sum_{j=i+1}^N \frac{1}{r_{ij}} \quad (2.5)$$

Where m_A is the mass of nucleus A , Z_A is the charge of nucleus A .

2.2 The Born-Oppenheimer Approximation

It is impossible to solve exactly the Schrodinger equation for systems that contain more than two bodies, such as atoms that contain more than one electron²⁹ or any molecules, and as such approximations need to be introduced. The Born-Oppenheimer approximation allows for the separation of the motion of the nuclei and the electrons by neglecting the motion of the atomic nuclei when describing the electrons in the system.³⁰

The approximation is based on the physical principle that since the mass of an atomic nucleus is much greater than that of an electron, the nuclei move much slower than the electrons when responding to stimuli and can be approximated as stationary. This allows for the separation of the Schrodinger equation into two separate equations: one for the nuclear component, equation 2.6, and one for the electronic component, equation 2.7.

$$H_{nuc}(R)\Psi_{nuc}(R) = E_{nuc}(R)\Psi_{nuc}(R) \quad (2.6)$$

$$H_{el}(r, R)\Psi_{el}(r, R) = E_{el}(R)\Psi_{el}(r, R) \quad (2.7)$$

It can be seen that the electronic Schrodinger equation is dependant on the coordinates of both the nuclei and the electrons, but as it is assumed that the nuclei are stationary, R is a constant, not a variable.

2.3 Hartree-Fock Theory

Hartree-Fock theory was developed to solve the electronic Schrodinger equation after the Born-Oppenheimer approximation has been invoked and serves a good starting point for more elaborate theoretical methods which are better approximations to the electronic Schrodinger equation.³¹

$$f(i)|\chi'_a\rangle = \varepsilon'_a|\chi'_a\rangle \quad (2.8)$$

Equation 2.8 shows the canonical Hartree-Fock equation, an eigenvalue equation where the one electron Fock operator, $f(i)$, acts on a spin orbital to give back the orbital energy, ε'_a , multiplied by that same spin orbital. The Fock orbital is defined as

$$f(i) = h(i) + V^{HF} \quad (2.9)$$

$h(i)$ is the core Hamiltonian operator and accounts for the kinetic energy of and potential energy arising from the attraction to the nuclei of the electron, as shown in equation 2.10.

$$h(i) = \frac{1}{2}\nabla_i^2 - \sum_{A=1}^M \frac{Z_A}{r_{iA}} \quad (2.10)$$

V^{HF} is the Hartree-Fock potential which accounts for the interaction between the electron and all other electrons it could possibly interact with, and is defined by equation 2.11.

$$V^{HF}(i) = \sum_{b \neq a} J_{ab}(i) + \sum_{b \neq a} K_{ab}(i) \quad (2.11)$$

The first term, J_{ab} , is the Coulomb operator, which represents the electrostatic potential felt by electron 1 due to the presence of an electron 2 in spin orbital b.

$$J_{ab}(X_1) = \int dx_2 \chi_b^*(X_2)\chi_b(X_2) \frac{1}{r_{12}} \quad (2.12)$$

The second term, K_{ab} , is the exchange operator.

$$K_{ab}(X_1)\chi_a(X_1) = \left[\int dx_2 \chi_b^*(X_2)\chi_a(X_2) \frac{1}{r_{12}} \right] \chi_b(X_1) \quad (2.13)$$

2.4 Second-Order Møller-Plesset Perturbation Theory

Møller-Plesset Perturbation Theory improves on Hartree-Fock by beginning to account for the electron-correlation effects and is the least costly ab initio method to do so, however it is also regarded as being much less accurate than the Coupled-Cluster methods that shall be discussed subsequently in section 2.5.³² The role that this method shall serve in this thesis is to provide ground state geometries to be compared to excited state geometries obtained using the ADC(2),

overviewed in section 2.6, as the ADC(2) is described as ‘MP2 for excited states’³³ and uses the MP2 ground state wavefunction and energy in it’s calculations.

In perturbation theory the total Hamiltonian H is separated into a reference Hamiltonian, $H^{(0)}$, from a reference Schrodinger equation

$$H^{(0)}\Psi_n^{(0)} = E_n^{(0)}\Psi_n^{(0)} \quad (2.14)$$

and a perturbation, V , to give equation 2.15.

$$H = H^{(0)} + \lambda V \quad (2.15)$$

λ is a parameter between 0 and 1 that has no dimensions.

Møller and Plesset suggested to use a HF calculation as the starting point of the perturbation expansion³² making their zeroth-order wavefunction $\Psi_0^{(0)}$ an eigenfunction of the Fock operator shown in equation 2.9.

In perturbation theory the energy and wavefunction are expressed as a sum of various terms

$$E_n = E_n^{(0)} + \lambda E_n^{(1)} + \lambda^2 E_n^{(2)} + \lambda^3 E_n^{(3)} + \dots \quad (2.16)$$

$$\Psi_n = \Psi_n^{(0)} + \lambda \Psi_n^{(1)} + \lambda^2 \Psi_n^{(2)} + \lambda^3 \Psi_n^{(3)} + \dots \quad (2.17)$$

where the superscript denotes the order of the correction energy. The first electron correction to HF theory occurs at the second order of perturbation theory (MP2) and is give as

$$E_{MP}^{(2)} = \sum_i^{occ.} \sum_{j>i}^{occ.} \sum_a^{vir.} \sum_{b>a}^{vir.} \frac{\iint X_i(1)X_j(2) \frac{1}{r_{12}} [X_a(1)X_b(2) - X_b(1)X_a(2)] dt_1 dt_2}{\epsilon_a + \epsilon_b - \epsilon_i - \epsilon_j} \quad (2.18)$$

2.5 Coupled-Cluster Theory

The second-order approximate coupled cluster singles and doubles model (CC2) was developed to provide an approximation for the more expensive coupled cluster singles and doubles method (CCSD) at a lower computational cost, and provides an energy that is considered to be of the

same quality as the MP2 energy.³⁴ The CC2 method can be used for both ground and excited state calculations, and shall be used to obtain ground and excited state geometries for the calculation of adiabatic excitation energies in this thesis.

Coupled-cluster theory begins with an exponential ansatz for the CC wavefunction.³⁵

$$|\Psi_{CC}\rangle = e^T |\Phi_0\rangle \quad (2.19)$$

$|\Phi_0\rangle$ is the HF wavefunction and T is the cluster operator, which can be expanded as a sum of cluster operators of different excitation levels as shown in equation 2.20.

$$T = T_1 + T_2 + \dots + T_N \quad (2.20)$$

where T_1 is the cluster operator for single excitations, T_2 is the cluster operator for double excitations, etc.

The operator e^T can be written as

$$e^T = 1 + T + \frac{T^2}{2!} + \frac{T^3}{3!} + \dots = 1 + C_1 + C_2 + \dots + C_N \quad (2.21)$$

where operator C_1 generates single excitations, C_2 double excitations, etc. After substituting equation 2.20 into equation 2.21 and gathering the corresponding cluster operators equations 2.22 and 2.23 can be produced.

$$C_1 = T_1 \quad (2.22)$$

$$C_2 = T_2 + \frac{1}{2} T_1^2 \quad (2.23)$$

Equation 2.22 shows that the single excitations are generated only by T_1 , and equation 2.23 shows how double excitations can be generated by either T_2 describing a simultaneous excitation of two electrons, or T_1^2 describing two independent simultaneous excitations. CCSD is truncated at the second order, meaning $T = T_1 + T_2$, and CC2 further simplifies on this by approximating the doubles equations as correct only through the first order.³⁴

2.6 Algebraic Diagrammatic Construction Scheme

The algebraic diagrammatic construction (ADC) scheme is used for the calculation of excited states and is more suited for the study of large molecules than other ab initio methods, as the Hermitian nature of the ADC matrix means that it does not have to compute two representations of the excited state that correspond to different eigenvectors, such as the case is for CC methods, as both of ADC's eigenvectors are identical.³³

Using a technique known as the intermediate state representation (ISR) expressions can be obtained for \mathbf{M} , a non-diagonal matrix representation of an effective Hamiltonian, and \mathbf{f} , a matrix of effective transition moments.

Beginning with the correlated ground-state wavefunction, Ψ_0 , a correlated excited-state basis $\{\Psi_J^0\}$ can be generated by acting on Ψ_0 with a series of excitation operators $\{C_J\}$ which represent single, double, etc. excitations as shown in equation 2.24

$$\{C_J\} \equiv \{\hat{c}_a^\dagger \hat{c}_r, \hat{c}_a^\dagger \hat{c}_b^\dagger \hat{c}_r \hat{c}_s, \dots\} \quad (2.24)$$

$$\Psi_J^0 = C_J \Psi_0 \quad (2.25)$$

Using the IS basis \mathbf{M} and \mathbf{f} can be expressed as

$$(\mathbf{M})_{IJ} = \langle \Psi_I | H - E_0^N | \Psi_J \rangle \quad (2.26)$$

$$(\mathbf{f})_{J,pq} = \langle \Psi_J | \hat{c}_p^\dagger \hat{c}_q | \Psi_0 \rangle \quad (2.27)$$

where E_0^N is the ground state energy. Choosing the n th order Møller-Plesset ground state as the starting point, Ψ_0 , when deriving the IS basis results in the n th order ADC(n) scheme for the excitation energies being obtained. For example, beginning with the MP2 ground-state wavefunction and energy returns the ADC(2) level excitation energies.³³

2.7 Basis Sets

A basis set is a set of one-particle functions used to build molecular orbitals when in a quantum mechanical setting. There are two main types of basis sets, Slater-Type Orbitals (STOs) and Gaussian-Type Orbitals (GTOs).

STOs have the functional form

$$\chi_{\zeta,n,l,m}(r, \theta, \varphi) = NY_{l,m}(\theta, \varphi)r^{n-1}e^{-\zeta r} \quad (2.28)$$

N is a normalizing constant, $Y_{l,m}$ is a spherical harmonic function and ζ is a constant that relates to the effective charge of the nucleus.

GTOs have the cartesian functional form

$$\chi_{\zeta,l_x,l_y,l_z}(x, y, z) = Nx^{l_x}y^{l_y}z^{l_z}e^{-\zeta r^2} \quad (2.29)$$

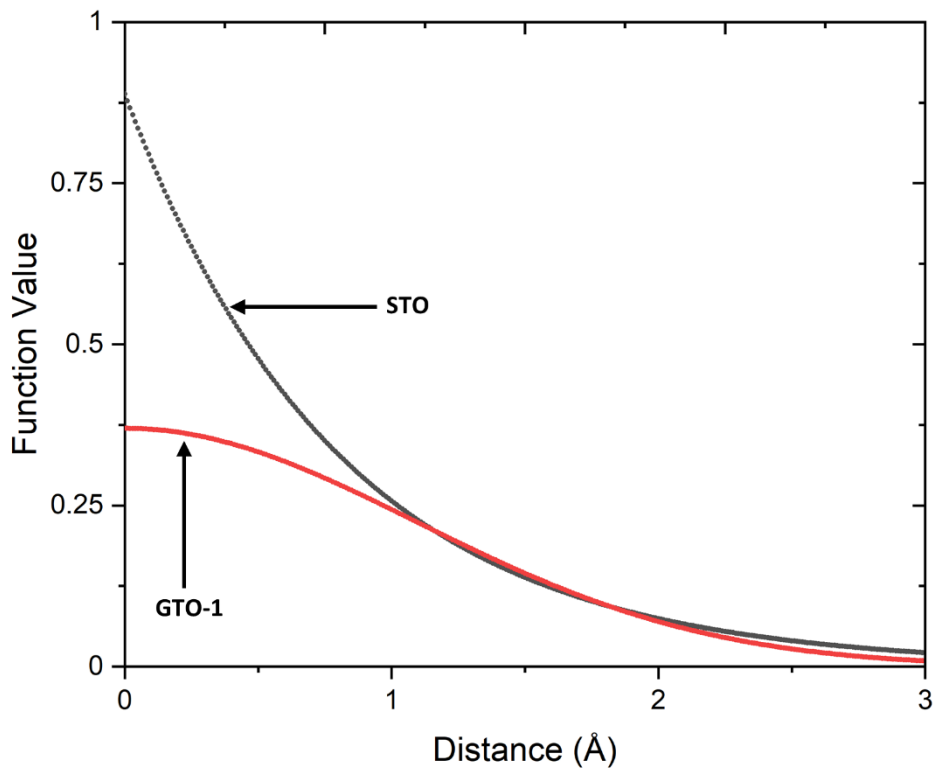


Figure 2.1 Comparison between Slater-Type Orbital STO and Gaussian-Type Orbital GTO

Figure 2.1 was constructed using the functional forms $GTO = \left(\frac{2\alpha}{\pi}\right)^{0.75} e^{-\alpha r^2}$ and

$STO = \left(\frac{\zeta^3}{\pi}\right) e^{-\zeta r}$, with values of $\zeta = 1.24$ and $\alpha = 0.4166$ being used to model orbitals for hydrogen.³⁶

Basis sets can be further defined as one of several types based on the number of functions used. A minimal basis set contains a single basis function, be it an STO or GTO, for each atomic orbital (AO) in the atom. For example, a H atom minimal basis set would have one 1s AO represented by a single basis function, and a C atom minimal basis set would have basis functions for a 1s, a 2s and three 2p AOs, for five in total.

Double- ζ (DZ) basis sets contain two basis functions for each AO; using the above example a C atom double- ζ basis set would contain ten total basis functions. A triple- ζ (TZ) basis set contains three basis functions for each AO, a quadruple- ζ (QZ) basis set contains four per AO, continuing this pattern through 5Z, 6Z, etc.

Basis sets can also be further qualified as split-valence basis sets, which use only one basis function for each core AO, and a larger basis for the valence AOs. For examples, a C atom split-valence double- ζ basis set would have a total of nine basis functions; one function for the 1s AO and two functions each for the 2s and three 2p AOs.

The quality of basis sets can be improved through the addition of further functions. Polarization functions, denoted by * or a letter (d,p) add flexibility to the basis sets which allows for charge polarization away from atomic distribution to occur. Diffuse functions, denoted by + or 'aug', have a small ζ exponent, meaning that the electron is held far away from the nucleus, which allows for weakly bonded electrons to localise further away from the density.

The aug-cc-pVDZ basis set, which contains both diffuse and polarization functions and is of double- ζ level, and the cc-pVTZ basis set, of triple- ζ level and containing polarization but no diffuse functions, shall be used in this thesis, and their ability to produce accurate values for the adiabatic excitation energy of 2,2'-bithiophene will be compared in the subsequent chapter.

3 Chapter 3

3.1 Introduction

The aim of this chapter is to obtain results for the change in geometry on excitation of unsubstituted trans- and cis-2,2'-bithiophene, as well as values for the excitation energy of the first singlet excited state, to serve as a comparison to the results for substituted trans and cis-2,2'-bithiophene that will be analysed subsequently in Chapter 4, in order to assess the changes caused to the geometries and the excitation energy by those substituted groups. The results in this chapter shall also be compared to experimental data in order to assess the accuracy of the methods and basis sets chosen.

3.2 Computational Methods

Ground and excited state geometry optimisation and frequency calculations were performed using TURBOMOLE 6.4.³⁷ From this point onwards and in all subsequent chapters 2,2'-bithiophene shall be abbreviated as 'BP'. Ground state geometries of trans- and cis-BP were obtained using MP2³⁸⁻⁴⁰ and CC2⁴¹, and the cc-pVTZ⁴² and aug-cc-pVDZ⁴³ basis sets, via the ricc2 module⁴⁴ and using an SMP parallelization scheme. Frequency calculations using the NumForce tool were performed on the obtained geometries to ensure that these ground-state structures represented true-minima on the potential energy surface; not transition-state geometries or saddle points. Excited state geometry optimisations of the first singlet excited state (S_1) were then performed at the CC2⁴⁵ and ADC2⁴⁶ level, again with both the cc-pVTZ and aug-cc-pVDZ basis sets, using the CC2 and MP2 ground state geometries respectively as inputs. For the correlation consistent basis sets the -aug prefix indicates the addition of one diffuse basis function of each function type that is in use for a given atom. Using the elements of the second period, Li-Ne, as an example, the aug-cc-pVDZ basis set contains 23 basis functions⁴², and the cc-pVTZ basis set contains 30 basis functions. Diffuse functions can become necessary when there

is the potential for hydrogen bonding or weak intramolecular forces, and as such it is expected that the calculations performed using the aug-cc-pVDZ basis set will provide the more accurate results.

The control files produced by these calculations were analysed using the TmoleX 4.1⁴⁷ graphical interface in order to view the geometries and molecular orbitals (MOs). Geometries were also viewed in the form of an .xyz file using Avogadro 1.2.0⁴⁸ to view the dihedral angles.

3.3 Results and Discussion

3.3.1 Unsubstituted trans-2,2'-bithiophene

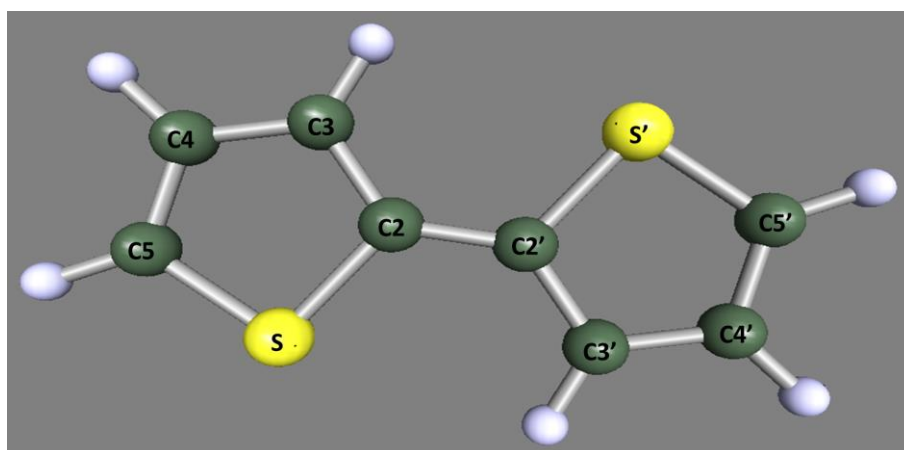


Figure 3.1 unsubstituted trans 2,2'-bithiophene

Table 3.1 displays the bond lengths and C2-S-S'-C2' dihedral angle as obtained from each ground state and excited state geometry optimisation. The first four rows show the ground state geometries and the latter four the excited state geometries. The respective equivalent bond lengths were identical in each thiophene ring and so have only been displayed once in the table. When the C2-S-S'-C2' dihedral angle is equal to 180°, the molecule is completely planar.

Table 3.1: Selected bond lengths and dihedral angle of unsubstituted *trans*-2,2'-bithiophene

Method	Basis set	Bond length /Å						C2-S-S'-C2' angle /°
		C2-C2'	C2-C3	C3-C4	C4-C5	C5-S	S-C2	
MP2	Aug-cc-pVDZ	1.454	1.398	1.421	1.392	1.729	1.741	147.3
CC2		1.454	1.398	1.425	1.391	1.736	1.748	148.6
MP2	cc-pVTZ	1.445	1.386	1.41	1.377	1.713	1.727	150.8
CC2		1.437	1.379	1.407	1.373	1.713	1.737	155.2
ADC2	Aug-cc-pVDZ	1.384	1.446	1.396	1.418	1.731	1.788	180
CC2		1.385	1.445	1.399	1.418	1.737	1.793	180
ADC2	cc-pVTZ	1.367	1.428	1.377	1.4	1.71	1.768	180
CC2		1.368	1.427	1.38	1.401	1.716	1.773	180

Table 3.2 displays the change in the bond lengths and the C2-S-S'-C2' dihedral angle shown in Table 3.1 on excitation by comparing the results of the relative ground and excited state geometry optimisations to each other. The MP2 ground state geometry is compared to the ADC(2) excited state geometry, as ADC(2) is seen as the direct equivalent to MP2 for excited state calculations³³.

Table 3.2: Changes in selected bond lengths and dihedral angle of *trans* 2,2'-bithiophene on excitation

Method	Basis set	Bond length change/Å						C2-S-S'-C2' angle change /°
		C2-C2'	C2-C3	C3-C4	C4-C5	C5-S	S-C2	
ADC(2)	Aug-cc-pVDZ	-0.07	0.048	-0.025	0.026	0.002	0.047	32.7
CC2		-0.069	0.047	-0.026	0.027	0.001	0.045	31.4
ADC(2)	cc-pVTZ	-0.078	0.042	-0.033	0.023	-0.003	0.041	29.2
CC2		-0.069	0.048	-0.027	0.028	0.003	0.036	24.8

Figure 3.2 shows the molecular orbitals (MOs) involved in the ground state to S_1 excitation and the percentage that this transition contributed to the overall excitation; specifically the ADC(2)/aug-cc-pVDZ calculation. Complete breakdowns of the contributors to the excitation for all four calculations levels are included in appendix 7.3 as table 7.1.

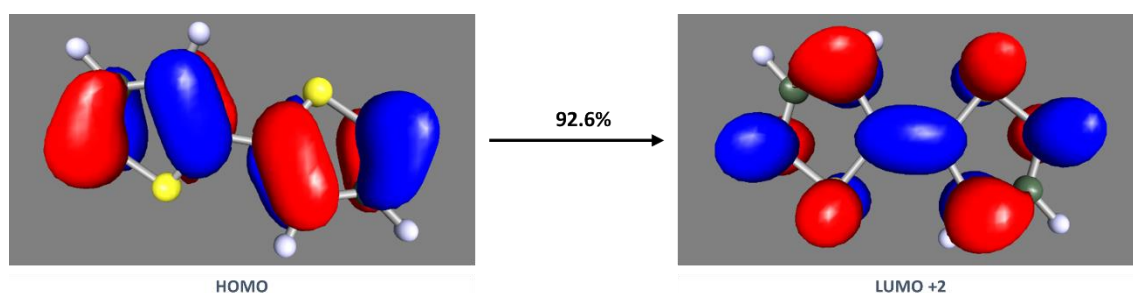


Figure 3.2 MOs of the ground state to S_1 excitation of *trans* 2,2'-bithiophene at the ADC(2)/aug-cc-pVDZ level

The excitation can be assigned as a π to π^* transition. The decrease in the central C2-C2' bond length can be attributed to the excitation from anti-bonding in the ground state to bonding character in the excited state, and the alternating increase, decrease, increase of the C-C bonds within the thiophene ring to the inversion of bonding and anti-bonding character from the ground to excited state MOs. Similarly, the S-C2 bond increases in length due to going from bonding character in the ground state to anti-bonding in the excited state, whilst the S-C5 bond remains almost unchanged on excitation as there is a node in both the ground and excited state MO.

3.3.2 Unsubstituted *cis*-2,2'-bithiophene

Table 3.3 shows the bonds lengths and C2-S-S'-C2' dihedral angle as obtained from each ground state and excited state geometry optimisation. In this case, when the C2-S-S'-C2' dihedral angle is equal to 0 the molecule is completely planar. As was the case with the *trans* configuration, respective equivalent bond lengths were identical in each thiophene ring.

Table 3.3 Selected bond lengths and dihedral angle of unsubstituted cis-2,2'-bithiophene

Method	Basis set	Bond length /Å						C2-S-S'-C2' angle /°
		C2-C2'	C2-C3	C3-C4	C4-C5	C5-S	S-C2	
MP2	Aug-cc-pVDZ	1.455	1.398	1.421	1.392	1.728	1.741	40.5
CC2		1.455	1.397	1.425	1.392	1.735	1.749	40.3
MP2	cc-pVTZ	1.438	1.379	1.404	1.373	1.706	1.72	33.5
CC2		1.438	1.379	1.407	1.374	1.712	1.727	32.9
ADC2	Aug-cc-pVDZ	1.386	1.445	1.394	1.42	1.727	1.79	0
CC2		1.387	1.444	1.397	1.421	1.733	1.797	0
ADC2	cc-pVTZ	1.368	1.425	1.376	1.404	1.705	1.773	0
CC2		1.37	1.424	1.379	1.405	1.71	1.779	0

Table 3.4 displays the change in the bond lengths and the C2-S-S'-C2' dihedral angle shown in Table 3.3 on excitation, using the same comparisons as with the trans configuration.

Table 3.4 Changes in selected bond lengths and dihedral angle of cis 2,2'-bithiophene on excitation

Method	Basis set	Bond length change/Å						C2-S-S'-C2' angle change /°
		C2-C2'	C2-C3	C3-C4	C4-C5	C5-S	S-C2	
ADC(2)	Aug-cc-pVDZ	-0.069	0.047	-0.027	0.028	-0.001	0.049	-40.5
CC2		-0.068	0.047	-0.028	0.029	-0.002	0.048	-40.3
ADC(2)	cc-pVTZ	-0.07	0.046	-0.028	0.031	-0.001	0.053	-33.5
CC2		-0.068	0.045	-0.028	0.031	-0.002	0.052	-32.9

For the calculations performed using the aug-cc-pVDZ basis set the changes in bond lengths on excitation of cis BP are almost identical to those of trans BP seen in Table 3.2, however there was a much greater deviation for the calculations performed using the unaugmented cc-pVTZ basis set, especially with regards to the S-C2 bonds.

Figure 3.3 shows the MOs involved in the ground state to S₁ excitation for cis BP; specifically using the results of the ADC(2)/aug-cc-pVDZ calculation. Table 7.2 in appendix 7.3 shows the complete breakdowns for all four calculation levels.

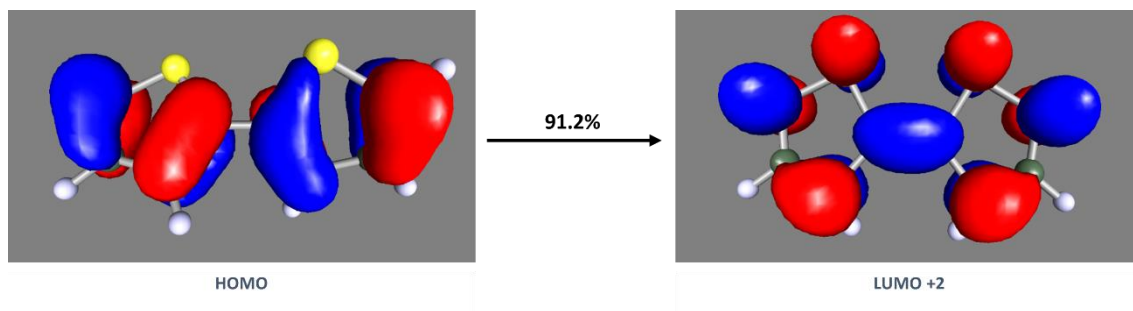


Figure 3.3 MOs of the ground state to S_1 excitation of *cis* 2,2'-bithiophene at the ADC(2)/aug-cc-pVDZ level

The bond length changes experienced by *cis* BP on excitation can be attributed to the same causes as for *trans* BP above.

3.3.3 Excitation Energies

Adiabatic excitation energies were calculated for both *trans* and *cis* BP using the energies of corresponding ground and excited state geometries. The results of these calculations are displayed in Tables 3.5 and 3.6.

Table 3.5 Adiabatic excitation energies of *trans* 2,2'-bithiophene

Basis Set	Method	Adiabatic excitation energy		
		/eV	/cm ⁻¹	Experimental /cm ⁻¹
AUG-cc-pVTZ	ADC(2)	3.8526	31073	31111
	CC2	3.8636	31162	
cc-pVTZ	ADC(2)	4.0059	32310	
	CC2	4.0315	32516	

Table 3.6 Adiabatic excitation energies of cis 2,2'-bithiophene

Basis Set	Method	Adiabatic excitation energy		
		/eV	/cm ⁻¹	Experimental / cm ⁻¹
AUG-cc-pVTZ	ADC(2)	3.8626	31154	31203
	CC2	3.8694	31209	
cc-pVTZ	ADC(2)	4.0019	32278	
	CC2	4.0127	32364	

J. Chadwick and B. Kohler used resonance-enhanced multiphoton ionization spectroscopy to obtain experimental values for the S₁ excitation of trans and cis BP, finding values of 31,111 cm⁻¹ for trans BP and 31203 cm⁻¹ for cis BP.⁴⁹ The calculations performed for this thesis using the aug-cc-pVDZ basis set are in very good agreement with these values for both trans, 31073 cm⁻¹ for ADC2 and 31162 cm⁻¹ for CC2, and cis BP, 31154 cm⁻¹ for ADC2 and 31209 cm⁻¹ for CC2. Comparatively, the calculations performed using the unagumented cc-pVTZ basis set have all overestimated the experimental energy results by ~1000 cm⁻¹. As such, only the aug-cc-pVDZ basis set will be used for calculations on substituted BP and thiophene oligomers in the subsequent chapters of this thesis.

3.4 Conclusion

Calculations performed on unsubstituted cis and trans BP using both the CC2 and ADC(2) methods with the aug-cc-pVDZ basis set have produced results for the adiabatic excitation energy that are in very good agreement with the experimental resonance-enhanced multiphoton ionization spectroscopy results of Chadwick and Kohler. All subsequent calculations in this thesis shall therefore be conducted using this basis set.

The CC2 and ADC(2) methods have produced results for the bond lengths that are generally in good agreement with each other, with the primary differences, although still small, being in the S-C bond lengths. However, the results for the changes in the bond lengths on excitation are in very good agreement with each other, differing by only 0.001Å for all bonds in both trans and

cis with the exception of the S-C2 bond of trans, which differs by 0.002Å, and as such both methods shall continue to be used.

4 Chapter 4

4.1 Introduction

The aim of this chapter is to obtain results for the changes in geometry on excitation, as well as values for the adiabatic excitation energy, of substituted trans- and cis-2,2'-bithiophene, and to compare the geometries, change in geometries and excitation energies to the values obtained in the previous chapter for unsubstituted trans- and cis-2,2'-bithiophene.

4.2 Selection of Substituted Groups and Substitution Positions

The following groups were selected as substituents; OH, formyl, nitro, nitroso, OC(H)O, OC(CH₃)O, phenyl and dimethylamino in the expectation that they would cause a variety of electronic and steric effects that would alter the excitation energy of the BP by affecting the conjugation of the molecule. The structures of these groups are shown below in figure 4.1. Atoms have been labelled according to the convention that will be used in the tables and discussion in the following section.

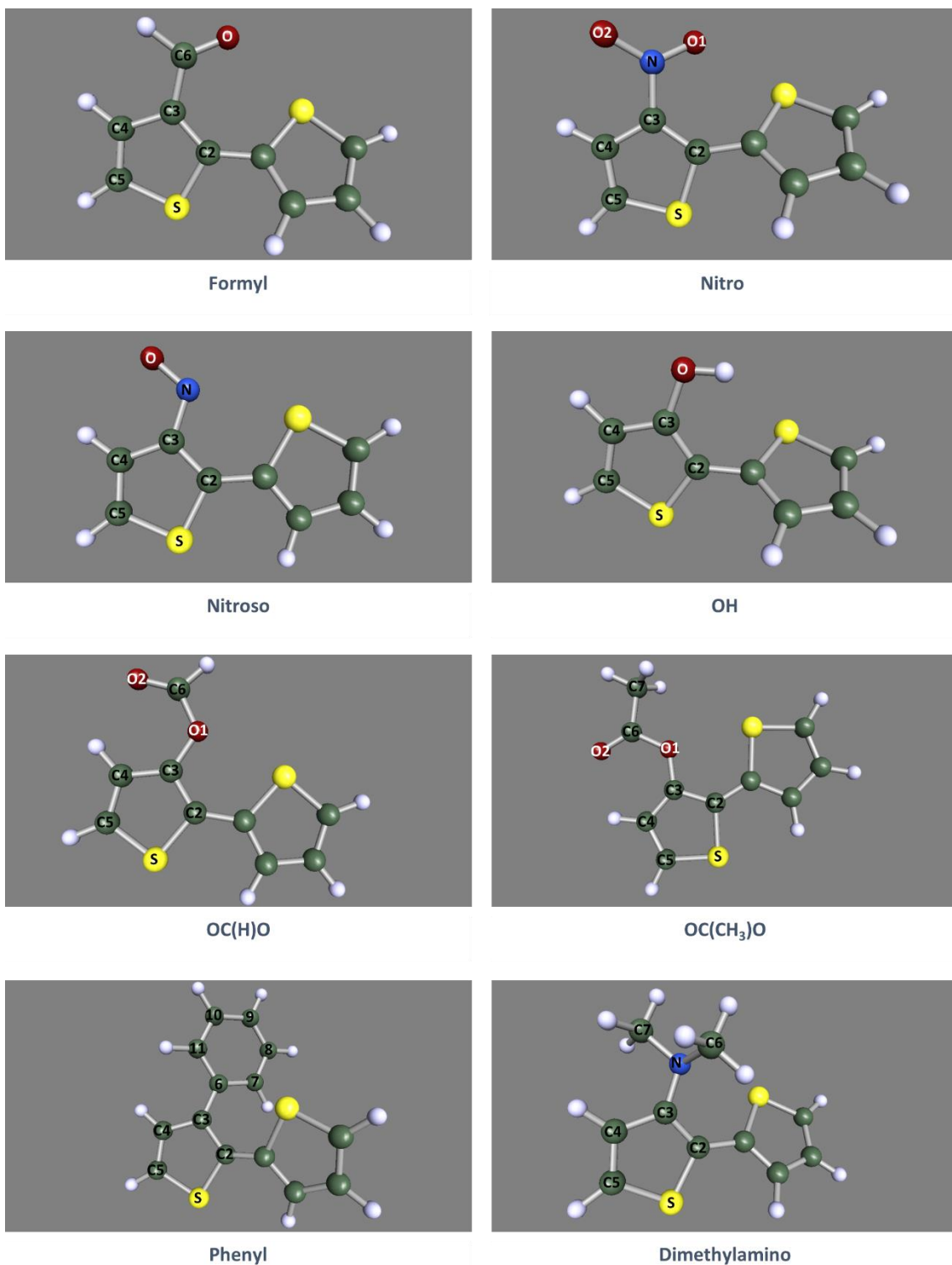


Figure 4.1 Structures of the selected substituents using 3 substituted trans-2,2'-bithiophene as an example

The substituents were chosen to provide a range of both electron withdrawing and electron donating groups, that were also of varying sizes. Dimethylamino groups would be expected to cause a large decrease in the excitation energy due to being strongly electron donating in nature,

however the size of the substituent could result in the molecule being bent further away from the preferred dihedral angle, causing a disruption in the conjugated system and therefore reducing the magnitude of this decrease. The two different types of acyloxy groups, OC(H)O and OC(CH₃)O, would both be expected to cause a reduction in the excitation energy, however the increased size of the substituent with the methyl group could cause a reduction in the magnitude of this decrease. OH groups are strongly donating in addition to being relatively small substituents, having basically no negative steric impact on the dihedral angle of the molecule, and so were expected to cause the greatest decrease in the excitation energy. Phenyl groups are weak electron donors, so their electronic effects could be expected to only cause a slight decrease in the excitation energy, however their large steric bulk could cause a significant impact on the dihedral angle of the molecule, especially depending on the position of the substituent, and so could instead cause a slight increase in the excitation energy.

Nitro groups have strong electron withdrawing effects and so a large increase in the excitation energy could be expected. Formyl groups have moderate electron withdrawing effects and so could be expected to cause a similarly moderate increase in the excitation energy. Nitroso groups are only weakly electron withdrawing, but are also relatively small substituents, and so could be expected to cause only a small increase in the excitation energy.

Substitutions were made singly at the C3 and C4 positions, and doubly at the C3/C3', C4/C4' and C3/C4' positions, as illustrated below in figure 4.2, using OH substituted trans-2,2'-bithiophene as the example. These will be referred to as 3 substituted, 3,3' substituted, 4' substituted, 4,4' substituted and 3,4' substituted in figures and in text.

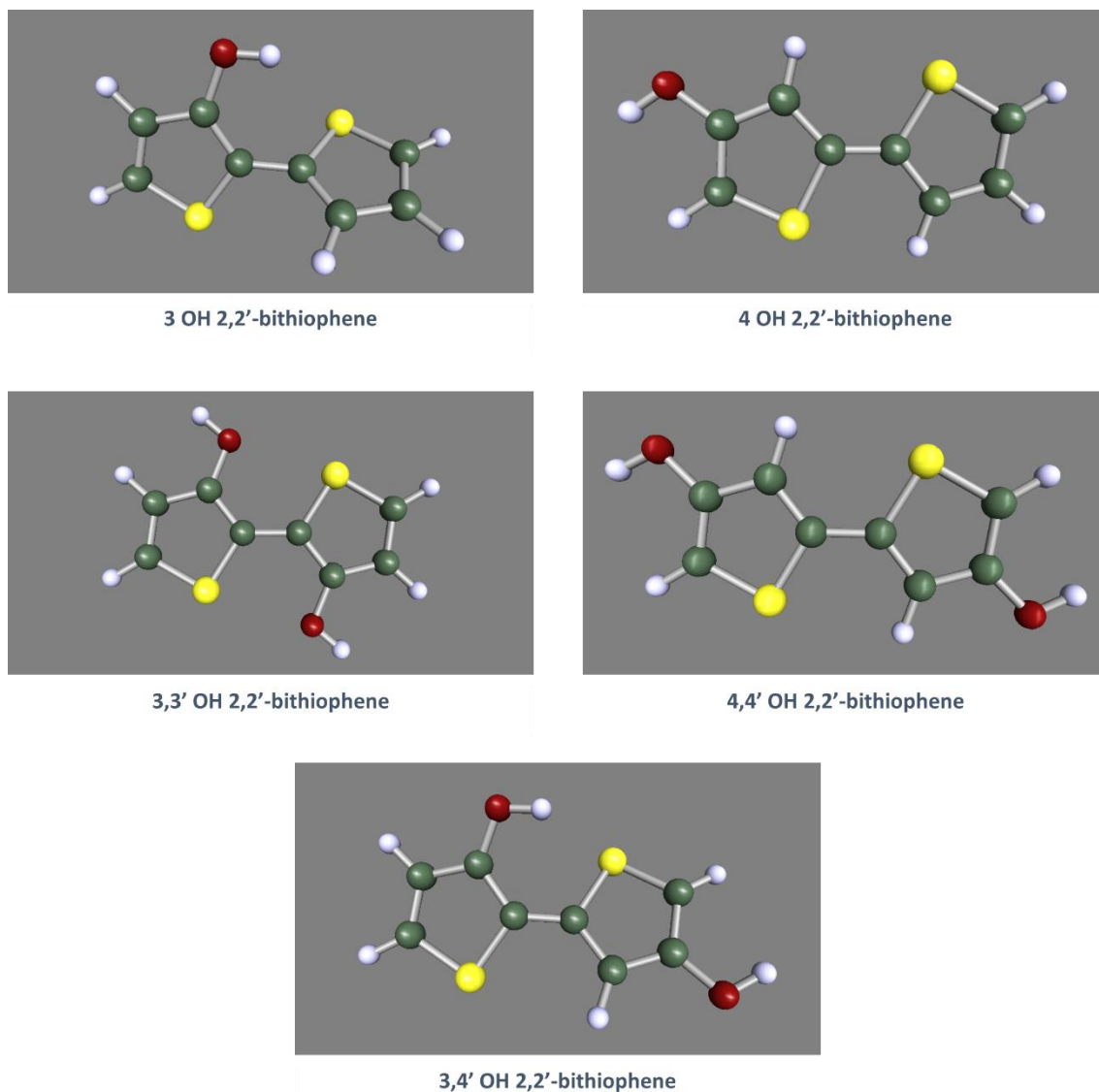


Figure 4.2 Diagram of substitution locations

4.3 Computational Methods

As with the calculations performed in Chapter 3 on unsubstituted BP, ground and excited state geometry optimisations were performing using TURBOMOLE 6.4. Ground state geometries were obtained at the MP2/aug-cc-pVDZ and CC2/aug-cc-pVDZ levels, and excited state geometries for the first singlet excited state were obtained at the CC2/aug-cc-pVDZ and ADC(2)/aug-cc-pVDZ levels, again using the *ricc2* module and an SMP parallelization scheme. The results of these calculations were visualised using the same software as in Chapter 3.

4.4 Substituted trans 2,2'-bithiophene Results and Discussion

The calculations involving the formyl, nitro and nitroso substituents all produced high values for the D1 diagnostic, indicating that 2,2'-bithiophene substituted with these groups has pronounced multi-reference ground state character and therefore MP2 and CC2 were inadequate to describe the ground state of the system correctly.⁵⁰ As such these methods cannot be expected to yield reasonable results for geometries and have been discounted.³³ The excited state geometry optimisations using these methods also involve performing a ground state geometry optimisation, meaning that these calculations also cannot be considered accurate.

4.4.1 OH substituted trans-2,2'-bithiophene

Selected bond lengths within the thiophene rings, and the C2-S-S'-C2' dihedral angle, of the ground state geometries of OH substituted trans BP, calculated at the MP2/aug-cc-pVDZ and CC2/aug-cc-pVDZ levels, are shown in tables 4.1 and 4.2. The first row of each table displays the bond lengths and dihedral angle of the unsubstituted trans BP ground state geometry, obtained at the respective levels in Chapter 3.

Table 4.1 Selected bond lengths and dihedral angle of the OH substituted BP ground state geometry at the MP2 level

Sub. pos.	Bond length / Å											C2-S-S'-C2' angle / °
	C2-C2'	C2-C3	C3-C4	C4-C5	C5-S	S-C2	C2'-C3'	C3'-C4'	C4'-C5'	C5'-S'	S'-C2'	
-	1.454	1.398	1.421	1.392	1.729	1.741	1.398	1.421	1.392	1.729	1.741	147.3
3	1.454	1.4	1.421	1.389	1.729	1.741	1.398	1.421	1.392	1.728	1.749	128.2
4	1.452	1.395	1.42	1.391	1.733	1.743	1.399	1.421	1.391	1.73	1.742	179.9
3,3'	1.446	1.402	1.418	1.39	1.726	1.75	1.402	1.418	1.39	1.726	1.75	180
4,4'	1.451	1.396	1.419	1.391	1.733	1.743	1.396	1.419	1.391	1.733	1.743	180

Table 4.2 Selected bond lengths and dihedral angle of the OH substituted BP ground state geometry at the CC2 level

Sub. pos.	Bond length /Å											C2-S-S'-C2' angle /°
	C2-C2'	C2-C3	C3-C4	C4-C5	C5-S	S-C2	C2'-C3'	C3'-C4'	C4'-C5'	C5'-S'	S'-C2'	
-	1.454	1.398	1.425	1.391	1.736	1.748	1.398	1.425	1.391	1.736	1.748	148.6
3	1.453	1.4	1.425	1.389	1.735	1.749	1.397	1.425	1.391	1.735	1.757	130.8
4	1.452	1.395	1.423	1.391	1.74	1.75	1.398	1.424	1.391	1.736	1.749	179.9
3,3'	1.446	1.401	1.423	1.39	1.734	1.757	1.401	1.423	1.39	1.734	1.757	180
3,4'	1.451	1.401	1.425	1.388	1.735	1.749	1.393	1.425	1.392	1.739	1.758	133.6

There have been no significant changes in any of the bond lengths of the ground state geometry upon the addition of an OH substituent, regardless of the substitution being made singly to one thiophene ring or doubly to both rings, and regardless of the location of the substitution. There have however been more significant changes in the dihedral angles; the dihedral angles of the 4 OH BP, 3,3' OH BP and 4,4' OH BP ground state geometries have all increased to become totally planar. Conversely, the ground state dihedral angle of 3 OH BP has decreased by $\sim 20^\circ$, and that of 3,4' OH BP by 15° , both becoming less planar compared to the unsubstituted ground state geometry.

Selected bond lengths and the C2-S-S'-C2' dihedral angle of the excited state geometries of OH substituted trans BP at the ADC(2)/aug-cc-pVDZ and CC2/aug-cc-pVDZ levels are shown in tables 4.3 and 4.4. As with the tables concerning the ground state geometries, the first row of each table includes bond lengths and the dihedral angle of the unsubstituted trans BP excited state geometry obtained at the respective level.

Table 4.3 Selected bond lengths and dihedral angle of the OH substituted BP excited state geometry at the ADC(2) level

Sub. pos.	Bond length / Å											C2-S-S'-C2' angle / °
	C2-C2'	C2-C3	C3-C4	C4-C5	C5-S	S-C2	C2'-C3'	C3'-C4'	C4'-C5'	C5'-S'	S'-C2'	
-	1.384	1.446	1.396	1.418	1.731	1.788	1.446	1.396	1.418	1.731	1.788	180
C3	1.388	1.463	1.396	1.411	1.751	1.779	1.447	1.396	1.412	1.746	1.79	159
C4	1.385	1.441	1.403	1.407	1.737	1.774	1.431	1.405	1.429	1.726	1.831	180
C3,C3'	1.393	1.447	1.4	1.41	1.746	1.783	1.447	1.4	1.41	1.746	1.783	155.4
C4,C4'	1.386	1.433	1.403	1.419	1.732	1.8	1.433	1.403	1.419	1.732	1.8	180

Table 4.4 Selected bond lengths and dihedral angle of the OH substituted BP excited state geometry at the CC2 level

Sub. pos.	Bond length / Å											C2-S-S'-C2' angle / °
	C2-C2'	C2-C3	C3-C4	C4-C5	C5-S	S-C2	C2'-C3'	C3'-C4'	C4'-C5'	C5'-S'	S'-C2'	
-	1.385	1.445	1.399	1.418	1.737	1.793	1.445	1.399	1.418	1.737	1.793	180
C3	1.394	1.458	1.405	1.404	1.761	1.778	1.441	1.399	1.415	1.749	1.802	153.5
C4	1.387	1.441	1.405	1.408	1.745	1.779	1.429	1.409	1.428	1.728	1.83	180
C3,C3'	1.394	1.446	1.404	1.408	1.75	1.788	1.446	1.404	1.408	1.75	1.788	154.1
C3,C4'	1.39	1.45	1.405	1.404	1.752	1.78	1.440	1.4	1.429	1.742	1.825	155.4

In comparison to the ground state geometries there are more noticeable changes in the bond lengths of the excited state geometries after substitution. Compared to the unsubstituted excited state, in 3 OH BP the C2-C3 bond has increased by 0.015 Å and the C5-S bond by ~0.02 Å, the S-C2 bond has decreased by ~0.01 Å and the C5'-S' has increased by ~0.015 Å. 4 OH BP has experienced only one small change in the substituted ring, C4-C5 has decreased by 0.01 Å, but has experienced more changes in the unsubstituted ring; C2'-C3' has decreased by ~0.015 Å, C3'-

C4' and C4'-C5' have both increased, and C5'-S' has decreased, by $\sim 0.01\text{\AA}$, and C2'-S' has increased by $\sim 0.04\text{\AA}$.

In 3,3' OH BP both thiophene rings have experienced the same changes; C4-C5 has decreased by $\sim 0.01\text{\AA}$ and C5-S has increased by $\sim 0.015\text{\AA}$. In 4,4' OH BP both thiophene rings also experience the same changes, with the only noticeable difference from the unsubstituted excited state being an increase of $\sim 0.15\text{\AA}$ for C5-S.

Finally, for 3,4' OH BP, C4-C5 has decreased $\sim 0.015\text{\AA}$ and C5-S has increased by $\sim 0.015\text{\AA}$. The bond lengths in this ring resembles those in one of the C3, C3' substituted rings. And C4'-C5' increased by $\sim 0.01\text{\AA}$ and S-C2 by $\sim 0.03\text{\AA}$.

In common with the ground state geometries, there have been more significant changes when it comes to the dihedral angles. Whilst the 4 OH BP and 4,4' OH BP excited state geometries have remained completely planar like that of unsubstituted BP, the dihedral angles of the other three substituted BPs have all decreased by $\sim 25^\circ$.

The changes of the bond lengths and dihedral angle on excitation are displayed in tables 4.5 and 4.6. As was the case with unsubstituted BP in Chapter 3, ground state geometries calculated at the MP2 level are compared to the excited state geometries obtained at the ADC(2) level.

Table 4.5 Changes in selected bond lengths and dihedral angle of OH substituted BP on excitation at the ADC(2) level

Sub. pos.	Bond length change / \AA											C2-S-S'-C2' angle change / $^\circ$
	C2-C2'	C2-C3	C3-C4	C4-C5	C5-S	S-C2	C2'-C3'	C3'-C4'	C4'-C5'	C5'-S'	S'-C2'	
-	-0.07	0.048	-0.025	0.026	0.002	0.047	0.048	-0.025	0.026	0.002	0.047	32.7
C3	-0.066	0.063	-0.025	0.022	0.022	0.038	0.049	-0.025	0.02	0.018	0.041	30.8
C4	-0.067	0.046	-0.017	0.016	0.004	0.031	0.032	-0.016	0.038	-0.004	0.089	0.1
C3,C3'	-0.053	0.045	-0.018	0.02	0.02	0.033	0.045	-0.018	0.02	0.02	0.033	-24.6
C4,C4'	-0.065	0.037	-0.016	0.028	-0.001	0.057	0.037	-0.016	0.028	-0.001	0.057	0

Table 4.6 Changes in selected bond lengths and dihedral angle of OH substituted BP on excitation at the CC2 level

Sub. pos.	Bond length change /Å											C2-S-S'-C2' angle change /°
	C2-C2'	C2-C3	C3-C4	C4-C5	C5-S	S-C2	C2'-C3'	C3'-C4'	C4'-C5'	C5'-S'	S'-C2'	
-	-0.069	0.047	-0.026	0.027	0.001	0.045	0.047	-0.026	0.027	0.001	0.045	31.4
C3	-0.059	0.058	-0.02	0.015	0.026	0.029	0.044	-0.026	0.024	0.014	0.045	22.7
C4	-0.065	0.046	-0.018	0.017	0.005	0.029	0.031	-0.015	0.037	-0.008	0.081	0.1
C3,C3'	-0.052	0.045	-0.019	0.018	0.016	0.031	0.045	-0.019	0.018	0.016	0.031	-25.9
C3,C4'	-0.061	0.049	-0.02	0.016	0.017	0.031	0.047	-0.025	0.037	0.003	0.067	21.8

Table 4.7 shows the changes on excitation of the bond lengths of the OH substituents, and the ground and excited state dihedral angles of the substituent relative to the thiophene ring it is substituted on to, at the different substitution locations.

Table 4.7 Changes in selected bond lengths and dihedral angles of OH substituents on excitation

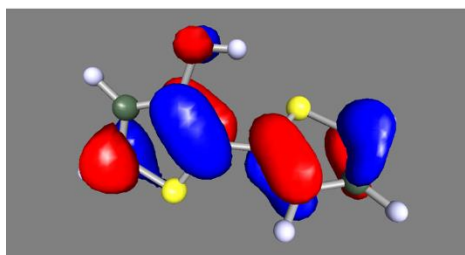
Sub. pos.	Method	Bond length change/Å		C2-C3-O-H angle /°			Bond length change/Å		C2'-C3'-O'-H' angle /°		
		C3-O	O-H	GS	EX	Dif	C3'-O	O-H	GS	EX	Dif
3	ADC(2)	-0.024	0.011	1.7	2.5	0.8					
	CC2	-0.024	0.016	1.1	6	4.9					
3,3'	ADC(2)	-0.018	0.004	180	179.1	-0.9	-0.018	0.004	180	179.1	-0.9
	CC2	-0.017	0.006	180	178.8	-1.2	-0.017	0.006	180	178.8	-1.2
Sub. pos.	Method	Bond length change/Å		C3-C4-O-H angle /°			Bond length change/Å		C3'-C4'-O'-H' angle /°		
		C4-O	O-H	GS	EX	Dif	C4'-O	O-H	GS	EX	Dif
4	ADC(2)	-0.027	0.003	180	180	0					
	CC2	-0.022	0.003	180	180	0					
4,4'	ADC(2)	-0.014	0.002	180	180	0	-0.014	0.002	180	180	0
3,4'	CC2	-0.015	0.012	0.9	2.5	1.6	-0.016	0.002	179.6	175.8	-3.8

In each case the C-O bond at the substitution location undergoes a decrease in length on excitation and the O-H bond remains basically unchanged, except for the case of 3 OH BP where it experiences an increase in length. In all cases, the dihedral angle used to measure the planarity of the substituent relative to the thiophene ring it is attached to remains close to completely

planar; $\sim 0^\circ$ in the case of 3 OH BP and the C3 substituted OH in 3,4' OH BP, meaning that the hydrogen is pointing towards the sulphur of the opposite thiophene ring, and $\sim 180^\circ$ in all other examples, meaning that the hydrogen is pointing away from the sulphur of the opposite thiophene ring.

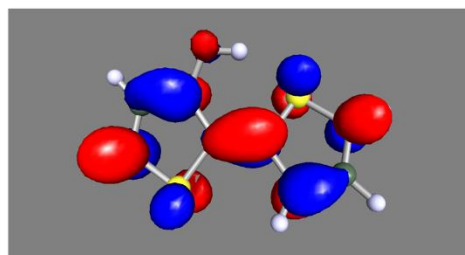
The MOs of OH substituted trans BP involved in the ground state to S_1 excitation are shown in below in figure 4.3. The percentage that this transition contributed to the overall excitation displayed, for this figure and all subsequent figures detailing MOs in this chapter, is from the ADC(2)/aug-cc-pVDZ calculation, as this level has the most calculations complete successfully. In the case where an ADC(2)/aug-cc-pVDZ calculation was not successful, the percentage from the CC2/aug-cc-pVDZ calculation is displayed instead. Complete breakdowns of the contributors to the excitations of all substituents and substitution positions are shown in appendix 7.4 as tables 7.3-7.8.

3 OH 2,2'-bithiophene



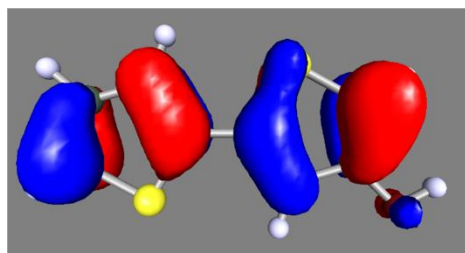
HOMO

84.5%



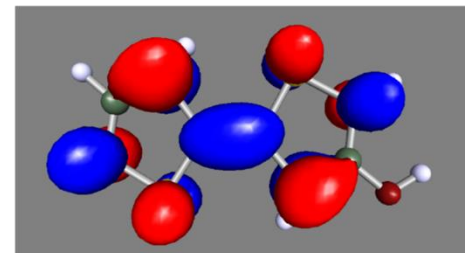
LUMO +2

4 OH 2,2'-bithiophene



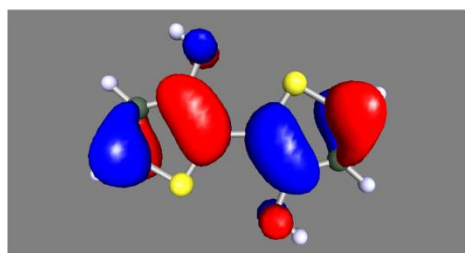
HOMO

85%



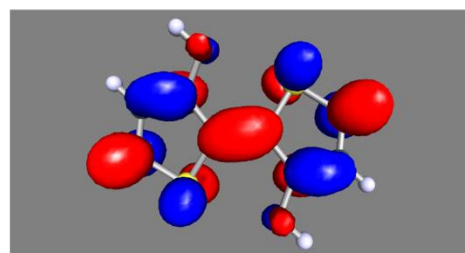
LUMO +2

3,3' OH 2,2'-bithiophene



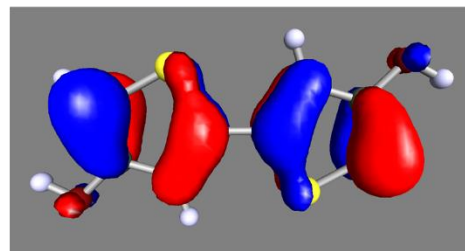
HOMO

79.2%



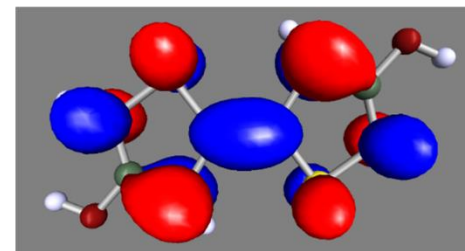
LUMO +5

4,4' OH 2,2'-bithiophene



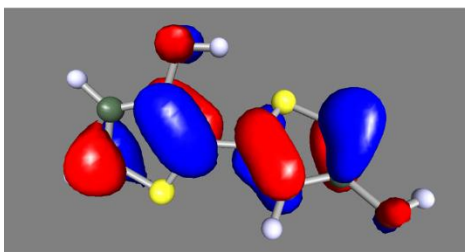
HOMO

88.2%



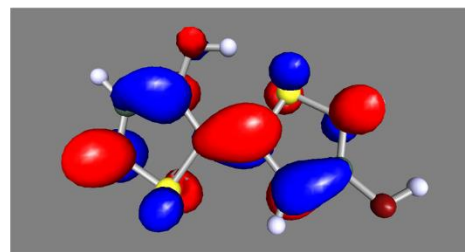
LUMO +2

3,4' OH 2,2'-bithiophene



HOMO

75.4%



LUMO +2

Figure 4.3 MOs involved in S_1 excitation of OH substituted *trans* 2,2'-bithiophene

The above can all be assigned as π to π^* transitions similarly to unsubstituted trans BP. Adiabatic excitation energies were calculated using the ground and excited state geometries and are presented in table 4.8.

Table 4.8 Adiabatic Excitation energies of OH substituted trans 2,2'-bithiophene

Substitution position	Method	Adiabatic excitation energy		Difference from unsubstituted	
		/eV	/cm ⁻¹	/eV	/cm ⁻¹
3	ADC(2)	3.8750	31254	0.02240	180.63
	CC2	3.8977	31437	0.03414	275.39
4	ADC(2)	3.5992	29030	-0.25341	-2043.9
	CC2	3.6625	29540	-0.20110	-1622
3,3'	ADC(2)	3.8488	31043	-0.00382	-30.84
	CC2	3.8760	31262	0.01245	100.41
4,4'	ADC(2)	3.5155	28354	-0.33710	-2718.9
3,4'	CC2	3.7732	30433	-0.09035	-728.70

4,4' OH BP has experienced the greatest decrease in excitation energy relative to unsubstituted trans BP, followed closely by 4 OH BP. Both have planar ground state geometries which could lead to increased conjugation and therefore reduce the excitation energy. 3 OH BP and 3,3' OH BP both experienced increases in excitation energy relative to unsubstituted BP (or very minor decrease), however only the 3 OH BP ground state geometry had a dihedral angle that was less planar than unsubstituted BP, as the 3,3' OH BP ground state geometry was totally similarly to 4 OH BP and 4,4' OH BP. There is no hydrogen bonding between hydroxy H and the S of the adjacent thiophene ring for 3 OH, as the OH group is angled away from the other thiophene ring.

4.4.2 OC(H)O Substituted trans-2,2'-bithiophene

Selected bond lengths and the C2-S-S'-C2' dihedral angle of the ground state geometries of OC(H)O substituted trans BP are shown in tables 4.9 and 4.10.

Table 4.9 Selected bond lengths and dihedral angle of the OC(H)O substituted BP ground state geometry at the MP2 level

Sub. pos.	Bond length /Å											C2-S-S'-C2' angle /°
	C2-C2'	C2-C3	C3-C4	C4-C5	C5-S	S-C2	C2'-C3'	C3'-C4'	C4'-C5'	C5'-S'	S'-C2'	
-	1.454	1.398	1.421	1.392	1.729	1.741	1.398	1.421	1.392	1.729	1.741	147.3
C3	1.45	1.402	1.424	1.388	1.728	1.74	1.402	1.418	1.392	1.727	1.747	180
C4	1.452	1.398	1.422	1.391	1.724	1.741	1.399	1.421	1.391	1.729	1.742	180
C3,C3'	1.446	1.398	1.414	1.389	1.73	1.742	1.398	1.414	1.389	1.73	1.742	152.1
C4,C4'	1.452	1.395	1.417	1.388	1.726	1.742	1.396	1.417	1.392	1.727	1.743	145.5
C3,C4'	1.451	1.397	1.416	1.39	1.729	1.736	1.395	1.416	1.391	1.727	1.743	135.7

Table 4.10 Selected bond lengths and dihedral angle of the OC(H)O substituted BP ground state geometry at the CC2 level

Sub. pos.	Bond length /Å											C2-S-S'-C2' angle /°
	C2-C2'	C2-C3	C3-C4	C4-C5	C5-S	S-C2	C2'-C3'	C3'-C4'	C4'-C5'	C5'-S'	S'-C2'	
-	1.454	1.398	1.425	1.391	1.736	1.748	1.398	1.425	1.391	1.736	1.748	148.6
C3	1.45	1.401	1.428	1.388	1.736	1.747	1.401	1.422	1.391	1.735	1.754	180
C4	1.452	1.398	1.426	1.39	1.731	1.749	1.398	1.424	1.391	1.736	1.749	180
C3,C3'	1.445	1.396	1.419	1.388	1.738	1.749	1.396	1.419	1.388	1.738	1.749	151.5
C4,C4'	1.452	1.395	1.421	1.387	1.733	1.75	1.395	1.421	1.391	1.734	1.751	146.6
C3,C4'	1.45	1.395	1.42	1.39	1.736	1.744	1.394	1.42	1.391	1.734	1.751	136.6

As with OH substituted trans BP there has been no significant changes to the ground state geometry, in terms of bond lengths, on substitution, regardless of substitution position, but there have been some more significant changes in the C2-S-S'-C2' dihedral angle. Both 3 and 4 OC(H)O BP have completely planar ground state geometries, whilst the dihedral angles of 3,3' and 4,4' OC(H)O BP have remained largely unchanged relative to the unsubstituted ground state geometry, only experiencing a change of ~2-3°. The dihedral angle of 3,4' OC(H)O BP has

decreased by $\sim 12^\circ$ to become less planar, an almost identical change to that of the 3,4' OH BP ground state.

Selected bond lengths and the C2-S-S'-C2' dihedral angle of the excited state geometries of OC(H)O substituted trans BP are shown in tables 4.11 and 4.12.

Table 4.11 Selected bond lengths and dihedral angle of the OC(H)O substituted BP excited state geometry at the ADC(2) level

Sub. pos.	Bond length /Å											C2-S-S'-C2' angle /°
	C2-C2'	C2-C3	C3-C4	C4-C5	C5-S	S-C2	C2'-C3'	C3'-C4'	C4'-C5'	C5'-S'	S'-C2'	
-	1.384	1.446	1.396	1.418	1.731	1.788	1.446	1.396	1.418	1.731	1.788	180
C3	1.385	1.453	1.396	1.418	1.731	1.787	1.453	1.396	1.412	1.738	1.781	180
C4	1.385	1.441	1.4	1.422	1.724	1.803	1.444	1.398	1.413	1.733	1.779	180
C3,C3'	1.386	1.453	1.4	1.408	1.735	1.783	1.453	1.4	1.408	1.735	1.783	154.2
C4,C4'	1.385	1.438	1.402	1.416	1.724	1.786	1.439	1.407	1.415	1.726	1.801	176.9
C3,C4'	1.382	1.454	1.396	1.417	1.728	1.786	1.450	1.391	1.416	1.737	1.795	176.8

Table 4.12 Selected bond lengths and dihedral angle of the OC(H)O substituted BP excited state geometry at the CC2 level

Sub. pos.	Bond length /Å											C2-S-S'-C2' angle /°
	C2-C2'	C2-C3	C3-C4	C4-C5	C5-S	S-C2	C2'-C3'	C3'-C4'	C4'-C5'	C5'-S'	S'-C2'	
-	1.385	1.445	1.399	1.418	1.737	1.793	1.445	1.399	1.418	1.737	1.793	180
C3	1.387	1.451	1.4	1.417	1.739	1.791	1.451	1.399	1.413	1.743	1.788	180
C4	1.386	1.439	1.404	1.422	1.728	1.807	1.444	1.402	1.413	1.74	1.785	180
C3,C3'	1.387	1.45	1.404	1.409	1.743	1.789	1.45	1.404	1.409	1.743	1.789	153.9
C4,C4'	1.386	1.437	1.405	1.417	1.73	1.795	1.438	1.408	1.415	1.732	1.803	176.2
C3,C4'	1.386	1.445	1.404	1.411	1.74	1.783	1.443	1.409	1.416	1.733	1.811	168.1

There are fewer notable changes in the bond lengths of the excited state geometries than for OH substituted BP. In 4 OC(H)O BP C5-S and S-C2 have decrease and increased by ~ 0.01 angstroms respectively, and in 4,4' OC(H)O BP S'-C2' in has increased by ~ 0.01 angstroms. In 3,4' OC(H)O BP C3'-C4' increases by ~ 0.01 angstroms and S'-C2' by ~ 0.02 angstroms relative to the unsubstituted excited state geometry. As with the ground state, the changes in the dihedral angle are more significant than those of the bond lengths, although not to such a degree as

when compared to OH substituted BP. The dihedral angles of the 3 and 4 OC(H)O BP excited state geometries remain unchanged at completely planar, and 4,4' OC(H)O BP has only experienced a very slight decrease of $\sim 3\text{-}4^\circ$ compared to the unsubstituted excited state geometry. The dihedral angle of 3,3' OC(H)O BP has decreased by $\sim 25^\circ$ and 3,4' OC(H)O BP by $\sim 10^\circ$.

The changes of the bond lengths and dihedral angle on excitation are displayed in tables 4.13 and 4.14.

Table 4.13 Changes in selected bond lengths and dihedral angle of OC(H)O substituted BP on excitation at the ADC(2) level

Sub. pos.	Bond length change / Å											C2-S-S'-C2' angle change / °
	C2-C2'	C2-C3	C3-C4	C4-C5	C5-S	S-C2	C2'-C3'	C3'-C4'	C4'-C5'	C5'-S'	S'-C2'	
-	-0.07	0.048	-0.025	0.026	0.002	0.047	0.048	-0.025	0.026	0.002	0.047	32.7
C3	-0.065	0.051	-0.028	0.03	0.003	0.047	0.051	-0.022	0.02	0.011	0.034	0
C4	-0.067	0.043	-0.022	0.031	0	0.062	0.045	-0.023	0.022	0.004	0.037	0
C3,C3'	-0.06	0.055	-0.014	0.019	0.005	0.041	0.055	-0.014	0.019	0.005	0.041	2.1
C4,C4'	-0.067	0.043	-0.015	0.028	-0.002	0.044	0.043	-0.01	0.023	-0.001	0.058	31.4
C3,C4'	-0.069	0.057	-0.02	0.027	-0.001	0.05	0.055	-0.025	0.025	0.01	0.052	41.1

Table 4.14 Changes in selected bond lengths and dihedral angle of OC(H)O substituted BP on excitation at the CC2 level

Sub. pos.	Bond length change / Å											C2-S-S'-C2' angle change / °
	C2-C2'	C2-C3	C3-C4	C4-C5	C5-S	S-C2	C2'-C3'	C3'-C4'	C4'-C5'	C5'-S'	S'-C2'	
-	-0.069	0.047	-0.026	0.027	0.001	0.045	0.047	-0.026	0.027	0.001	0.045	31.4
C3	-0.063	0.05	-0.028	0.029	0.003	0.044	0.05	-0.023	0.022	0.008	0.034	0
C4	-0.066	0.041	-0.022	0.032	-0.003	0.058	0.046	-0.022	0.022	0.004	0.036	0
C3,C3'	-0.058	0.054	-0.015	0.021	0.005	0.04	0.054	-0.015	0.021	0.005	0.04	2.4
C4,C4'	-0.066	0.042	-0.016	0.03	-0.003	0.045	0.043	-0.013	0.024	-0.002	0.052	29.6
C3,C4'	-0.064	0.05	-0.016	0.021	0.004	0.039	0.049	-0.011	0.025	-0.001	0.06	31.5

Table 4.15 shows the changes on excitation of the bond lengths and the dihedral angle of the OC(H)O substituents at the different substitution locations.

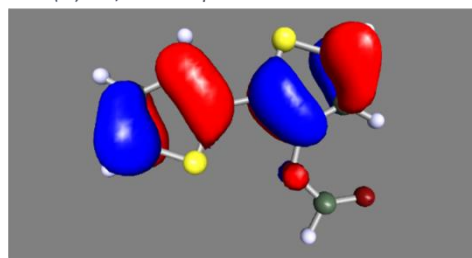
Table 4.15 Changes in selected bond lengths and dihedral angles of OC(H)O substituents on excitation

Sub. pos.	Method	Bond length change/Å			C2-C3-O1-C6 /°			Bond length change/Å			C2'-C3'-O1'-C6' /°		
		C4-O	O1-C6	C6-O2	GS	EX	Dif	C3'-O	O1-C6'	C6'-O2'	GS	EX	Dif
3	ADC(2)	-0.017	0.009	0.001	179.9	180	0.1						
	CC2	-0.016	0.01	0.002	179.9	180	0.1						
3,3'	ADC(2)	-0.012	0.002	-0.002	78.6	171.8	93.2	-0.017	-0.007	0.006	78.6	171.8	93.2
	CC2	-0.016	-0.006	0.007	75.2	170.1	94.9	-0.016	-0.006	0.007	75.2	170.1	94.9
Sub. pos.	Method	Bond length change/Å			C3-C4-O1-C6 /°			Bond length change/Å			C3'-C4'-O1'-C6' /°		
		C4-O	O1-C6	C6-O2	GS	EX	Dif	C4'-O	O1-C6'	C6'-O2'	GS	EX	Dif
4	ADC(2)	-0.016	0.016	-0.005	180	180	0						
	CC2	-0.014	0.015	-0.004	180	180	0						
4,4'	ADC(2)	-0.012	0.002	-0.002	127.5	179.8	52.3	-0.019	0.012	-0.002	62.6	156.6	94
	CC2	-0.014	0.005	-0.002	129.1	180	50.9	-0.015	0.009	-0.001	61.4	149	87.6
Sub. pos.	Method	Bond length change/Å			C2-C3-O1-C6 /°			Bond length change/Å			C3'-C4'-O1'-C6' /°		
		C3-O	O1-C6	C6-O2	GS	EX	Dif	C4'-O	O1-C6'	C6'-O2'	GS	EX	Dif
3,4'	ADC(2)	-0.02	0	0.003	63.8	179.9	116.1	-0.009	0.004	-0.001	113.3	123.2	9.9
	CC2	-0.014	-0.003	0.002	62.2	176.2	114	-0.021	0.014	-0.002	114.5	24.3	-90.2

In 3 and 4 OC(H)O BP the substituents experienced effectively no change in planarity on excitation, both remaining totally planar relative to the thiophene ring they are attached to. 3,3', 4,4' and 3,4' OC(H)O BP however all experience significantly changes in the planarity of the substituents relative to their respective thiophene rings; in 3,3' substituted BP the substituents both begin close to perpendicular relative to their thiophene rings and experience a large increase in the dihedral angle to become close to completely planar. In 4,4' and 3,4' OC(H)O BP both substituted groups being ~50-60° out of plane from their respective thiophene rings in the ground state geometry and increase to become close to totally planar on excitation.

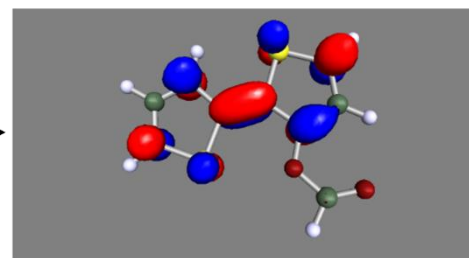
The MOs of OC(H)O BP involved in the ground state to S₁ excitation are shown below in Figure 4.4.

3 OC(H)O 2,2'-bithiophene



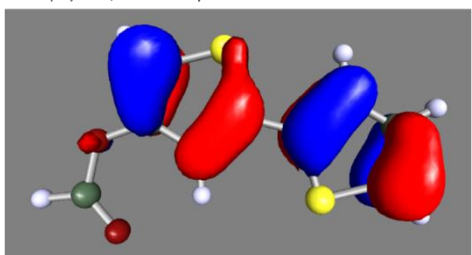
HOMO

93.7%



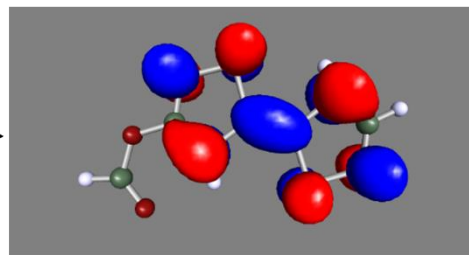
LUMO +2

4 OC(H)O 2,2'-bithiophene



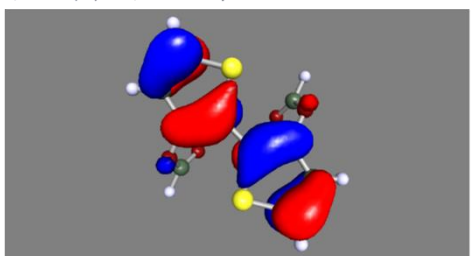
HOMO

90.8%



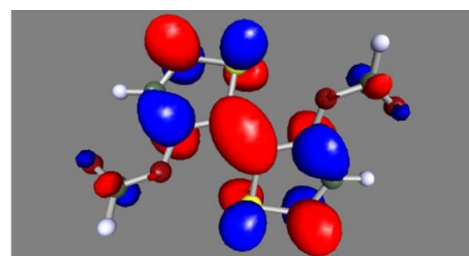
LUMO +1

3,3' OC(H)O 2,2'-bithiophene



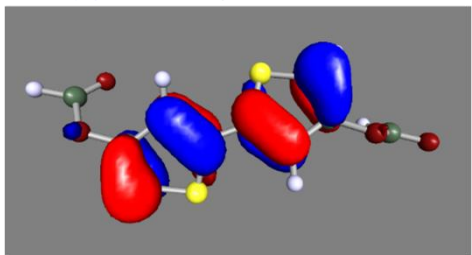
HOMO

90.5%



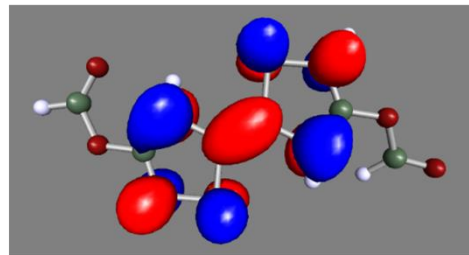
LUMO +2

4,4' OC(H)O 2,2'-bithiophene



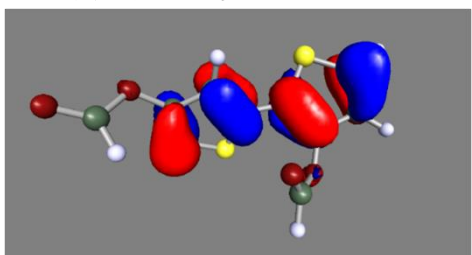
HOMO

89.6%



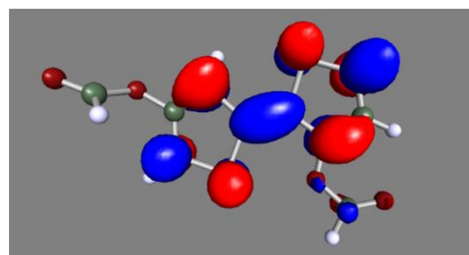
LUMO

3,4' OC(H)O 2,2'-bithiophene



HOMO

92.7%



LUMO

Figure 4.4 MOs involved in S_1 excitation of OC(H)O substituted *trans* 2,2'-bithiophene

As with OH substituted BP all can be assigned as π to π^* transitions. Note the change in planarity relative to the thiophene rings of the substituent groups of 3,3' and 4,4' OC(H)O BP, and of the C3 position substituent in 3,4' OC(H)O BP.

Adiabatic excitation energies were calculated from the ground and excited state geometries and are shown in table 4.16.

Table 4.16 Adiabatic Excitation energies of OC(H)O substituted *trans* 2,2'-bithiophene

Substitution position	Method	Adiabatic excitation energy		Difference to unsubstituted	
		/eV	/cm ⁻¹	/eV	/cm ⁻¹
3	ADC(2)	3.8385	30959	-0.01413	-113.97
	CC2	3.8551	31094	-0.00844	-68.07
4	ADC(2)	3.7249	30043	-0.12768	-1029.8
	CC2	3.7515	30257	-0.11214	-904.45
33	ADC(2)	3.9451	31819	0.09251	746.13
	CC2	3.9585	31927	0.09488	765.22
44	ADC(2)	3.6699	29600	-0.18266	-1473.3
	CC2	3.7058	29889	-0.15782	-1272.9
34	ADC(2)	3.8719	31229	0.01932	155.83
	CC2	3.8432	30997	-0.02040	-164.51

As with OH substituted BP, 4,4' and 4 OC(H)O BP experience the greatest decrease in the excitation energy relative to unsubstituted BP, although unlike OH substituted BP only 4 OC(H)O BP has a planar ground state, with 4,4' have a ground state dihedral angle almost identical to unsubstituted BP. The excitation energy of 3,3' OC(H)O BP experiences a relatively large increase, and while it does have a slightly more planar ground state than unsubstituted BP, this angle does not change significantly on excitation. The excitation energy of 3,3' OC(H)O BP is greater than that of unsubstituted BP.

4.4.3 OC(CH₃)O Substituted trans 2,2'-bithiophene

Selected bond lengths and the C2-S-S'-C2' dihedral angle of the ground state geometries of OC(H)O substituted trans BP are shown in tables 4.17 and 4.18.

Table 4.17 Selected bond lengths and dihedral angle of the OC(CH₃)O substituted BP ground state geometry at the MP2 level

Sub. pos.	Bond length /Å											C2-S-S'-C2' angle /°
	C2-C2'	C2-C3	C3-C4	C4-C5	C5-S	S-C2	C2'-C3'	C3'-C4'	C4'-C5'	C5'-S'	S'-C2'	
-	1.454	1.398	1.421	1.392	1.729	1.741	1.398	1.421	1.392	1.729	1.741	147.3
C3	1.45	1.397	1.416	1.39	1.731	1.737	1.398	1.421	1.391	1.729	1.743	140.9
C4	1.452	1.398	1.422	1.392	1.724	1.741	1.399	1.421	1.391	1.73	1.742	180
C3,C3'	1.444	1.399	1.414	1.388	1.73	1.745	1.399	1.414	1.388	1.73	1.745	180
C4,C4'	1.451	1.396	1.419	1.39	1.727	1.743	1.395	1.418	1.388	1.727	1.743	147
C3,C4'	1.452	1.397	1.416	1.391	1.73	1.734	1.393	1.417	1.391	1.727	1.744	128.3

Table 4.18 Selected bond lengths and dihedral angle of the OC(CH₃)O substituted BP ground state geometry at the CC2 level

Sub. pos.	Bond length /Å											C2-S-S'-C2' angle /°
	C2-C2'	C2-C3	C3-C4	C4-C5	C5-S	S-C2	C2'-C3'	C3'-C4'	C4'-C5'	C5'-S'	S'-C2'	
-	1.454	1.398	1.425	1.391	1.736	1.748	1.398	1.425	1.391	1.736	1.748	148.6
C3	1.449	1.396	1.42	1.39	1.738	1.744	1.397	1.424	1.391	1.736	1.751	141.8
C4,C4'	1.451	1.394	1.422	1.388	1.734	1.751	1.395	1.423	1.39	1.734	1.751	148

The bond lengths of the OC(CH₃)O substituted BP ground state geometries are almost identical to their OC(H)O substituted equivalents shown in tables 4.9 and 4.10, and consequently so are the bond length differences when compared to the unsubstituted ground state geometry. The dihedral angles are also nearly identical to their OC(H)O substituted equivalents for 4 and 4,4' OC(CH₃)O BP, however whilst the dihedral angle the 3 OC(H)O BP ground state geometry is completely planar, the dihedral angle of the 3 OC(CH₃)O substituted ground state geometry has only decreased slightly by ~7° compared to that of the unsubstituted ground state, and the dihedral angle of the 3,3' OC(CH₃)O BP ground state geometry is completely planar compared to ~150° for its OC(H)O substituted equivalent. The dihedral angle of the 3,4' OC(CH₃)O ground

state geometry has decreased by $\sim 20^\circ$ relative to the unsubstituted ground state geometry, a greater magnitude of decrease than its OC(H)O equivalent.

Selected bond lengths and the C2-S-S'-C2' dihedral angle of the excited state geometries of OC(CH₃)O substituted trans BP are shown in tables 4.19 and 4.20.

Table 4.19 Selected bond lengths and dihedral angle of the OC(CH₃)O substituted BP excited state geometry at the ADC(2) level

Sub. pos.	Bond length /Å											C2-S-S'-C2' angle /°
	C2-C2'	C2-C3	C3-C4	C4-C5	C5-S	S-C2	C2'-C3'	C3'-C4'	C4'-C5'	C5'-S'	S'-C2'	
-	1.384	1.446	1.396	1.418	1.731	1.788	1.446	1.396	1.418	1.731	1.788	180
C3	1.385	1.454	1.396	1.418	1.733	1.785	1.453	1.395	1.412	1.739	1.783	180
C4	1.385	1.439	1.403	1.424	1.723	1.806	1.444	1.399	1.412	1.734	1.778	180
C3,C3'	1.388	1.447	1.386	1.417	1.732	1.784	1.457	1.396	1.403	1.746	1.772	169.7
C4,C4'	1.385	1.44	1.398	1.413	1.731	1.79	1.437	1.405	1.422	1.721	1.8	178.1
C3,C4'	1.383	1.448	1.395	1.409	1.737	1.777	1.443	1.392	1.421	1.728	1.804	163.4

Table 4.20 Selected bond lengths and dihedral angle of the OC(CH₃)O substituted BP excited state geometry at the CC2 level

Sub. pos.	Bond length /Å											C2-S-S'-C2' angle /°
	C2-C2'	C2-C3	C3-C4	C4-C5	C5-S	S-C2	C2'-C3'	C3'-C4'	C4'-C5'	C5'-S'	S'-C2'	
-	1.385	1.445	1.399	1.418	1.737	1.793	1.445	1.399	1.418	1.737	1.793	180
C3	1.387	1.452	1.401	1.416	1.742	1.787	1.45	1.399	1.413	1.744	1.79	179.9
C4,C4'	1.386	1.439	1.401	1.413	1.738	1.796	1.436	1.408	1.423	1.727	1.805	177.6

As was the case concerning the ground state geometries, the bond lengths of the excited state geometries are almost identical to their respective OC(H)O equivalents, and therefore also the unsubstituted excited state, save for 3,4' OC(CH₃)O BP where C4-C5 and C2-S have both decreased by $\sim 0.01\text{Å}$ and S'-C2' by $\sim 0.015\text{Å}$ relative to the unsubstituted excited state geometry. In terms of dihedral angles, 3 and 4 OC(CH₃)O BP are completely planar, as were 3 and 4 OC(H)O BP. The 4,4' OC(CH₃)O BP has only experienced a very slight decrease of $\sim 3^\circ$ compared to the unsubstituted excited state geometry, almost identical to the OC(H)O substituted equivalent, whereas 3,3' and 3,4' have experienced changes of $\sim 10^\circ$ and 15° respectively.

Due to the similarities between the ground and excited state geometries of OC(H)O and OC(CH₃)O substituted BP at each corresponding substitution positions, their bond length changes on excitation are almost identical. As such the changes in bond lengths and dihedral angles on excitation of OC(CH₃)O substituted BP at the ADC(2)/aug-cc-pVDZ and CC2/aug-cc-pVDZ levels have been included in appendix 7.4 as tables 7.9 and 7.10 instead of being included here.

The changes on excitation of the bond lengths and dihedral angle of the OC(CH₃)O substituents at each substitution location are shown in table 4.21.

Table 4.21 Changes in selected bond lengths and dihedral angles of OC(CH₃)O substituents on excitation

Sub. pos.	Method	Bond length change/Å			C2-C3-O1-C6 /°			Bond length change/Å			C2'-C3'-O1'-C6' /°		
		C4-O	O1-C6	C6-O2	GS	EX	Dif	C3'-O	O1-C6'	C6'-O2'	GS	EX	Dif
3	ADC(2)	-0.022	-0.003	0.003	66.1	180	113.9						
	CC2	-0.021	-0.004	0.003	64.6	179.9	115.3						
3,3'	ADC(2)	-0.011	0.01	0	89.9	77.9	-12	-0.028	0.034	0.005	89.9	52.1	-37.8
Sub. pos.	Method	Bond length change/Å			C3-C4-O1-C6 /°			Bond length change/Å			C3'-C4'-O1'-C6' /°		
		C4-O	O1-C6	C6-O2	GS	EX	Dif	C4'-O	O1-C6'	C6'-O2'	GS	EX	Dif
4	ADC(2)	-0.019	0.022	-0.006	180	180	0						
4,4'	ADC(2)	-0.005	0.005	-0.001	96.9	94.7	-2.2	-0.02	0.013	-0.004	126.5	179.6	53.1
	CC2	-0.009	0.012	-0.004	128.5	94.4	-34.1	-0.114	0.006	-0.001	97	179.6	82.6
Sub. pos.	Method	Bond length change/Å			C2-C3-O1-C6 /°			Bond length change/Å			C3'-C4'-O1'-C6' /°		
		C3-O	O1-C6	C6-O2	GS	EX	Dif	C4'-O	O1-C6'	C6'-O2'	GS	EX	Dif
3,4'	ADC(2)	-0.009	0.012	-0.004	59.7	56.9	-2.8	-0.114	0.006	-0.001	83.7	84.2	0.5

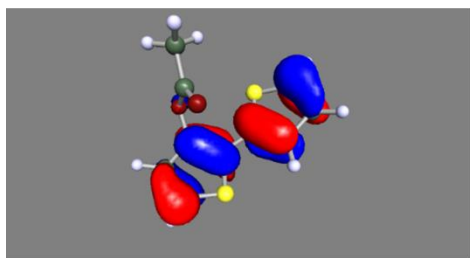
In several cases there have been significant changes on excitation of the planarity of the substituent groups relative to their thiophene rings. In 3 OC(CH₃)O BP the substituent has gone from being ~25° away from perpendicular to the thiophene ring in the ground state geometry to completely planar on excitation, with the second oxygen atom oriented away from the sulphur of the opposite thiophene ring. In 3,3' OC(CH₃)O BP both substituents began as completely perpendicular in the ground state geometry and became more planar on excitation, although in this case the second oxygen atom was oriented towards the sulphur of the opposite thiophene ring. There is some discrepancy between the dihedral angles obtain using the

different methods for the substituents of 4,4' OC(CH₃)O BP; for the calculations performed at the ADC(2) level one of the substituents begins perpendicular and remains so on excitation, whilst the other begins approximately midway between being perpendicular and planar and becomes completely planar on excitation. For the calculations performed at the CC2 level these changes appear to occur to the opposite substituent, with the OC(CH₃)O that is perpendicular in the ground state becoming completely planar in the excited state, and the substituent at the midway point becoming perpendicular on excitation.

Both 4 and 3,4' OC(CH₃)O BP do not experience significant changes in the dihedral angles of the substituents on excitation; in 4 OC(CH₃)O BP the substituent begins and remains completely planar relative to the thiophene ring, whilst in 3,4' OC(CH₃)O BP the substituent at position C3 remains approximately midway between planar and perpendicular, and the substituent at position C4' remains roughly perpendicular to the thiophene ring.

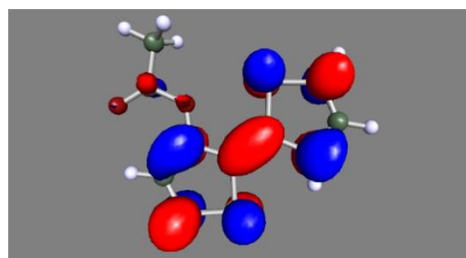
The MOs of OC(CH₃)O substituted BP that are involved in the ground state to S₁ excitation are shown below in Figure 4.5.

3 $OC(CH_3)O$ 2,2'-bithiophene



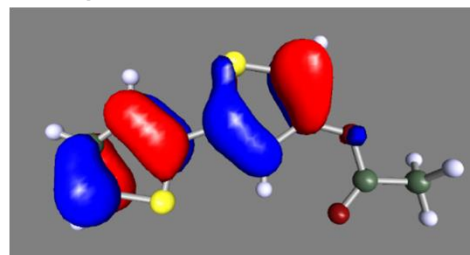
HOMO

91.4%



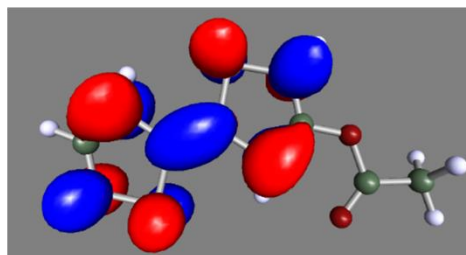
LUMO +3

4 $OC(CH_3)O$ 2,2'-bithiophene



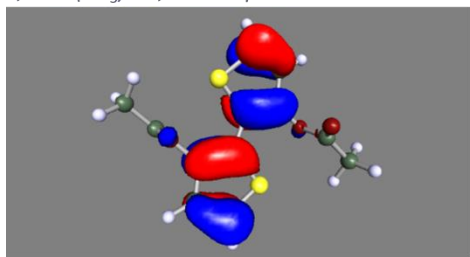
HOMO

90.1%



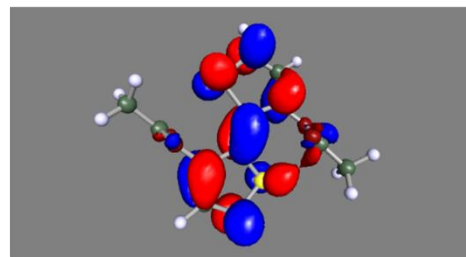
LUMO +2

3,3' $OC(CH_3)O$ 2,2'-bithiophene



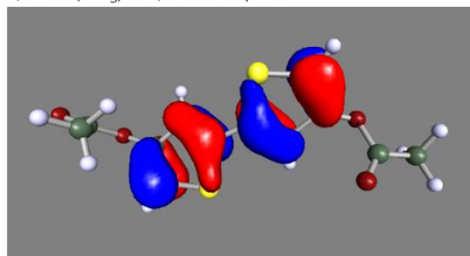
HOMO

65.8%



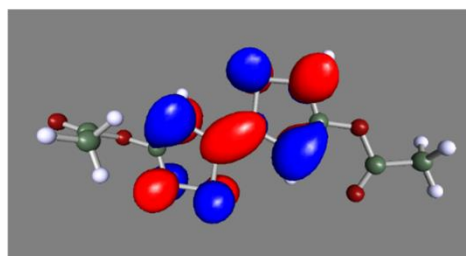
LUMO +3

4,4' $OC(CH_3)O$ 2,2'-bithiophene



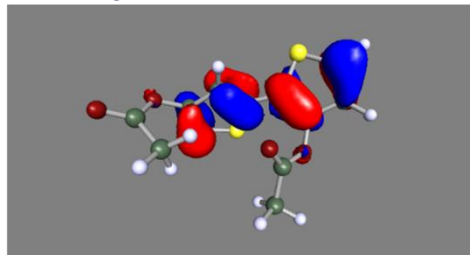
HOMO

89.7%



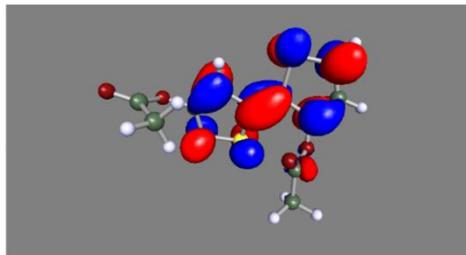
LUMO

3,4' $OC(CH_3)O$ 2,2'-bithiophene



HOMO

76.9%



LUMO

Figure 4.5 MOs involved in S_1 excitation of $OC(CH_3)O$ substituted *trans* 2,2'-bithiophene

Again, all can be assigned as π to π^* transitions. Note the change in dihedral angle relative to the thiophene ring of the substituent of 3 OC(CH₃)O BP to completely planar on excitation, and the nearly perpendicular angle of one substituent in 4,4' OC(CH₃)O BP and the C4 position substituent in 3,4' OC(CH₃)O BP.

The ground and excited state geometries were used to calculate adiabatic excitation energies which are tabulated below in table 4.22.

Table 4.22 Adiabatic Excitation energies of OC(CH₃)O substituted *trans* 2,2'-bithiophene

Substitution position	Method	Adiabatic excitation energy		Difference to unsubstituted	
		/eV	/cm ⁻¹	/eV	/cm ⁻¹
3	ADC(2)	3.9322	31715	0.07957	641.81
	CC2	3.9541	31892	0.09051	730.00
4	ADC(2)	3.6998	29841	-0.15279	-1232.3
33	ADC(2)	3.9131	31561	0.06046	487.61
44	ADC(2)	3.6868	29736	-0.16583	-1337.5
	CC2	3.7122	29941	-0.15140	-1221.1
34	ADC(2)	3.8551	31093	0.00249	20.04

As was the case for OH and OC(H)O substituent BP 4 and 4,4' substituted have experienced the greatest decreases in excitation energy relative to unsubstituted BP, with the values obtained having magnitudes roughly comparable to OC(H)O substituted BP. All other substitution locations have experienced an increase in the adiabatic excitation energy compared to unsubstituted BP, with 3 OC(CH₃)O BP experiencing the greatest increase.

4.4.4 Phenyl Substituted trans-2,2'-bithiophene

Tables 4.23 and 4.24 display selected bond lengths within the thiophene rings and the C2-S-S'-C2' dihedral angle of the ground state geometries of phenyl substituted trans BP.

Table 4.23 Selected bond lengths and dihedral angle of the phenyl substituted BP ground state geometry at the MP2 level

Sub. pos.	Bond length / Å											C2-S-S'-C2' angle / °
	C2-C2'	C2-C3	C3-C4	C4-C5	C5-S	S-C2	C2'-C3'	C3'-C4'	C4'-C5'	C5'-S'	S'-C2'	
-	1.454	1.398	1.421	1.392	1.729	1.741	1.398	1.421	1.392	1.729	1.741	147.3
C3	1.456	1.405	1.426	1.391	1.729	1.738	1.399	1.421	1.393	1.727	1.74	127.1
C4	1.452	1.397	1.426	1.398	1.726	1.742	1.399	1.421	1.392	1.729	1.741	149.3
C3,C3'	1.457	1.406	1.427	1.391	1.728	1.735	1.406	1.427	1.391	1.728	1.735	115.7
C4,C4'	1.451	1.398	1.426	1.398	1.726	1.742	1.398	1.426	1.398	1.726	1.742	151.1
C3,C4'	1.456	1.406	1.426	1.391	1.729	1.738	1.397	1.426	1.4	1.723	1.74	126

Table 4.24 Selected bond lengths and dihedral angle of the phenyl substituted BP ground state geometry at the CC2 level

Sub. pos.	Bond length / Å											C2-S-S'-C2' angle / °
	C2-C2'	C2-C3	C3-C4	C4-C5	C5-S	S-C2	C2'-C3'	C3'-C4'	C4'-C5'	C5'-S'	S'-C2'	
-	1.454	1.398	1.425	1.391	1.736	1.748	1.398	1.425	1.391	1.736	1.748	148.6
C3	1.456	1.404	1.43	1.39	1.735	1.746	1.398	1.425	1.393	1.734	1.748	127.2
C4	1.452	1.396	1.43	1.397	1.733	1.749	1.398	1.425	1.391	1.736	1.749	150.9
C3,C3'	1.457	1.405	1.431	1.391	1.735	1.744	1.405	1.431	1.391	1.735	1.744	115.7
C4,C4'	1.451	1.397	1.43	1.398	1.734	1.75	1.397	1.43	1.398	1.734	1.75	152.9
C3,C4'	1.455	1.404	1.43	1.39	1.736	1.746	1.396	1.43	1.399	1.731	1.749	126.2

As with previous substituted groups there are few differences between the bond lengths of the unsubstituted and substituted ground state geometries. Whilst the bond lengths of the ground state have not varied greatly with regards to the substitution position, this is the first time in which several of the different substitution locations have produced identical bond lengths; the bond lengths of the substituted ring of 4 phenyl BP are identical to either ring of 4,4' phenyl BP, and the position C3 substituted thiophene ring in 3,4' phenyl BP has bond lengths identical to

the substituted ring of 3 phenyl BP, which are both also almost identical to either ring of 3,3' phenyl BP. Again, as with other substituted groups there are more significant differences between the dihedral angles at different substitution positions. Both 3 and 3,4' phenyl BP have decreased by $\sim 20^\circ$ compared to the unsubstituted ground state geometry dihedral angle, and 3,3' phenyl BP has decreased even further by $\sim 30^\circ$, all becoming less planar. This is to be expected as the steric hindrance caused by having the large phenyl rings substituted at a position close to the central C-C bond is likely to twist the molecule out of the plane. The 4 and 4,4' phenyl BP ground state geometries have dihedral angles slightly more planar, $\sim 2-4^\circ$, than the unsubstituted ground state geometry.

Selected bond lengths and the C2-S-S'-C2' dihedral angle of the excited state geometries of phenyl substituted trans BP are shown in tables 4.25 and 4.26.

Table 4.25 Selected bond lengths and dihedral angle of the phenyl substituted BP excited state geometry at the ADC(2) level

Sub. pos.	Bond length /Å											C2-S-S'-C2' angle /°
	C2-C2'	C2-C3	C3-C4	C4-C5	C5-S	S-C2	C2'-C3'	C3'-C4'	C4'-C5'	C5'-S'	S'-C2'	
-	1.384	1.446	1.396	1.418	1.731	1.788	1.446	1.396	1.418	1.731	1.788	180
C3	1.392	1.465	1.423	1.39	1.751	1.769	1.434	1.396	1.42	1.715	1.806	155.7
C4	1.388	1.435	1.409	1.434	1.719	1.804	1.443	1.4	1.411	1.737	1.777	180
C3,C3'	1.39	1.459	1.41	1.403	1.731	1.788	1.459	1.41	1.403	1.731	1.788	148.2
C4,C4'	1.387	1.439	1.407	1.426	1.727	1.792	1.439	1.407	1.426	1.727	1.792	179.2
C3,C4'	1.393	1.461	1.425	1.388	1.751	1.769	1.427	1.409	1.429	1.71	1.816	155.3

Table 4.26 Selected bond lengths and dihedral angle of the phenyl substituted BP excited state geometry at the CC2 level

Sub. pos.	Bond length /Å											C2-S-S'-C2' angle /°
	C2-C2'	C2-C3	C3-C4	C4-C5	C5-S	S-C2	C2'-C3'	C3'-C4'	C4'-C5'	C5'-S'	S'-C2'	
-	1.385	1.445	1.399	1.418	1.737	1.793	1.445	1.399	1.418	1.737	1.793	180
C3	1.393	1.463	1.428	1.388	1.759	1.773	1.431	1.4	1.421	1.721	1.818	156
C4	1.389	1.433	1.413	1.435	1.724	1.811	1.441	1.404	1.41	1.744	1.783	180
C3,C3'	1.391	1.457	1.414	1.403	1.739	1.796	1.457	1.414	1.403	1.739	1.796	148.4
C4,C4'	1.389	1.437	1.411	1.426	1.733	1.798	1.437	1.411	1.426	1.733	1.798	178.9
C3,C4'	1.395	1.458	1.431	1.387	1.76	1.774	1.424	1.413	1.43	1.715	1.828	155.8

Phenyl substituted BP has provided the first examples in this thesis so far in which there have been noticeable deviations from the unsubstituted excited state geometry in terms of bond lengths; in 3 phenyl BP C2-C3 increased by $\sim 0.02\text{\AA}$ and the C3-C4 and C4-C5 bonds increased and decreased respectively by $\sim 0.03\text{\AA}$. C5-S and C2-S have also increased and decreased respectively by $\sim 0.02\text{\AA}$. The unsubstituted thiophene ring has also experienced changes relative to its counterpart in the unsubstituted ground state geometry; C2'-C3' decreased by $\sim 0.01\text{\AA}$, C5'-S' decreased by $\sim 0.015\text{\AA}$ and C2'-S' decreased by $\sim 0.025\text{\AA}$. 3,3' phenyl BP has undergone the same pattern of changes as the substituted ring in 3 phenyl BP when considering the C-C bonds within the thiophene ring, but with a lesser magnitudes of change, however both of its S-C bonds have remained very similar to those in the unsubstituted excited state geometry.

In 4 phenyl BP, C2-C3 and C3-C4 have decreased and increased by $\sim 0.01\text{\AA}$ respectively relative to the unsubstituted excited state, and C4-C5 has increased by $\sim 0.015\text{\AA}$, in contrast to the decrease this bond experienced in 3 and 3,3' phenyl BP. Bonds C5-S and C2-S have decreased and increased by ~ 0.015 respectively, again following the inverse of the pattern of changes experienced in 3 and 3,3' phenyl BP. In the unsubstituted ring C2'-S' has decreased by $\sim 0.01\text{\AA}$. As with 3 and 3,3' phenyl BP, 4,4' phenyl BP has followed the same pattern of changes as 4 phenyl BP but with smaller magnitudes of change.

In 3,4' phenyl BP the C3 substituted thiophene ring has experienced the same changes, compared to the unsubstituted excited state geometry, as the substituted ring in 3 phenyl BP, whilst the C4 substituted ring has also experienced fairly significant changes compared to the unsubstituted excited state geometry; C2'-C3' decreased by $\sim 0.02\text{\AA}$, C3'-C4' increased by $\sim 0.015\text{\AA}$, C4'-C5' increased by $\sim 0.01\text{\AA}$, C5'-S' decreased by $\sim 0.02\text{\AA}$ and C2'-S' increased by $\sim 0.035\text{\AA}$.

The dihedral angles of 4 and 4,4' phenyl BP are completely planar, similarly to the unsubstituted excited state geometry, whilst both 3 and 3,4' phenyl BP decreased by $\sim 25^\circ$. Again, as was the

case with the ground state geometry, 3,3' phenyl BP experienced the greatest decrease in the dihedral angle compared to the unsubstituted geometry, decreasing by $\sim 30^\circ$.

The changes of the bond lengths and dihedral angle on excitation of phenyl substituted BP are displayed in tables 4.27 and 4.28.

Table 4.27 Changes in selected bond lengths and dihedral angle of phenyl substituted BP on excitation at the ADC(2) level

Sub. pos.	Bond length change / Å											C2-S-S'-C2' angle change /°
	C2-C2'	C2-C3	C3-C4	C4-C5	C5-S	S-C2	C2'-C3'	C3'-C4'	C4'-C5'	C5'-S'	S'-C2'	
-	-0.07	0.048	-0.025	0.026	0.002	0.047	0.048	-0.025	0.026	0.002	0.047	32.7
C3	-0.064	0.06	-0.003	-0.001	0.022	0.031	0.035	-0.025	0.027	-0.012	0.066	28.6
C4	-0.064	0.038	-0.017	0.036	-0.007	0.062	0.044	-0.021	0.019	0.008	0.036	30.7
C3,C3'	-0.067	0.053	-0.017	0.012	0.003	0.053	0.053	-0.017	0.012	0.003	0.053	32.5
C4,C4'	-0.064	0.041	-0.019	0.028	0.001	0.05	0.041	-0.019	0.028	0.001	0.05	28.1
C3,C4'	-0.063	0.055	-0.001	-0.003	0.022	0.031	0.03	-0.017	0.029	-0.013	0.076	29.3

Table 4.28 Changes in selected bond lengths and dihedral angle of phenyl substituted BP on excitation at the CC2 level

Sub. pos.	Bond length change / Å											C2-S-S'-C2' angle change /°
	C2-C2'	C2-C3	C3-C4	C4-C5	C5-S	S-C2	C2'-C3'	C3'-C4'	C4'-C5'	C5'-S'	S'-C2'	
-	-0.069	0.047	-0.026	0.027	0.001	0.045	0.047	-0.026	0.027	0.001	0.045	31.4
C3	-0.063	0.059	-0.002	-0.002	0.024	0.027	0.033	-0.025	0.028	-0.013	0.07	28.8
C4	-0.063	0.037	-0.017	0.038	-0.009	0.062	0.043	-0.021	0.019	0.008	0.034	29.1
C3,C3'	-0.066	0.052	-0.017	0.012	0.004	0.052	0.052	-0.017	0.012	0.004	0.052	32.7
C4,C4'	-0.062	0.04	-0.019	0.028	-0.001	0.048	0.04	-0.019	0.028	-0.001	0.048	26
C3,C4'	-0.06	0.054	0.001	-0.003	0.024	0.028	0.028	-0.017	0.031	-0.016	0.079	29.6

Table 4.29 shows the changes on excitation of the dihedral angle of the phenyl substituents at the different substitution locations. The bond lengths within the phenyl rings only experience minor changes on excitation and so have been omitted here and instead included in appendix 7.4 in tables 7.11 and 7.12.

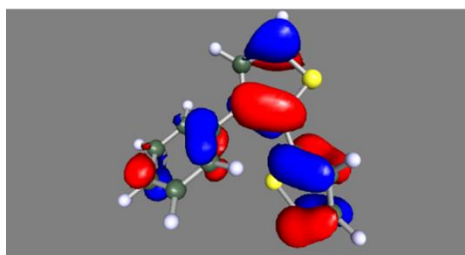
Table 4.29 Changes in dihedral angles of phenyl substituents on excitation

Substitution position	Method	C2-C3-C6-C7 /°			C2'-C3'-C6'-C7' /°		
		GS	EX	Dif	GS	EX	Dif
3	ADC(2)	45.1	23.5	-21.6			
	CC2	45.1	22.4	-22			
3,3'	ADC(2)	37.8	29.2	-8.6	37.8	29.2	-8.6
	CC2	37	28.9	-8.1	37	28.9	-8.1
Substitution position	Method	C3-C4-C6-C7 /°			C3'-C4'-C6'-C7' /°		
		GS	EX	Dif	GS	EX	Dif
4	ADC(2)	37.4	0	-37.4			
	CC2	37	0	-37			
4,4'	ADC(2)	37.5	24.6	-12.9	37.5	24.6	-12.9
	CC2	37.1	22.9	-14.2	37.1	22.9	-14.2
Substitution position	Method	C2-C3-C6-C7 /°			C3'-C4'-C6'-C7' /°		
		GS	EX	Dif	GS	EX	Dif
3,4'	ADC(2)	44.5	23.7	-20.8	37	26.2	-10.8
	CC2	43.8	22.4	-21.4	36.6	25.4	-11.2

Regardless of substitution position all the phenyl substituents begin as roughly halfway between planar and perpendicular, relative to their thiophene rings, in the ground state, with the phenyl ring of 3 phenyl BP and the C3 position phenyl of 3,4' phenyl BP being almost exactly half way, and the dihedral angles of all other phenyl rings being almost identical at $\sim 37^\circ$. The phenyl of 4 phenyl BP becomes completely planar on excitation, whilst all other phenyl rings also become more planar with respect to their thiophene rings, decreasing to a dihedral angle of $\sim 25^\circ$ regardless of substitution position.

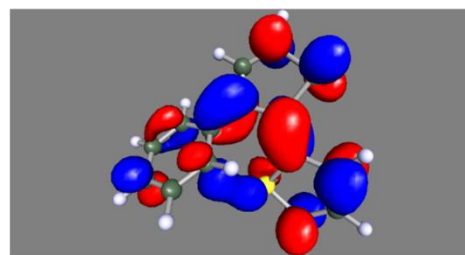
The MOs of phenyl substituted BP that are involved in the ground state to S_1 excitation are shown below in Figure 4.6.

3 phenyl 2,2'-bithiophene



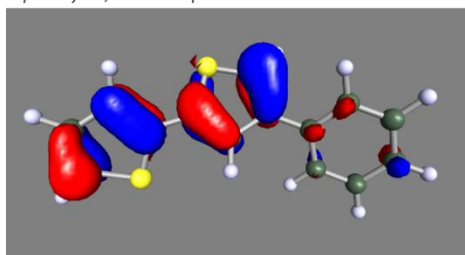
HOMO

89.6%



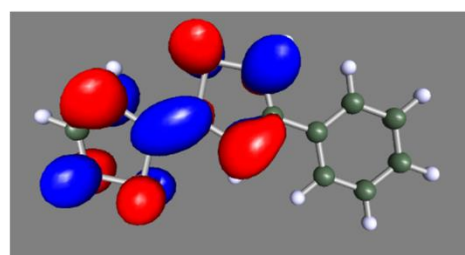
LUMO

4 phenyl 2,2'-bithiophene



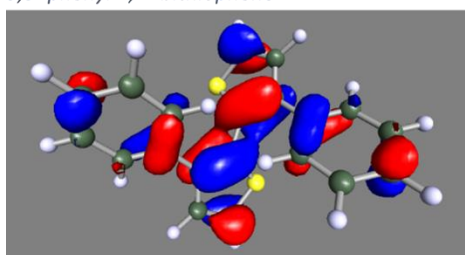
HOMO

90.2%



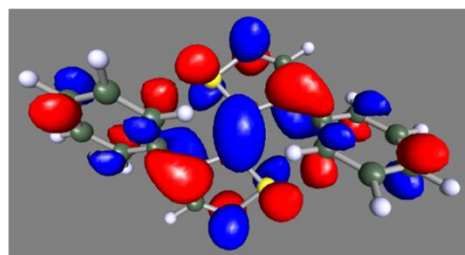
LUMO + 2

3,3' phenyl 2,2'-bithiophene



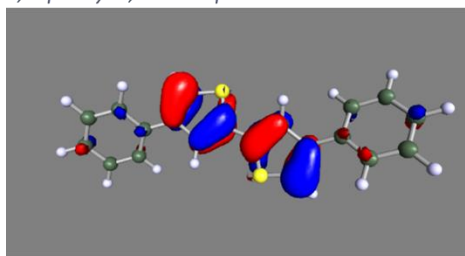
HOMO

93.3%



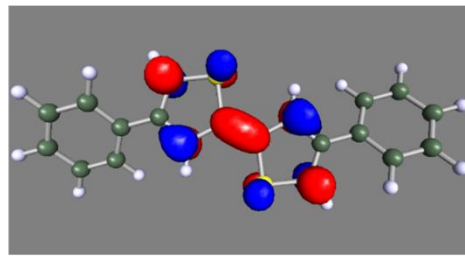
LUMO

4,4' phenyl 2,2'-bithiophene



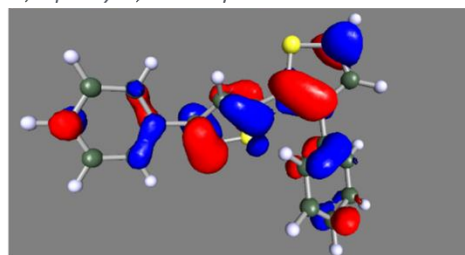
HOMO

88.8%



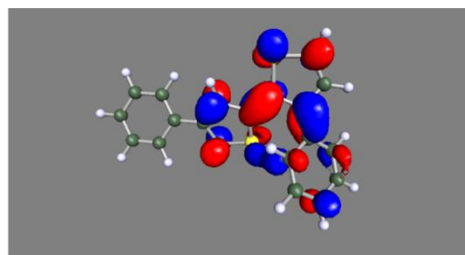
LUMO + 2

3,4' phenyl 2,2'-bithiophene



HOMO

89.1%



LUMO

Figure 4.6 MOs involved in S_1 excitation of phenyl substituted *trans* 2,2'-bithiophene

These can be assigned as π to π^* transitions and the lack of significant changes for the bond lengths within the substituent groups can be attributed to the electron density associated with these bonds not being involved in the transition to the first excited state.

Adiabatic excitation energies were calculated using the ground and excited state geometries and are shown in table 4.30.

Table 4.30 Adiabatic Excitation energies of phenyl substituted *trans* 2,2'-bithiophene

Substitution position	Method	Adiabatic excitation energy		Difference to unsubstituted	
		/eV	/cm ⁻¹	/eV	/cm ⁻¹
3	ADC(2)	3.4544	27861	-0.39824	-3212
	CC2	3.4305	27669	-0.43308	-3493
4	ADC(2)	3.7213	30014	-0.13132	-1059.2
	CC2	3.7295	30081	-0.13404	-1081.1
33	ADC(2)	3.3177	26759	-0.53486	-4314
	CC2	3.3003	26619	-0.56328	-4543.2
44	ADC(2)	3.6294	29273	-0.22321	-1800.3
	CC2	3.6403	29361	-0.22325	-1800.6
34	ADC(2)	3.3337	26888	-0.51891	-4185.3
	CC2	3.3048	26655	-0.55881	-4507.1

Phenyl substituted BP is the first case in this thesis where there has been a decrease in the excitation energy relative to unsubstituted BP regardless of substitution position, and where are all of the decreases are of a significant magnitude; the smallest decrease seen here, that of 4 phenyl BP, is approximately equivalent to the greatest decreases seen for both OC(H)O and OC(CH₃)O substituted BP. This is contrary to the predictions made in section 4.2. The greatest decreases are experienced by 3,3' and 3,4' phenyl BP, also in contrast to the previous substituted BP examples, followed by 3 phenyl BP. The 4,4' and 4' phenyl BP experience the smallest decreases in the excitation energy relative to unsubstituted BP. This is somewhat counter intuitive as all three of these have less planar ground states, and less planar excited states, than that unsubstituted BP, whilst 4 and 4,4' phenyl BP have more planar ground states and planar excited states.

4.4.5 Dimethylamino Substituted trans-2,2'-bithiophene

Selected bond lengths and the C2-S-S'-C2' dihedral angle of the ground state geometries of dimethylamino substituted trans BP are shown in tables 4.31 and 4.32.

Table 4.31 Selected bond lengths and dihedral angle of the dimethylamino substituted BP ground state geometry at the MP2 level

Sub. pos.	Bond length /Å											C2-S-S'-C2' angle /°
	C2-C2'	C2-C3	C3-C4	C4-C5	C5-S	S-C2	C2'-C3'	C3'-C4'	C4'-C5'	C5'-S'	S'-C2'	
-	1.454	1.398	1.421	1.392	1.729	1.741	1.398	1.421	1.392	1.729	1.741	147.3
C3	1.45	1.407	1.427	1.391	1.728	1.738	1.401	1.42	1.391	1.73	1.747	149.1
C4	1.452	1.394	1.43	1.401	1.732	1.74	1.399	1.421	1.391	1.73	1.741	148.2
C3,C3'	1.449	1.409	1.427	1.391	1.727	1.741	1.409	1.427	1.391	1.727	1.741	134.8
C4,C4'	1.451	1.394	1.43	1.401	1.732	1.741	1.394	1.43	1.401	1.732	1.741	149.7
C3,C4'	1.449	1.406	1.427	1.39	1.73	1.739	1.397	1.427	1.4	1.733	1.747	154.2

Table 4.32 Selected bond lengths and dihedral angle of the dimethylamino substituted BP ground state geometry at the CC2 level

Sub. pos.	Bond length /Å											C2-S-S'-C2' angle /°
	C2-C2'	C2-C3	C3-C4	C4-C5	C5-S	S-C2	C2'-C3'	C3'-C4'	C4'-C5'	C5'-S'	S'-C2'	
-	1.454	1.398	1.425	1.391	1.736	1.748	1.398	1.425	1.391	1.736	1.748	148.6
C3	1.45	1.406	1.432	1.39	1.736	1.746	1.4	1.424	1.391	1.738	1.756	150.8
C4	1.452	1.393	1.434	1.401	1.739	1.747	1.398	1.425	1.391	1.736	1.749	149.8
C3,C3'	1.448	1.408	1.432	1.391	1.735	1.75	1.408	1.432	1.391	1.735	1.75	135.6
C4,C4'	1.451	1.393	1.434	1.401	1.74	1.747	1.393	1.434	1.401	1.74	1.747	151.2
C3,C4'	1.448	1.406	1.432	1.39	1.737	1.747	1.396	1.432	1.4	1.742	1.755	155.9

There have only been minor changes to the ground state geometries on substitution with regards to the bond angles, as seen in OH, OC(H)O and OC(CH₃)O substituted and conversely to phenyl substituted. The 3,3' dimethylamino BP, as well as the C3 substituted ring in 3 and 3,4' dimethylamino BP, all have nearly identical bond lengths and have all seen increases of ~0.01Å for C2-C3. The substituted ring in 4 dimethylamino BP and both thiophene rings in 4,4' dimethylamino BP likewise have identical bond lengths to each other, with all three C-C bonds

within the thiophene rings undergoing an increase of $\sim 0.01\text{\AA}$ compared to the unsubstituted ground state geometry. There have also been less significant changes in the dihedral angles when compared to other substituted BP, with both 3, 4 and 4,4' dimethylamino BP differing from the unsubstituted ground state dihedral by a few degrees. The 3,4' dimethylamino BP has increased by $\sim 7^\circ$ and become slightly more planar than the unsubstituted geometry, and 3,3' dimethylamino BP has undergone the most significant change with a decrease of $\sim 13^\circ$, decreasing in planarity relative to the unsubstituted ground state geometry.

Tables 4.33 and 4.34 show selected bond lengths within the thiophene rings and the C2-S-S'-C2' dihedral angle of the excited state geometries of dimethylamino substituted BP.

Table 4.33 Selected bond lengths and dihedral angle of the dimethylamino substituted BP excited state geometry at the ADC(2) level

Sub. pos.	Bond length / \AA											C2-S-S'-C2' angle / $^\circ$
	C2-C2'	C2-C3	C3-C4	C4-C5	C5-S	S-C2	C2'-C3'	C3'-C4'	C4'-C5'	C5'-S'	S'-C2'	
-	1.384	1.446	1.396	1.418	1.731	1.788	1.446	1.396	1.418	1.731	1.788	180
C3	1.399	1.445	1.413	1.398	1.769	1.76	1.429	1.407	1.409	1.742	1.799	145.5
C4	1.394	1.433	1.434	1.432	1.737	1.83	1.43	1.411	1.399	1.745	1.769	178.9
C3,C3'	1.394	1.449	1.412	1.403	1.758	1.783	1.449	1.412	1.403	1.758	1.783	141.6
C4,C4'	1.394	1.424	1.421	1.407	1.744	1.768	1.434	1.434	1.432	1.739	1.829	179.1
C3,C4'	1.388	1.441	1.413	1.4	1.753	1.77	1.430	1.433	1.43	1.735	1.838	156.1

Table 4.34 Selected bond lengths and dihedral angle of the dimethylamino substituted BP excited state geometry at the CC2 level

Sub. pos.	Bond length / \AA											C2-S-S'-C2' angle / $^\circ$
	C2-C2'	C2-C3	C3-C4	C4-C5	C5-S	S-C2	C2'-C3'	C3'-C4'	C4'-C5'	C5'-S'	S'-C2'	
-	1.385	1.445	1.399	1.418	1.737	1.793	1.445	1.399	1.418	1.737	1.793	180
C3	1.399	1.445	1.417	1.399	1.773	1.768	1.428	1.409	1.411	1.749	1.81	144.7
C4	1.396	1.428	1.44	1.429	1.74	1.827	1.429	1.413	1.399	1.752	1.774	178.8
C3,C3'	1.395	1.447	1.415	1.403	1.765	1.79	1.447	1.415	1.403	1.765	1.79	141.2
C4,C4'	1.395	1.425	1.424	1.409	1.751	1.772	1.429	1.439	1.429	1.741	1.827	179
C3,C4'	1.392	1.441	1.416	1.4	1.766	1.775	1.419	1.435	1.426	1.736	1.839	149.7

As with phenyl substituted BP there have been more significant changes to the bond lengths on excitation when compared to the unsubstituted excited state geometry. In 3 dimethylamino BP both the substituted and unsubstituted thiophene rings have seen more significant changes, with C3-C4 and C4-C5 having increased and decreasing by $\sim 0.02\text{\AA}$ respectively, C5-S increased by $\sim 0.035\text{\AA}$ and C2-S decreased by $\sim 0.025\text{\AA}$, S'-C2' and C2'-C3' increased and decreased by $\sim 0.015\text{\AA}$ respectively, and C3'-C4' and C5'-S' have both increased by $\sim 0.01\text{\AA}$ compared to the unsubstituted excited state geometry.

In 4 dimethylamino BP C2-C3 has decreased $\sim 0.15\text{\AA}$, C3-C4 and S-C2 have increased $\sim 0.04\text{\AA}$ and C4-C5 has increased $\sim 0.01\text{\AA}$. As with 3 dimethylamino BP the unsubstituted ring has also undergone more significant changes when compared to the other substituents; C2'-C3' decreased $\sim 0.015\text{\AA}$, C3'-C4' increased $\sim 0.015\text{\AA}$, C4'-C5' decreased $\sim 0.02\text{\AA}$, C5'-S' increased $\sim 0.015\text{\AA}$ and S'-C2' decreased $\sim 0.02\text{\AA}$ relative to the unsubstituted geometry.

The 3,3' dimethylamino BP shows the same changes with regards to the C-C bonds as 3 dimethylamino BP, whereas C5-S experiences a change of lesser magnitude in comparison and C2-S barely changes at all. Each thiophene ring of 4,4' dimethylamino BP experienced different changes; in one ring C2-C3 decreased by $\sim 0.02\text{\AA}$, C3-C4 increased by $\sim 0.025\text{\AA}$, C4-C5 decreased $\sim 0.01\text{\AA}$, C5-S increased $\sim 0.015\text{\AA}$, and C2-S decreased $\sim 0.02\text{\AA}$, and in the other ring the changes experienced are almost identical to the substituted ring in 4 dimethylamino BP. For 3,4' dimethylamino BP the C3 substituted ring experiences the same changes as the substituted ring of 3 dimethylamino BP but with lesser magnitude of changes for C-S bonds, and in the C4' substituted ring C2'-C3' decreased $\sim 0.025\text{\AA}$, C3'-C4' increased $\sim 0.04\text{\AA}$ and S'-C2' increased $\sim 0.045\text{\AA}$.

The dihedral angle of the 4 and 4,4' dimethylamino BP excited state geometries remained almost completely planar, similarly to the unsubstituted excited state geometry, whilst both 3 and 3,3' dimethylamino BP decreased by $\sim 35^\circ$ and 40° respectively. The dihedral angle of the 3,4' dimethylamino BP geometry experienced a smaller, but still significant, decrease of $\sim 25\text{-}30^\circ$.

The changes of the bond lengths and dihedral angle on excitation of dimethylamino substituted BP are displayed in tables 4.35 and 4.36.

Table 4.35 Changes in selected bond lengths and dihedral angle of dimethylamino substituted BP on excitation at the ADC(2) level

Sub. pos.	Bond length change /Å											C2-S-S'-C2' angle change /°
	C2-C2'	C2-C3	C3-C4	C4-C5	C5-S	S-C2	C2'-C3'	C3'-C4'	C4'-C5'	C5'-S'	S'-C2'	
-	-0.07	0.048	-0.025	0.026	0.002	0.047	0.048	-0.025	0.026	0.002	0.047	32.7
C3	-0.051	0.038	-0.014	0.007	0.041	0.022	0.028	-0.013	0.018	0.012	0.052	-3.6
C4	-0.058	0.039	0.004	0.031	0.005	0.09	0.031	-0.01	0.008	0.015	0.028	30.7
C3,C3'	-0.055	0.04	-0.015	0.012	0.031	0.042	0.04	-0.015	0.012	0.031	0.042	6.8
C4,C4'	-0.057	0.03	-0.009	0.006	0.012	0.027	0.04	0.004	0.031	0.007	0.088	29.4
C3,C4'	-0.061	0.035	-0.014	0.01	0.023	0.031	0.033	0.006	0.03	0.002	0.091	1.9

Table 4.36 Changes in selected bond lengths and dihedral angle of dimethylamino substituted BP on excitation at the CC2 level

Sub. pos.	Bond length change /Å											C2-S-S'-C2' angle change /°
	C2-C2'	C2-C3	C3-C4	C4-C5	C5-S	S-C2	C2'-C3'	C3'-C4'	C4'-C5'	C5'-S'	S'-C2'	
-	-0.069	0.047	-0.026	0.027	0.001	0.045	0.047	-0.026	0.027	0.001	0.045	31.4
C3	-0.051	0.039	-0.015	0.009	0.037	0.022	0.028	-0.015	0.02	0.011	0.054	-6.1
C4	-0.056	0.035	0.006	0.028	0.001	0.08	0.031	-0.012	0.008	0.016	0.025	29
C3,C3'	-0.053	0.039	-0.017	0.012	0.03	0.04	0.039	-0.017	0.012	0.03	0.04	5.6
C4,C4'	-0.056	0.032	-0.01	0.008	0.011	0.025	0.036	0.005	0.028	0.001	0.08	27.8
C3,C4'	-0.056	0.035	-0.016	0.01	0.029	0.028	0.023	0.003	0.026	-0.006	0.084	-6.2

The changes upon excitation of the bond lengths of the dimethylamino substituents at the different substitution locations are shown in table 4.37, and the changes in dihedral angles of the substituent methyl groups upon excitation are shown in table 4.38.

Table 4.37 Changes in selected bond lengths of dimethylamino substituents on excitation

Substitution position	Method	Bond length change/Å					
		C3-N	N-C	N-C	C3'-N'	N'-C'	N'-C'
3	ADC(2)	-0.016	0	-0.005			
	CC2	-0.017	0	-0.004			
3,3'	ADC(2)	-0.027	0.002	-0.003	-0.027	0.002	-0.003
	CC2	-0.025	0.003	-0.002	-0.025	0.003	-0.002
Substitution position	Method	Bond length change/Å					
		C4-N	N-C	N-C	C4'-N'	N'-C'	N'-C'
4	ADC(2)	-0.054	-0.002	0.002			
	CC2	-0.047	-0.003	0.002			
4,4'	ADC(2)	0.002	-0.002	0	-0.054	-0.003	0.003
	CC2	0.001	-0.002	0	0.051	-0.004	0.002
Substitution position	Method	Bond length change/Å					
		C3-N	N-C	N-C	C4'-N'	N'-C'	N'-C'
3,4'	ADC(2)	-0.011	0	-0.003	-0.054	-0.005	0.001
	CC2	-0.014	-0.002	-0.004	-0.043	-0.006	0.001

Table 4.38 Table 4.39 Changes in dihedral angles of dimethylamino substituent methyl groups on excitation

Sub. pos.	Method	C2-C3-N-C6 /°			C2-C3-N-C7 /°			C2'-C3'-N'-C6' /°			C2'-C3'-N'-C7' /°		
		GS	EX	Dif	GS	EX	Dif	GS	EX	Dif	GS	EX	Dif
3	ADC(2)	72.3	55.6	-16.7	160.6	154.5	-6.1						
	CC2	72.1	55.5	-16.6	160.7	155.3	-5.4						
3,3'	ADC(2)	64.5	55.1	-9.4	167.7	166.6	-1.1	64.5	55.1	-9.4	167.7	166.6	-1.1
	CC2	63.7	55.3	-8.4	168.3	166.7	-1.6	63.7	55.3	-8.4	168.3	166.7	-1.6
Sub. pos.	Method	C3-C4-N-C6 /°			C3-C4-N-C7 /°			C3'-C4'-N'-C6' /°			C3'-C4'-N'-C7' /°		
		GS	EX	Dif	GS	EX	Dif	GS	EX	Dif	GS	EX	Dif
4	ADC(2)	48.8	6.5	-42.3	178	171.4	-6.6						
	CC2	47.4	7.6	-39.8	177	171.4	-5.6						
4,4'	ADC(2)	48.6	45.3	-3.3	177.9	175.1	-2.8	48.6	6.4	-42.2	177.8	171.4	-6.4
	CC2	47.5	41.2	-6.3	177	172	-5	47.5	7.3	-40.2	177	171.3	-5.7
Sub. pos.	Method	C2-C3-N-C6 /°			C2-C3-N-C7 /°			C3'-C4'-N'-C6' /°			C3'-C4'-N'-C7' /°		
		GS	EX	Dif	GS	EX	Dif	GS	EX	Dif	GS	EX	Dif
3,4'	ADC(2)	75.1	67.6	-7.5	157.9	161.5	3.6	49.8	9.6	-40.2	178.5	172.1	-6.4
	CC2	74.8	63.6	-11.2	158.1	160.4	2.3	48.2	5.5	-42.7	177.3	166.6	-10.7

In both 3 and 3,3' dimethylamino BP, and the C3 substituted dimethylamino group of 3,4' dimethylamino BP, one of the substituent methyl groups begins close to perpendicular relative to the thiophene ring, more so in the case of 3 and 3,4' dimethylamino BP, and all become slightly, $\sim 10^\circ$ for 3,3' and 3,4', and $\sim 17^\circ$ for 3', more planar. The other methyl group in the substituent at these positions begins close to planar relative to the thiophene ring in the ground state, and only experiences slight changes of $\sim 1-4^\circ$ on excitation for 3,3' and 3,4' dimethylamino BP. In 4 dimethylamino BP, the C4 position group in 3,4' dimethylamino BP and for one of the groups in 4,4' dimethylamino BP, one substituent methyl group begins approximately midway between planar and perpendicular relative to the thiophene ring in the ground state and becomes close to completely planar on excitation, whilst the other methyl group begins almost totally planar and experiences a decrease of $\sim 5-10^\circ$, resulting in the two methyl groups becoming more planar relative to the thiophene ring and each other. The other dimethylamino group in 4,4' dimethylamino BP has one methyl begin and remain at the halfway mark between planar and perpendicular, and the other methyl group beginning and remaining almost completely planar relative to the thiophene ring.

The MOs of dimethylamino substituted BP that are involved in the ground state to S_1 excitation are shown below in Figures 4.7 and 4.8

3 dimethylamino 2,2'-bithiophene

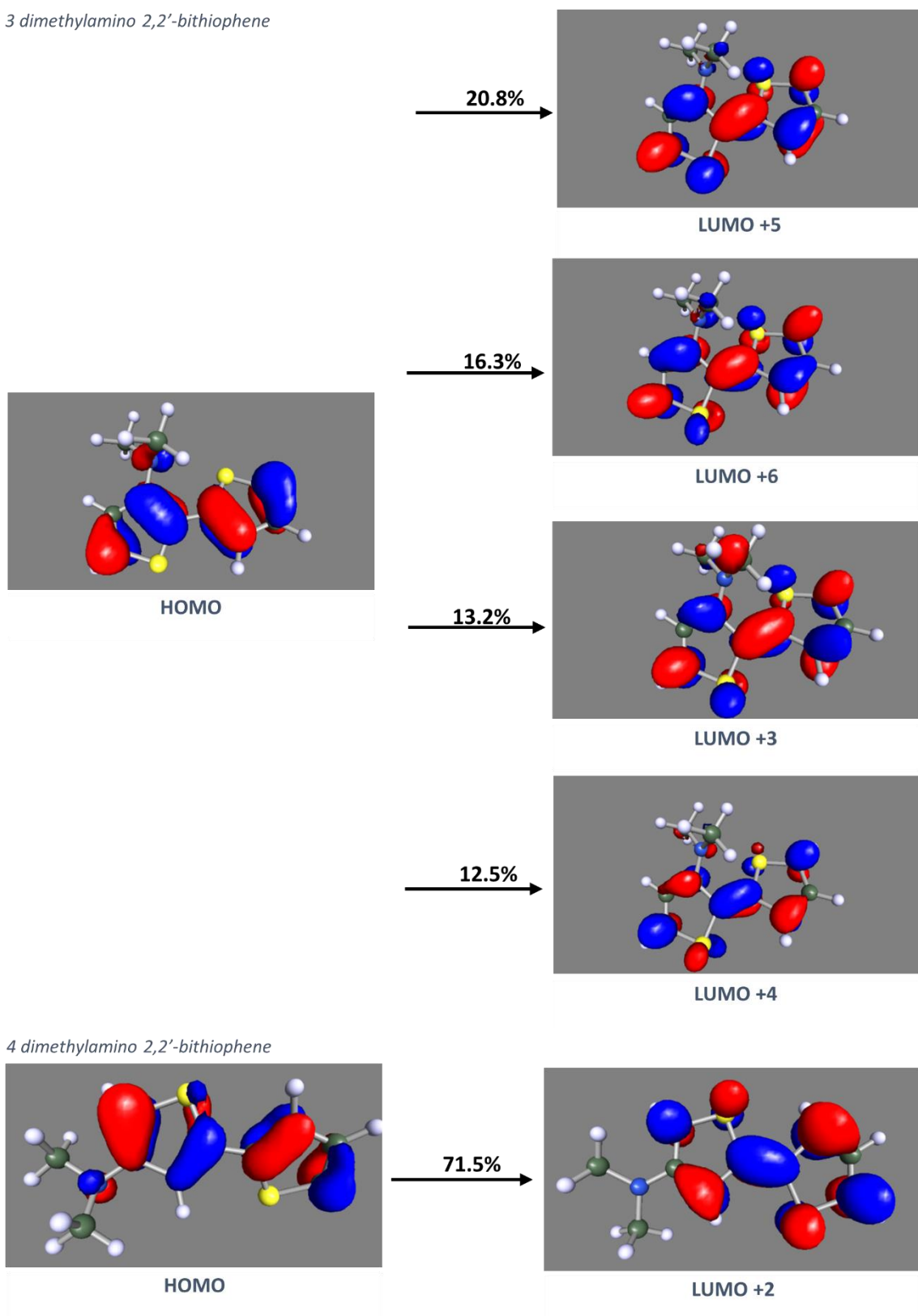
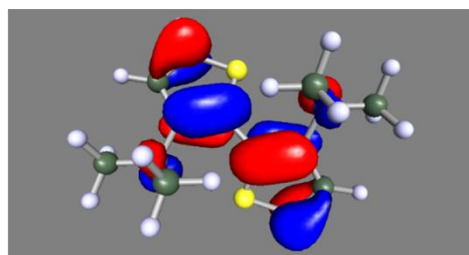


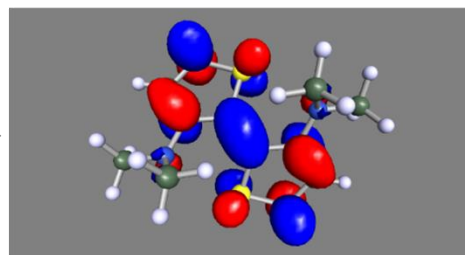
Figure 4.7 MOs involved in S_1 excitation of singly dimethylamino substituted trans 2,2'-bithiophene

3,3' dimethylamino 2,2'-bithiophene



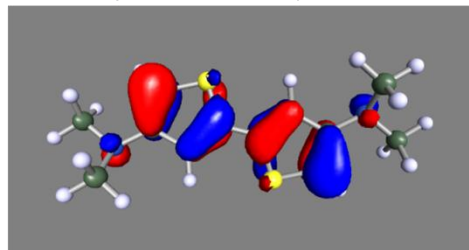
HOMO

64.5%



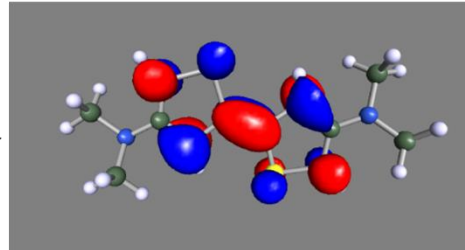
LUMO + 8

4,4' dimethylamino 2,2'-bithiophene



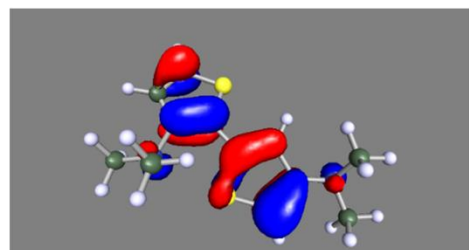
HOMO

68.4%



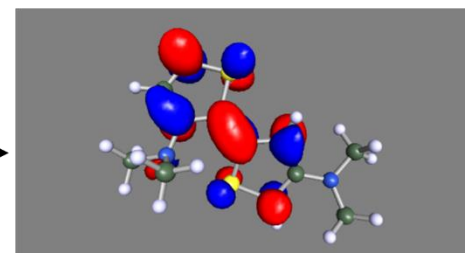
LUMO + 2

3,4' dimethylamino 2,2'-bithiophene



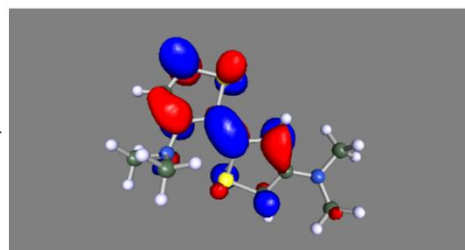
HOMO

40.8%



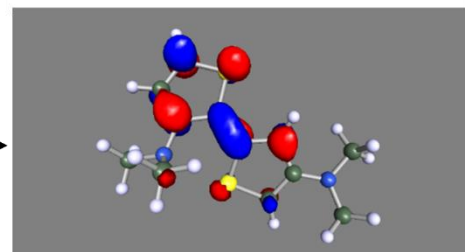
LUMO + 3

22.9%



LUMO + 6

12.1%



LUMO + 5

Figure 4.8 MOs involved in S_1 excitation of doubly dimethylamino substituted *trans* 2,2'-bithiophene

The transitions can be assigned as π to π^* star like all previous discussed substituents. Adiabatic excitation energies were obtained using the ground and excited state geometries and are shown in table 4.39.

Table 4.40 Adiabatic Excitation energies of dimethylamino substituted *trans* 2,2'-bithiophene

Substitution position	Method	Adiabatic excitation energy		Difference to unsubstituted	
		/eV	/cm ⁻¹	/eV	/cm ⁻¹
3	ADC(2)	3.3183	26764	-0.53435	-4309.8
	CC2	3.3381	26924	-0.52549	-4238.3
4	ADC(2)	3.1071	25060	-0.74553	-6013.1
	CC2	3.2030	25834	-0.66056	-5327.8
33	ADC(2)	3.2293	26046	-0.62333	-5027.5
	CC2	3.2530	26237	-0.61060	-4924.9
44	ADC(2)	3.1096	25080	-0.74304	-5993
	CC2	3.2001	25811	-0.66345	-5351
34	ADC(2)	3.0149	24317	-0.83767	-6756.2
	CC2	3.0926	24944	-0.77097	-6218.3

As with phenyl substituted BP all dimethylamino substitutions have resulted in decreases in the excitation relative to unsubstituted BP, and in more significant decreases than any substitution position for OH, OC(H)O and OC(CH₃)O substituted BP. The 3,4' dimethylamino BP has experienced the greatest decrease, followed by 4 and 4,4' dimethylamino BP. The 3,4' dimethylamino BP has the most planar ground state, but does not undergo any change in planarity on excitation, whilst 4 and 4,4' dimethylamino BP have both ground and excited state dihedral angles roughly equivalent to unsubstituted BP. The 3,3' and 3' dimethylamino BP have experienced the smallest, but still very significant, decreases in excitation energy. Both 3 and 3,3' dimethylamino BP have similar ground state dihedral angles to unsubstituted BP and whilst 3,3' dimethylamino BP experienced an increase similar to that of 3,4' dimethylamino BP, 3 dimethylamino BP actually becomes less planar on excitation.

4.5 Substituted Cis-2,2'-bithiophene Results and Discussion

Due to the similarities with regards to bond lengths between substituted cis BP and both unsubstituted cis BP and substituted trans BP, only changes in dihedral angles will be discussed here. The bond lengths of the ground and excited state geometries of OH, OC(H)O, OC(CH₃)O, phenyl and dimethylamino substituted cis BP are displayed in appendix 7.4 as tables 7.13 through 7.22. Changes in the bond lengths of the substituents are also shown in appendix 7.4 as tables 7.23 through 7.28. The MOs that are involved in the ground state to S₁ excitations are shown in appendix 7.4 as figures 7.1 to 7.6, with breakdowns of the contributions of each transition to the overall excitation listed in tables 7.29 to 7.34.

4.5.1 OH substituted cis-2,2'-bithiophene

The ground and excited state geometry S-C2-C2'-S' dihedral angle and dihedral angles of the OH group(s) relative to the thiophene ring are shown in table 4.40. No results were obtained for either 3 or 3,3' OH BP.

Table 4.41 Thiophene ring and substituent dihedral angles of OH substituted cis-2,2'-bithiophene

Substitution. pos.	Method	S-C2-C2'-S' /°			C3-C4-O-H /°			C3'-C4'-O'-H' /°		
		GS	EX	Dif	GS	EX	Dif	GS	EX	Dif
4	ADC(2)	0	0	0	0	0	0			
	CC2	0	0	0	0	0	0			
4,4'	ADC(2)	0.1	0	-0.1	180	180	0	0	0	0
	CC2	0.1	0	-0.1	180	180	0	0	0	0
Substitution. pos.	Method	S-C2-C2'-S' /°			C2-C3-O-H /°			C3'-C4'-O'-H' /°		
		GS	EX	Dif	GS	EX	Dif	GS	EX	Dif
3,4'	ADC(2)	0.1	0	-0.1	180	180	0	180	180	0
	CC2	0.1	3.6	3.5	180	179.8	-0.2	180	179.9	-0.1

Regardless of substitution location the dihedral angles of both the ground and excited state geometries are all completely planar, compared to the dihedral angle of ~40° for unsubstituted cis-2,2'-bithiophene as seen in Chapter 3. The planarity of the substituents relative to their

thiophene ring is also completely planar in both the ground and excited state geometries regardless of substitution position, with the only outlier being a slight deviation from planarity, $\sim 4^\circ$ for the C3 position OH group of 3,4' OH BP calculated at the CC2 level.

Adiabatic excitation energies were calculated from the ground and excited state geometries and are displayed in table 4.41.

Table 4.42 Adiabatic Excitation energies of OH substituted cis 2,2'-bithiophene

Substitution position	Method	Adiabatic excitation energy		Difference to unsubstituted	
		/eV	/cm ⁻¹	/eV	/cm ⁻¹
4	ADC(2)	3.4981	28214	-0.36445	-2939.5
	CC2	3.5573	28692	-0.31212	-2517.4
44	ADC(2)	3.3772	27239	-0.48539	-3914.9
	CC2	3.4344	27700	-0.43505	-3509
34	ADC(2)	3.5877	28937	-0.27490	-2217.2
	CC2	3.6529	29463	-0.21648	-1746

In contrast to trans OH substituted trans BP, 3,4' OH cis BP has caused a significant decrease in the excitation energy relative to unsubstituted cis BP. As with trans substituted BP 4,4' and 4' have experienced the greatest decrease in the excitation energy, however all the decreases displayed here are of a greater magnitude than their trans equivalents.

4.5.2 OC(H)O Substituted cis 2,2'-bithiophene

The ground and excited state geometry S-C2-C2'-S' dihedral angle and dihedral angles of the OC(H)O group(s) relative to the thiophene ring are shown in table 4.42. No results were obtained for 3,3' OC(H)O BP.

Table 4.43 Thiophene ring and substituent dihedral angles of OC(H)O substituted cis-2,2'-bithiophene

Substitution. pos.	Method	S-C2-C2'-S' /°			C2-C3-O1-C6 /°			C2'-C3'-O1'-C6' /°		
		GS	EX	Dif	GS	EX	Dif	GS	EX	Dif
3	ADC(2)	50.2	13.5	-36.7	65.6	54.1	-11.5			
	CC2	51.1	12.4	-38.7	64.1	51.4	-12.7			
Substitution. pos.	Method	S-C2-C2'-S' /°			C3-C4-O1-C6 /°			C3'-C4'-O1'-C6' /°		
		GS	EX	Dif	GS	EX	Dif	GS	EX	Dif
4	ADC(2)	41	0	-41	127.1	180	52.9			
	CC2	40.7	0	-40.7	128.7	180	51.3			
4,4'	ADC(2)	0	0	0	180	180	0	180	180	0
	CC2	0	0	0	180	180	0	180	180	0
Substitution. pos.	Method	S-C2-C2'-S' /°			C2-C3-O1-C6 /°			C3'-C4'-O1'-C6' /°		
		GS	EX	Dif	GS	EX	Dif	GS	EX	Dif
3,4'	CC2	38.5	7	-31.5	57.4	59	1.6	119.6	139.9	20.3

Unlike OH substituted BP, there is more variation in the dihedral angle depending on substitution position, with 4,4' OC(H)O BP decreasing when substituted by ~40° to have a completely planar ground state geometry and the ground state dihedral angle of 3 OC(H)O BP increasing by ~10° compared to that of unsubstituted cis BP. 4 and 3,4' OC(H)O BP both remain very similar to the unsubstituted ground state geometry. In terms of the excited state geometries both 4 and 4,4' OC(H)O have completely planar geometries as does unsubstituted BP, whilst 3,4' OC(H)O deviated slightly from planarity.

The substituents of 4,4' OC(H)O begin and remain completely planar on excitation, whilst that of 4 OC(H)O increased to become planar. In 3,4' OC(H)O BP the C3 position substituent is ~30° from perpendicular relative to its thiophene ring and does not change significantly on excitation, whilst the C4 position OC(H)O group begins ~30° from perpendicular but becomes more planar

on excitation. In 3 OC(H)O BP the substituent begins $\sim 25^\circ$ from perpendicular relative to the thiophene ring and only became $\sim 10^\circ$ more planar on excitation.

Adiabatic excitation energies were calculated using the ground and excited state geometries and are shown in table 4.43.

Table 4.44 Adiabatic Excitation energies of OC(H)O substituted cis 2,2'-bithiophene

Substitution position	Method	Adiabatic excitation energy		Difference to unsubstituted	
		/eV	/cm ⁻¹	/eV	/cm ⁻¹
3	ADC(2)	3.9151	31577	0.05250	423.46
	CC2	3.9025	31476	0.03311	267.07
4	ADC(2)	3.7702	30409	-0.09237	-745.01
	CC2	3.7886	30557	-0.08080	-651.73
4,4'	ADC(2)	3.6015	29048	-0.26111	-2106
	CC2	3.6252	29239	-0.24423	-1970
3,4'	CC2	3.8656	31178	-0.00381	-30.76

As was the case with OC(H)O substituted trans BP, 4,4' OC(H)O cis BP has experienced the greatest decrease in excitation energy relative to its respective unsubstituted BP, followed by 4 OC(H)O BP, though in the case of substituted cis BP there is a greater difference between the magnitudes of the decreases in excitation energies for these two different substitutions. The 3 OC(H)O BP has a greater excitation energy than unsubstituted BP in contrast to its trans equivalent, which caused a slight decrease, which could be attributed to the trans ground state being completely planar, whilst the cis has decreased in planarity relative to unsubstituted BP.

4.5.3 OC(CH₃)O Substituted cis-2,2-bithiophene

The ground and excited state geometry S-C2-C2'-S' dihedral angle and dihedral angles of the OC(CH₃)O group(s) relative to the thiophene ring are shown in table 4.44.

Table 4.45 Thiophene ring and substituent dihedral angles of OC(CH₃)O substituted cis-2,2'-bithiophene

Substitution. pos.	Method	S-C2-C2'-S' /°			C2-C3-O1-C6 /°			C2'-C3'-O1'-C6' /°		
		GS	EX	Dif	GS	EX	Dif	GS	EX	Dif
3	ADC(2)	57	0	-57	86.1	180	93.9			
	CC2	58.1	3.9	-54.2	84.1	176	91.9			
Substitution. pos.	Method	S-C2-C2'-S' /°			C3-C4-O1-C6 /°			C3'-C4'-O1'-C6' /°		
		GS	EX	Dif	GS	EX	Dif	GS	EX	Dif
4	ADC(2)	41	0	-41	127	179.9	52.9			
	CC2	40.7	0	-40.7	128.8	179.9	51.1			
4,4'	ADC(2)	39.4	0	-39.4	121.6	180	58.4	121.9	180	58.1
	CC2	38.7	0	-38.7	124.2	179.9	55.7	124.2	179.9	55.7
Substitution. pos.	Method	S-C2-C2'-S' /°			C2-C3-O1-C6 /°			C3'-C4'-O1'-C6' /°		
		GS	EX	Dif	GS	EX	Dif	GS	EX	Dif
3,4'	ADC(2)	30.8	1.3	-29.5	68.4	71.6	3.2	83.2	6.2	-77
	CC2	31.6	7.6	-24	66.4	67.9	1.5	82.6	1.9	-80.7

As with OC(H)O BP there is little deviation in the dihedral angles from the unsubstituted ground state geometry, with only 3 and 3,4' OC(CH₃)O BP having increased by ~16° and decreased by ~10° respectively. There are even fewer differences from unsubstituted BP with regards to the dihedral angle of the excited state geometry, with 3 and 3,4' deviating slightly depending on the method used in the calculations.

The substituent of 3 OC(CH₃)O BP begins as perpendicular to the thiophene ring in the ground state and become planar on excitation. In both 4 and 4,4' OC(CH₃)O BP the substituents begin approximately midway between perpendicular and planar in the ground state and become completely planar on excitation. Finally in 3,4' OC(CH₃)O BP the C3 position substituent begins ~30° from perpendicular and become more so on excitation, whilst the C4 position substituent

begins almost completely planar in the ground state geometry and becomes almost completely planar in the excited state geometry.

Adiabatic excitation energies were calculated using the ground and excited state geometries and are displayed in table 4.45.

Table 4.46 Adiabatic Excitation energies of OC(CH₃)O substituted cis 2,2'-bithiophene

Substitution position	Method	Adiabatic excitation energy		Difference to unsubstituted	
		/eV	/cm ⁻¹	/eV	/cm ⁻¹
3	ADC(2)	3.9342	31731	0.07157	577.24
	CC2	3.9398	31777	0.07041	567.86
4	ADC(2)	3.7608	30333	-0.10175	-820.64
	CC2	3.7802	30490	-0.08918	-719.32
44	ADC(2)	3.6762	29650	-0.18640	-1503.5
	CC2	3.6949	29801	-0.17456	-1407.9
34	ADC(2)	3.7102	29925	-0.15241	-1229.2
	CC2	3.7447	30203	-0.12474	-1006.1

As with OH and OC(H)O substituted BP, 4,4' OC(CH₃)O BP has produced the greatest decrease in excitation energy relative to unsubstituted BP. 3,4' OC(CH₃)O BP occupies the midrange value for the decrease in excitation energy, and as with 3 OC(H)O BP, 3 OC(CH₃)O BP has a greater excitation energy than unsubstituted cis BP.

4.5.4 Phenyl Substituted cis-2,2-bithiophene

The ground and excited state geometry S-C2-C2'-S' dihedral angle and dihedral angles of the phenyl group(s) relative to the thiophene ring are shown in table 4.46. No results were obtained for 3 or 3,4' phenyl BP.

Table 4.47 Thiophene ring and substituent dihedral angles of phenyl substituted cis-2,2'-bithiophene

Substitution. pos.	Method	S-C2-C2'-S' /°			C2-C3-C6-C7 /°			C2'-C3'-C6'-C7' /°		
		GS	EX	Dif	GS	EX	Dif	GS	EX	Dif
3,3'	ADC(2)	61.1	36.4	-24.7	42.3	18.6	-23.7	42.3	18.6	-23.7
	CC2	62.7	37	-25.7	41.5	17.5	-24	41.5	17.5	-24
Substitution. pos.	Method	S-C2-C2'-S' /°			C3-C4-C6-C7 /°			C3'-C4'-C6'-C7' /°		
		GS	EX	Dif	GS	EX	Dif	GS	EX	Dif
4	ADC(2)	38.4	0.1	-38.3	37.5	19.9	-17.6			
	CC2	38.1	0.2	-37.9	37.1	14	-23.1			
4,4'	ADC(2)	0	0	0	37.7	24.6	-13.1	37.7	24.6	-13.1

The 3,3' phenyl BP has both ground and excited state dihedral angles that are significantly less planar than unsubstituted BP; by ~20° and 37° respectively. The dihedral angles of 4 phenyl BP are almost identical to the respective angles in unsubstituted cis BP, whilst both the ground and excited state dihedral angles of 4,4' phenyl BP are completely planar. As seen for phenyl substituted trans BP, the ground state dihedral angles relative to the thiophene rings of phenyl groups substituted at C3 positions are ~43° and those of phenyl groups attached at C4 positions are ~37°. Likewise, as with phenyl substituted trans BP they all become more planar on excitation, although to a slightly more planar value of ~20° in the case of cis 3,3' and 4 phenyl BP.

The ground and excited state geometries were used to calculate the adiabatic excitation energies and are displayed in table 4.47.

Table 4.48 Adiabatic Excitation energies of phenyl substituted cis 2,2'-bithiophene

Substitution position	Method	Adiabatic excitation energy		Difference to unsubstituted	
		/eV	/cm ⁻¹	/eV	/cm ⁻¹
4	ADC(2)	3.7338	30115	-0.12880	-1038.8
	CC2	3.7393	30159.	-0.13014	-1049.7
33	ADC(2)	3.2216	25984	-0.64096	-5169.7
	CC2	3.1918	25744	-0.67760	-5465.2
44	ADC(2)	3.6014	290478	-0.26114	-2106.2

As was the case with phenyl substituted trans BP, 3,3' phenyl BP has experienced the greatest decreases in excitation energy relative to unsubstituted BP, by an even greater magnitude than its trans configuration counterpart. Cis 4 and 4,4' phenyl BP has produced a decrease in the excitation energy of comparable magnitude to the trans equivalents, especially in the case of 4 phenyl BP.

4.5.5 Dimethylamino Substituted cis-2,2-bithiophene

The ground and excited state geometry S-C2-C2'-S' dihedral angle and dihedral angles of the dimethylamino group(s) relative to the thiophene ring are shown in table 4.48.

Table 4.49 Thiophene ring and substituent dihedral angles of dimethylamino substituted cis-2,2'-bithiophene

Sub. pos.	Method	S-C2-C2'-S' /°			C2-C3-N-C6 /°			C2-C3-N-C7 /°			C2'-C3'-N'-C6' /°			C2'-C3'-N'-C7' /°		
		GS	EX	Dif	GS	EX	Dif	GS	EX	Dif	GS	EX	Dif	GS	EX	Dif
3	ADC(2)	40.7	33.3	-7.4	63.3	47.2	-16.1	169.6	165.8	-3.8						
	CC2	42.6	33.1	-9.5	61.6	47.3	-14.3	171.1	166.6	-4.5						
3,3'	ADC(2)	45.8	26.2	-19.6	51.6	34.2	-17.4	175.8	175.7	-0.1	51.6	34.3	-17.3	175.8	175.7	-0.1
	CC2	45.9	26.6	-19.3	51.2	34.1	-17.1	175.8	175.8	0	51.2	34.2	-17	175.8	175.8	0
Sub. pos.	Method	S-C2-C2'-S'			C3-C4-N-C6 /°			C3-C4-N-C7 /°			C3'-C4'-N'-C6' /°			C3'-C4'-N'-C7' /°		
		GS	EX	Dif	GS	EX	Dif	GS	EX	Dif	GS	EX	Dif	GS	EX	Dif
4	ADC(2)	40.3	1.7	-38.6	49	6.8	-42.2	178.1	170.9	-7.2						
	CC2	39.7	1.2	-38.5	47.7	7.6	-40.1	177.1	170.7	-6.4						
4,4'	ADC(2)	0.1	0	-0.1	50.8	14.5	-36.3	179.5	166.5	-13	50.8	14.5	-36.3	179.5	166.5	-13
	CC2	0.1	0	-0.1	49.7	15.3	-34.4	178.6	165.9	-12.7	49.7	15.3	-34.4	178.6	165.9	-12.7
Sub. pos.	Method	S-C2-C2'-S'			C2-C3-N-C6 /°			C2-C3-N-C7 /°			C3'-C4'-N'-C6' /°			C3'-C4'-N'-C7' /°		
		GS	EX	Dif	GS	EX	Dif	GS	EX	Dif	GS	EX	Dif	GS	EX	Dif
3,4'	ADC(2)	37.2	8.6	-28.6	64.3	63.4	-0.9	168.9	170.4	1.5	49.8	3.9	-45.9	178.7	169.7	-9
	CC2	35.7	8.5	-27.2	63.2	62.4	-0.8	169.8	171.3	1.5	48.4	3.5	-44.9	177.6	168.8	-8.8

The ground state dihedral angles do not vary considerably with regards to substitution position, with the exception of 4,4' dimethylamino which has a completely planar ground state geometry, with those of 3 and 4 dimethylamino BP being almost identical to that of the unsubstituted geometry, and 3,4' and 3,3' dimethylamino BP being ~5° more planar and less planar respectively. On excitation the dihedral angle of 4,4' and 4' are completely and effectively planar respectively, as is the unsubstituted excited state geometry. The excited state dihedral angle of 3,4' dimethylamino BP deviates from planarity, and therefore the excited state geometry of unsubstituted cis BP, by ~9°, whilst those of 3 and 3,3' dimethylamino BP deviate more considerably by ~33° and 26° respectively.

The changes of the dihedral angles of the substituents of dimethylamino substituted cis BP follow the same patterns as their equivalent trans configurations, with the difference that the two methyl groups begin and end slightly more planar relative to the thiophene rings for the cis case, except for 4 dimethylamino BP where the trans and cis angles are basically identical.

Adiabatic excitation energies were calculated from the ground and excited state geometries and are listed in table 4.49.

Table 4.50 Adiabatic Excitation energies of dimethylamino substituted cis 2,2'-bithiophene

Substitution position	Method	Adiabatic excitation energy		Difference to unsubstituted	
		/eV	/cm ⁻¹	/eV	/cm ⁻¹
3	ADC(2)	3.3955	27386	-0.46711	-3767.5
	CC2	3.4291	27658	-0.44030	-3551.2
4	ADC(2)	3.1289	25236	-0.73370	-5917.7
	CC2	3.2200	25971	-0.64944	-5238.1
33	ADC(2)	3.2828	26477	-0.57979	-4676
	CC2	3.3330	26882	-0.53641	-4326
44	ADC(2)	3.0732	24787	-0.78934	-6366
	CC2	3.1367	25299	-0.73272	-5910
34	ADC(2)	3.0741	24794	-0.78847	-6359
	CC2	3.1669	25543	-0.70249	-5666

In common with trans dimethylamino BP, 3,4' and 4,4' and 4' experience the largest decreases in excitation energy when compared to unsubstituted BP, although in the case of 3,4' and 4,4' there is a less clear distinction between the magnitudes of the changes in excitation energy at these substitution positions. As opposed to OH substituted cis BP the magnitudes of these decrease are slightly less than their trans equivalents with the exception of the value obtained for 4,4' dimethylamino BP at the ADC(2) level.

4.6 Conclusion

Usable results for formyl, nitro and nitroso substituted BP could not be obtained using the CC2 and ADC(2) methods due to the high multi-reference character of their ground states. The most

significant changes to the ground state geometries on substitution occurred in terms of the S-C2-C2'-S' dihedral angles, with only minimal changes in bond lengths within the thiophene rings for most substituents regardless of substitution position. All excitations could be characterised as π to π^* transitions, as is the case for unsubstituted BP as shown in Chapter 3, and in line with previous studies of substituted bithiophene.^{15, 18-20}

With regards to substituted trans BP, dimethylamino substituted BP has experienced the greatest decrease in adiabatic excitation energy compared to unsubstituted BP, almost regardless of substitution position; the four greatest decreases in excitation energy all occur for dimethylamino substituted BP, followed closely by 3,3' phenyl BP, then 3 dimethylamino BP, and 3 and 3,4' phenyl BP. The significant decreases caused by the phenyl substituents, especially at the C3 positions where these large substituted groups are close to the central C2-C2' bond that determines the planarity and affects the conjugation of the molecule, is contrary to the predictions made in section 4.2 and to the findings of Casanovas et al where 3,3' carboxylic acid substituted bithiophene was found to have a greater energy gap when compared to both 3,4' and 4,4' carboxylic acid substituted bithiophene.¹⁶

The mid ranges of the excitation energy decreases are occupied by the 4 and 4,4' substituted OH, Phenyl, OC(H)O and OC(CH₃)O substituted BPs, with 4,4' substituted BP generally experiencing a greater decrease than 4 substituted BP. The OH, OC(H)O and OC(CH₃)O 3, 3,3' and 3,4' substitutions experienced the lowest decreases in the excitation energy compared to unsubstituted BP, with several of these having a greater excitation energy. The ranked results for substituted trans BP, from greatest to lowest decrease, are shown below in table 4.50.

Table 4.51 Ranking of the change in adiabatic excitation energies of substituted compared to unsubstituted trans 2,2'-bithiophene

ADC(2)				CC2			
1	3,4' dimethylainio	13	4,4' OC(CH ₃)O	1	3,4' dimethylainio	13	4 phenyl
2	4 dimethylainio	14	4 OC(CH ₃)O	2	4,4' dimethylainio	14	4 OC(H)O
3	4,4' dimethylainio	15	4 phenyl	3	4 dimethylainio	15	3,4' OH
4	3,3' dimethylainio	16	4 OC(H)O	4	3,3' dimethylainio	16	3,4 OC(H)O
5	3,3' phenyl	17	3 OC(H)O	5	3,3' phenyl	17	3 OC(H)O
6	3 dimethylainio	18	3,3' OH	6	3,4' phenyl	18	3,3' OH
7	3,4' phenyl	19	3,4' OC(CH ₃)O	7	3 dimethylainio	19	3 OH
8	3 phenyl	20	3,4 OC(H)O	8	3 phenyl	20	3 OC(CH ₃)O
9	4,4 OH	21	3 OH	9	4,4' Phenyl	21	3,3' OC(H)O
10	4 OH	22	3,3' OC(CH ₃)O	10	4 OH		
11	4,4' Phenyl	23	3 OC(CH ₃)O	11	4,4' OC(H)O		
12	4,4' OC(H)O	24	3,3 OC(H)O	12	4,4' OC(CH ₃)O		

The trends differ slightly for substituted cis BP; the greatest decreases relative to unsubstituted BP are still experienced by dimethylamino substituted BP and 3,3' phenyl substituted BP, but in this configuration OH substituted BP experiences much greater decreases in the excitation energy regardless of the substitution position. These are followed by 4,4' phenyl BP and 4,4' OC(H)O BP, then 4,4' and 3,4' OC(CH₃)O BP. The 4 phenyl, OC(H)O and OC(CH₃)O BP experience the smallest decrease in the excitation energy relative to unsubstituted cis BP, whilst 3 OC(H)O and OC(CH₃)O BP experience an increase in the excitation energy, in common with trans BP. The ranked results for substituted cis BP, from greatest to lowest decrease, are shown below in table 4.51. Whilst there have been previous investigations into bithiophene substituted at the 3,3', 3,4' and 4,4' positions, the area of interest of these studies has been the torsional potential as opposed to adiabatic excitation energies obtained in this report.^{15, 16, 19, 21, 22}

Table 4.52 Ranking of the change in adiabatic excitation energies of substituted compared to unsubstituted cis 2,2'-bithiophene

ADC(2)				CC2			
1	4,4' dimethylainio	11	3,4' OH	1	4,4' dimethylainio	11	4,4' OC(H)O
2	3,4' dimethylainio	12	4,4' phenyl	2	3,4' dimethylainio	12	3,4' OH
3	4 dimethylainio	13	4,4' OC(H)O	3	3,3' phenyl	13	4,4' OC(CH ₃)O
4	3,3' phenyl	14	4,4' OC(CH ₃)O	4	3,3' OH	14	4 phenyl
5	3,3' dimethylainio	15	3,4' OC(CH ₃)O	5	4 dimethylainio	15	3,4' OC(CH ₃)O
6	3,3' OH	16	4 phenyl	6	3,3' dimethylainio	16	4 OC(CH ₃)O
7	4,4' OH	17	4 OC(CH ₃)O	7	3 dimethylainio	17	4 OC(H)O
8	3 dimethylainio	18	4 OC(H)O	8	4,4' OH	18	3,4' OC(H)O
9	4 OH	19	3 OC(H)O	9	3,3' OC(H)O	19	3 OC(H)O
10	3,3' OH	20	3 OC(CH ₃)O	10	4 OH	20	3 OC(CH ₃)O

5 Chapter 5

5.1 Introduction

The aim of this chapter is to obtain ground and excited state geometries of unsubstituted thiophene oligomers of three and four repeat units, as well as for their OH and OC(H)O substituted counterparts. These will be used to calculate adiabatic excitation energies to be used alongside the dimer results obtained in Chapters 3 and 4 to perform an extrapolation to an excitation energy of a theoretical polymer of infinite length.

5.2 Linkage and Substitution Positions

Linkages were made between the C2 and C5 positions of the three and four repeat unit oligomers. Substitutions were made at the C3 positions, meaning that the first two thiophene rings were substituted at C3,3' relative to each other, whilst the second and third thiophene rings, and the third and fourth in the case of the tetramer, are substituted at the C3,C4' positions relative to each other. In each case sulphur atoms were oriented trans to each other in the input geometries. Figure 5.1 illustrates the above details using the OH substituted tetramer as an example; important carbon atoms have been labelled.

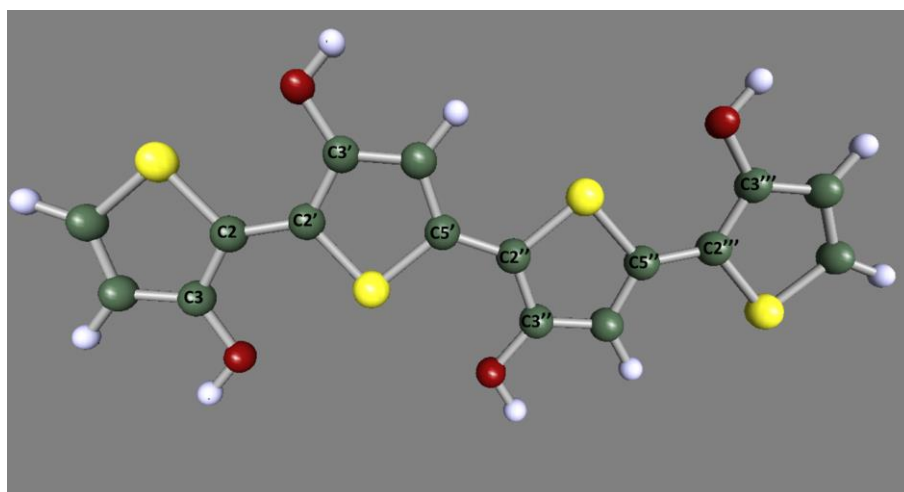


Figure 5.1 OH substituted tetrathiophene

The phenyl and dimethylamino groups were deemed too large for calculations involving oligomers with these substituents to be feasible within a reasonable time, and so were discounted. Due to the similarities between the OC(H)O and OC(CH₃)O, both in structure and in the results they produced previously in chapter 3, only the smaller substituent, OC(H)O, was selected for calculations, and so OC(CH₃)O was also discounted.

5.3 Computational Methods

Ground and excited state geometry calculations were performed using TURBOMOLE 6.4. Ground state geometries were obtained at the MP2/aug-cc-pVDZ and CC2/aug-cc-pVDZ levels, excited state geometries were obtained at the ADC(2)/aug-cc-pVDZ and CC2/aug-cc-pVDZ levels.

5.4 Results and Discussion

5.4.1 Geometries

Selected bond lengths of the ground and excited state geometries of unsubstituted thiophene, terthiophene and tetrathiophene, as well as each of their OH and OC(H)O substituted equivalents, are shown in appendix 7.5 as tables 7.35 through 7.42. As seen with unsubstituted and substituted BP investigated in Chapter 4, there are only very small differences, with regards to the bond angles within the thiophene rings, between the ground state geometries of the unsubstituted and substituted oligomers, and between the unsubstituted and substituted excited state geometries. However, as with substituted BP in Chapter 3, there are some more significant changes in the dihedral angles of each pair of thiophene rings on substitution, which for the trimers are shown below in table 5.1.

Table 5.1 Dihedral angles of unsubstituted and substituted terthiophene

Substituted group	Method	S-C2-C2'-S'			S'-C5'-C2''-S''		
		GS	EX	Diff	GS	EX	Diff
-	ADC(2)	153	180	27	153	180	27
	CC2	154.7	180	25.3	154.7	180	25.3
OH	ADC(2)	125.6	156.7	31.1	178.9	179.6	0.7
	CC2	126.5	157.8	31.3	178.9	179.9	1
OC(H)O	ADC(2)	71.3	27.8	-43.5	138.2	175.8	37.6
	CC2	73.6	27.9	-45.7	139.1	175.6	36.5

The ground state dihedral angle of the first two thiophene rings of the OH substituted trimer has deviated from that of the unsubstituted trimer by $\sim 27^\circ$, becoming less planar, whilst the ground state dihedral angle of the second and third rings has increased by ~ 25 on substitution to become almost completely planar. With regards to the excited state geometries, the dihedral angle of the first two rings also differs from that of the unsubstituted trimer, now by $\sim 23^\circ$, but for the second and third rings the dihedral angle is now almost identical to its unsubstituted equivalent.

The dihedral angles of the OC(H)O substituted trimer differ even more greatly from those of the unsubstituted trimer, with the first two rings (those that are substituted the positions 3,3' relative to each other) actually optimising in a cis configuration. The ground state dihedral angle of the second and third rings differs by a lesser degree than for its OH substituted equivalent, experiencing a decrease of $\sim 15^\circ$ relative to the equivalent angle in the unsubstituted ground state, and in the excited state only differs slightly by $\sim 4^\circ$, as with the corresponding dihedral angle of the OH substituted trimer.

Table 5.2 shows the dihedral angles of each pair of thiophene rings in the ground and excited states of the unsubstituted and substituted tetramers.

Table 5.2 Dihedral angles of unsubstituted and substituted tetrathiophene

Substituted group	Method	S-C2-C2'-S'			S'-C5'-C2''-S''			S''-C5''-C2'''-S'''		
		GS	EX	Diff	GS	EX	Dif	GS	EX	Diff
-	ADC(2)	154	180	26	160.1	180	19.9	154	180	26
	CC2	156.2	180	23.8	162.8	180	17.2	156.2	180	23.8
OH	ADC(2)	180	180	0	180	180	0	180	180	0
	CC2	180	180	0	180	180	0	180	180	0
OC(H)O	CC2	148.3	179.9	31.6	147.8	176.8	29	149.4	173.4	24

The OH substituted tetramer is completely planar, with the dihedral angles between all the thiophene rings being equal to 180°, both in the ground and excited state. The dihedral angles of the OC(H)O substituted tetramer do not differ significantly from those of the unsubstituted tetramer in either the ground or the excited state geometries. In the ground state the dihedral angle of the first two ring is ~6° less planar than that of the unsubstituted tetramer, and in the excited state is almost identical to it. The central dihedral angle, between the second and third thiophene rings, is ~12° less planar than the dihedral angle of the unsubstituted tetramer in the ground state and ~3° in the excited state, and the dihedral angle between the third and fourth rings is ~5° less planar than its unsubstituted equivalent in the ground state and ~6° in the excited state.

There are no significant changes of the bond lengths within the substituted groups on excitation for either the substituted trimers or tetramers; tables containing these bond lengths have been included in appendix 7.5 as table 7.43. As with the dihedral angles of the thiophene rings, there are more pronounced changes in the planarity of the substituted groups relative to the thiophene ring they are substituted to, on excitation; these angles are shown below in table 5.3.

Table 5.3 Dihedral angles of OH and OC(H)O substituents

Method	C2-C3-O-H			C2'-C3'-O'-H'			C2''-C3''-O''-H''			C2'''-C3'''-O'''-H'''		
	GS	EX	Dif	GS	EX	Dif	GS	EX	Dif	GS	EX	Dif
ADC(2)	177	178	1	2	7.7	5.7	179.6	178.5	-1.1			
CC2	176.9	177.5	0.6	1.2	7.4	6.2	179.6	179	-0.6			
ADC(2)	179.9	180	0.1	179.9	180	0.1	179.9	180	0.1	179.9	180	0.1
CC2	179.8	180	0.2	179.8	180	0.2	179.9	180	0.1	179.9	180	0.1
Method	C2-C3-C-O			C2'-C3'-C'-O'			C2''-C3''-C''-O''			C2'''-C3'''-C'''-O'''		
	GS	EX	Dif	GS	EX	Dif	GS	EX	Dif	GS	EX	Dif
ADC(2)	49.3	51.4	2.1	46.3	48	1.7	55.9	83	27.1			
CC2	47.9	48.7	0.8	44.3	49.6	5.3	54.9	81.1	26.2			
CC2	62.9	84.7	21.8	67.6	132.3	64.7	64.8	176.6	111.8	63.5	79.6	16.1

The OH groups of the substituted trimer and tetramer remain almost completely planar in both the ground and excited states; with the greatest fluctuation being a decrease in planarity of $\sim 6^\circ$ on excitation for the OH group attached to the central ring in the trimer. In the OC(H)O substituted trimer the substituted group attached to ring three becomes almost perpendicular relative the thiophene ring on excitation, and for the OC(H)O substituted tetramer this similarly happens to two of the substituents, those attached to rings one and four. The other two substituents experience an increase in the dihedral angle large enough to go from cis, where the substituent is oriented towards the adjacent thiophene ring, to trans, where the substituent is oriented away from the adjacent ring, both becoming more planar relative to their thiophene rings; with the substituent attached to ring three becoming almost completely planar.

The most significant dihedral angle changes are detailed below in figures 5.2 and 5.3 below.

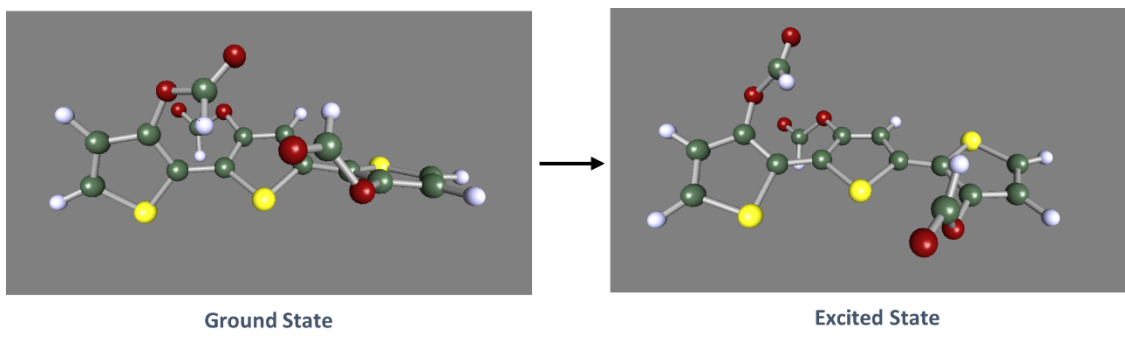


Figure 5.2 Geometry change of OC(H)O substituted terthiophene on excitation

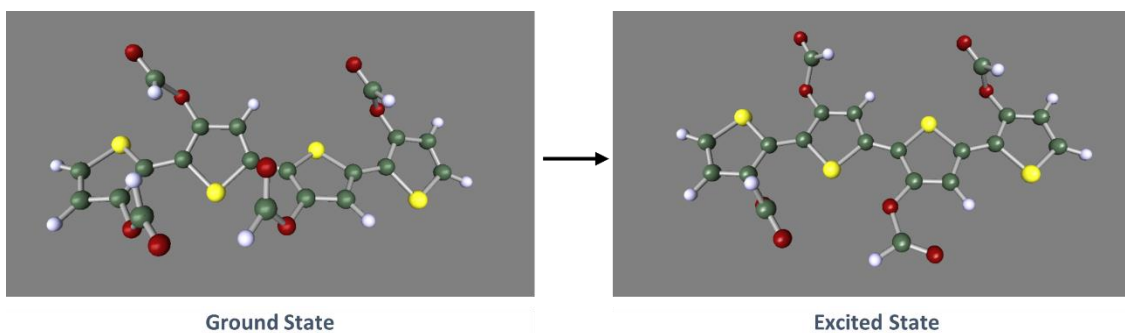


Figure 5.3 Geometry change of OC(H)O substituted tetrathiophene on excitation

5.4.2 Excitation Energies and Extrapolation

Adiabatic excitation energies were calculated for the unsubstituted and substituted oligomers using the relevant ground and excited state geometries. The trimer adiabatic excitation energies are presented in table 5.4 and the tetramer adiabatic excitation energies are shown in table 5.5.

Table 5.4 Adiabatic excitation energies of unsubstituted and substituted terthiophene

Substituted group	Method	Adiabatic excitation energy		Difference from unsubstituted	
		/eV	/cm ⁻¹	/eV	/cm ⁻¹
-	ADC(2)	3.2089	25881		
	CC2	3.2204	25974		
OH	ADC(2)	3.1138	25114	-0.09509	-766.96
	CC2	3.1947	25767	-0.02571	-207.33
OC(H)O	ADC(2)	3.4604	27910	0.251536	2028.7
	CC2	3.4991	28222	0.278635	2247.3

Table 5.5 Adiabatic excitation energies of unsubstituted and substituted tetrathiophene

Substituted group	Method	Adiabatic excitation energy		Difference from unsubstituted	
		/eV	/cm ⁻¹	/eV	/cm ⁻¹
-	ADC(2)	2.8399	22905		
	CC2	2.8499	22986		
OH	ADC(2)	2.4675	19902	-0.37234	-3003.1
	CC2	2.5910	20898	-0.25892	-2088.3
OC(H)O	ADC(2)				
	CC2	2.9616	23887	0.11164	900.47

It is possible to obtain an approximation for a property of a polymer at a theoretical infinite chain length by extrapolating the linear curve of the property, in the case of this thesis the excitation energy, against the reciprocal of the number of repeat units.⁵¹ This produces a linear fit and the value obtained when the reciprocal of the repeat units is zero, the y intercept, will be the value of the energy at this 'infinite' length. The linearity of this representation is only maintained when using oligomers up to 12 repeat units of length.^{51, 52} After this more advanced models are required to perform the extrapolation, however calculations on oligomers of this size are outside of the scope of this thesis due to the computational and associated time cost of conducting them.⁵³

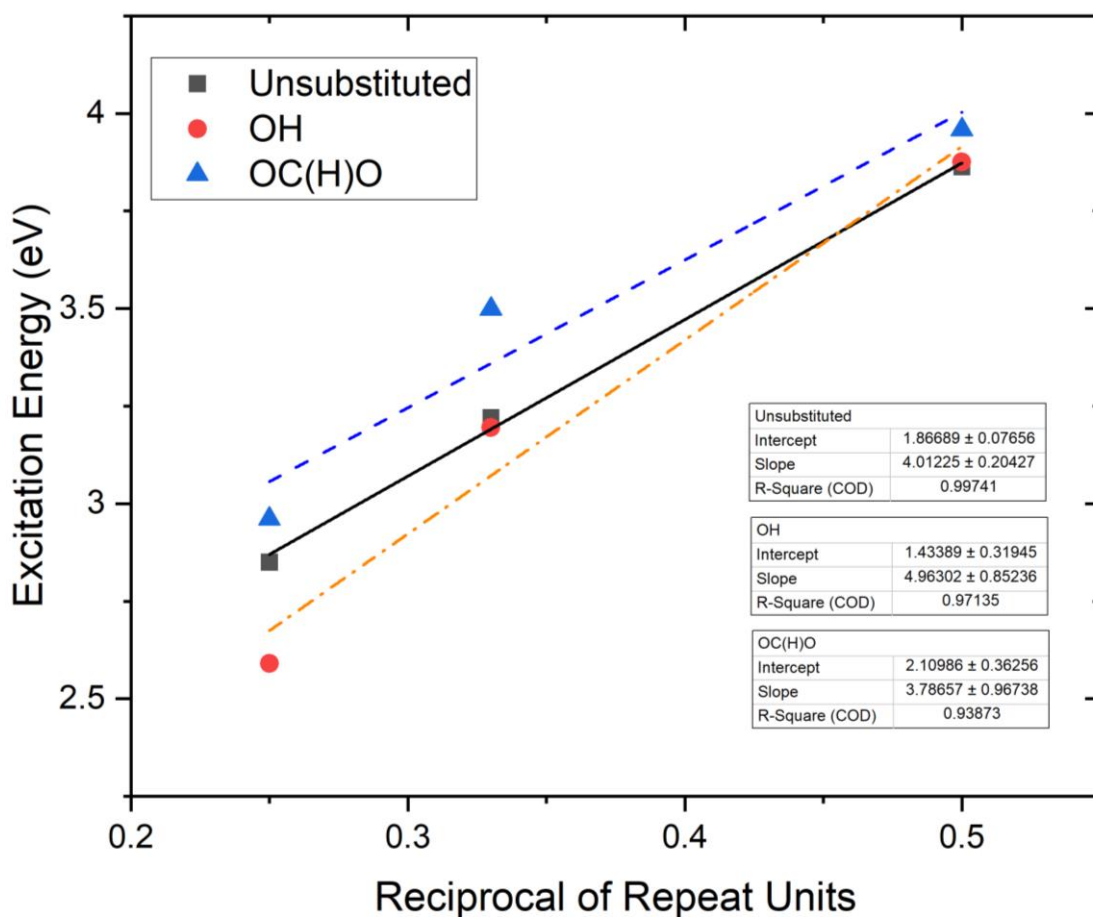


Figure 5.4 Extrapolation to an infinite length of the adiabatic excitation energy of unsubstituted, OH and OC(H)O substituted oligomers at the CC2/aug-cc-pVDZ level

Figure 5.4 shows the results of the extrapolation to an infinite polymer length using the geometries obtained at the CC2/aug-cc-pVDZ level. The unsubstituted polymer would have an adiabatic excitation energy of 1.867 eV, the OC(H)O substituted polymer has experienced an increase relative to this and obtained a value of 2.110 eV, whilst the OH substituted polymer has seen a decrease relative to the unsubstituted polymer and produced a value of 1.434 eV. It should be noted that the substituted oligomer extrapolations have both produced large errors of 22.3% and 17.2% for OH and OC(H)O substituted respectively. Reducing these could require the calculation of oligomers of greater numbers of repeat units, however this is outside the scope of this thesis due to the computational cost.

5.5 Conclusion

Values for the excitation of theoretical substituted polythiophene have been obtained as 2.110 eV for an OC(H)O substituted polymer and 1.434 eV for an OH substituted polymer. The energy of visible light ranges from ~ 1.8 to ~ 3.5 eV and as such both of these theoretical excitation energies, in particular that of the OH substituted polythiophene, can be considered low enough to cause significant energy loss through thermalization as the energy of the incident light could easily exceed the energy of the ground state to S_1 excitation. However, the values predicted by extrapolations using oligomers of up to 12 repeat units are typically underestimations of the actual values⁵², in order to obtain more a more accurate prediction oligomers of higher repeat units would have to be used, something that is not feasible using the CC2 and ADC(2) methods.

In the previously mentioned study by Casanovas et al thiophene oligomers of up to seven repeat units were investigated, with carboxylic acid groups substituted on every thiophene ring as was the case for the OH and OC(H)O groups investigated by this report.¹⁶ De Oliveira et al studied OC(H)O substituted oligothiophenes of up to six repeat units, however substitutions were only made to one or two of the thiophene rings, as opposed to every ring in the oligomer as in this report.²³

6 Chapter 6

6.1 Conclusion

Ab initio calculations have been performed on unsubstituted cis and trans BP using the CC2 and ADC(2) methods and the aug-cc-pVDZ basis set to obtain ground and excited state geometries subsequently used to obtain values for the adiabatic excitation energies that agree very well both with each other and with the experimental results of Chadwick and Kohler.⁴⁹

Ground and excited state geometries were then obtained for OH, OC(H)O, OC(CH₃)O, phenyl and dimethylamino substituted cis and trans BP, with substitutions made singly at the 3 and 4 positions, and doubly at the 3,3' , 3,4' and 4,4' positions. The most significant changes to the geometries on substitution occurred in terms of the S-C2-C2'-S' dihedral angles, with only minimal changes in bond lengths within the thiophene rings for most substituents regardless of substitution position. Adiabatic excitation energies were calculated using the ground and excited state energies, and all excitations were characterised as π to π^* transitions in line with previous studies on substituted BP.^{15, 18-20}

For both trans and cis BP the dimethylamino substituent was found to cause the greatest decrease in the adiabatic excitation energy in comparison to unsubstituted BP, almost regardless of substitution position, having excitation energies in the range of ~ 24000 to 27000 cm^{-1} compared to the unsubstituted values of 31111 and 31203 cm^{-1} for trans and cis BP respectively. The phenyl substituent caused a greater decrease in the adiabatic excitation energy than predicted, with the substitutions at the 3, 3,3' and 3,4' causing a greater decrease than those at the 4 and 4,4' positions, also contrary to prediction. Position 4 and 4,4' substituted OH, Phenyl, OC(H)O and OC(CH₃)O substituted BP produced mid-range excitation energy decreases with values in the 28000 to 30000 cm^{-1} range , with 4,4' substituted BP generally experiencing a greater decreases than 4 substituted BP. The OH, OC(H)O and OC(CH₃)O 3, 3,3' and 3,4' substitutions experienced the lowest decreases in the excitation energy compared to

unsubstituted BP, with 3 and 3,3' OH, 3,3' OC(H)O and 3 and 3,3' OC(CH₃)O all resulting in a slight increase in excitation energy compared unsubstituted BP. Previous studies on the effects of substitution groups at the 3,3', 3,4 and 4,4' positions have focused on torsional potentials, this report seeks to provide new information by primarily studying adiabatic excitation energies.^{15,}

16, 19, 21, 22, 54

A final series of calculations were performed to obtain ground and excited state geometries for unsubstituted, OH and OC(H)O substituted oligomers of three and four repeat units. The reciprocal of the repeat units against adiabatic excitation energy determined using these geometries was plotted to extrapolate to the excitation energy of a theoretical substituted polythiophene of infinite length, giving values of 2.110 eV for an OC(H)O substituted polymer and 1.434 eV for an OH substituted polymer. However, the values predicted by extrapolations using oligomers of 12 or less repeat units are typically underestimations of the actual values and using the CC2 and ADC(2) methods to perform calculations on oligomers of higher repeat units, in order to obtain more a more accurate prediction, is not feasible within the scope of this project.⁵²

6.2 Potential Areas of Further Study

This project could be further developed by performing the calculations on the higher repeat unit oligomers required to obtain accurate predictions for a theoretical substituted polythiophene of infinite length, as discussed in Chapter 5. Another area for further study is the addition of a typical electron acceptor found in OPVs, such as the fullerenes mentioned in Chapter 1, to the substituted BPs and investigate the effect this has on the adiabatic excitation energies. However, the size of these acceptor molecules may incur too great a computational cost for these calculations to be feasible using the methods selected for this report.

7 Appendix

7.3 Chapter 3 Supplementary Material

Table 7.1 Contributors to the S_1 excitation of *trans* 2,2'-bithiophene

Basis set	ADC(2)			CC2		
	Occupied	Virtual	%	Occupied	Virtual	%
Aug-cc-pVDZ	HOMO	LUMO +2	92.6	HOMO	LUMO +2	92.6
	HOMO -2	LUMO +2	2.2	HOMO -2	LUMO +2	1.9
cc-pVDZ	HOMO	LUMO	93.7	HOMO	LUMO	93.8
	HOMO -2	LUMO	1.9	HOMO -2	LUMO	2.2

Table 7.2 Contributors to the S_1 excitation of *cis* 2,2'-bithiophene

Basis set	ADC(2)			CC2		
	Occupied	Virtual	%	Occupied	Virtual	%
Aug-cc-pVDZ	HOMO	LUMO +2	91.2	HOMO	LUMO +2	92.2
	HOMO -1	LUMO +2	3.9	HOMO -1	LUMO +2	3.5
cc-pVDZ	HOMO	LUMO	91.6	HOMO	LUMO	91.4
	HOMO -1	LUMO	4.7	HOMO -1	LUMO	4.4

7.4 Chapter 4 Supplementary Material

Table 7.3 Contributors to the S_1 excitation of OH substituted *trans* 2,2'-bithiophene

Substitution Position	ADC(2)			CC2		
	Occupied	Virtual	%	Occupied	Virtual	%
3	HOMO	LUMO +2	84.5	HOMO	LUMO +2	72.3
	HOMO	LUMO +3	2.9	HOMO	LUMO +3	12.6
	HOMO	LUMO	2.8	HOMO	LUMO	2.6
	HOMO -1	LUMO +2	1	HOMO -1	LUMO +2	1.4
				HOMO	LUMO +4	1.2
Substitution Position	ADC(2)			CC2		
	Occupied	Virtual	%	Occupied	Virtual	%
4	HOMO	LUMO +2	85	HOMO	LUMO +2	87.1
	HOMO -1	LUMO +2	8.1	HOMO -1	LUMO +2	6
Substitution Position	ADC(2)			CC2		
	Occupied	Virtual	%	Occupied	Virtual	%
3,3'	HOMO	LUMO +5	79.2	HOMO	LUMO +5	72.1
	HOMO	LUMO	8.8	HOMO	LUMO	12.4
	HOMO	LUMO +4	2.2	HOMO	LUMO +4	4
	HOMO	LUMO +3	1.2	HOMO	LUMO +3	2
Substitution Position	ADC(2)			CC2		
	Occupied	Virtual	%	Occupied	Virtual	%
4,4'	HOMO	LUMO +2	88.2			
	HOMO -2	LUMO +2	6.2			
Substitution Position	ADC(2)			CC2		
	Occupied	Virtual	%	Occupied	Virtual	%
3,4'				HOMO	LUMO +2	75.4
				HOMO	LUMO	11.4
				HOMO -1	LUMO +2	1.6
				HOMO -2	LUMO +2	1.3

Table 7.4 Contributors to the S_1 excitation of OC(H)O substituted *trans* 2,2'-bithiophene

Substitution Position	ADC(2)			CC2		
	Occupied	Virtual	%	Occupied	Virtual	%
3	HOMO	LUMO +2	93.7	HOMO	LUMO +2	93.3
Substitution Position	ADC(2)			CC2		
	Occupied	Virtual	%	Occupied	Virtual	%
4	HOMO	LUMO +1	90.8	HOMO	LUMO +1	91.4
	HOMO -2	LUMO +1	2.2	HOMO -2	LUMO +1	1.8
	HOMO -1	LUMO +1	1.7	HOMO -1	LUMO +1	1.2
Substitution Position	ADC(2)			CC2		
	Occupied	Virtual	%	Occupied	Virtual	%
3,3'	HOMO	LUMO +2	90.5	HOMO	LUMO +2	88.5
	HOMO	LUMO	2.1	HOMO	LUMO	3.3
Substitution Position	ADC(2)			CC2		
	Occupied	Virtual	%	Occupied	Virtual	%
4,4'	HOMO	LUMO	89.6	HOMO	LUMO	90.5
	HOMO -2	LUMO	4.1	HOMO -2	LUMO	3.4
Substitution Position	ADC(2)			CC2		
	Occupied	Virtual	%	Occupied	Virtual	%
3,4'	HOMO	LUMO	92.7	HOMO	LUMO	89.9
	HOMO -2	LUMO	1.1	HOMO -1	LUMO	2.5

Table 7.5 Contributors to the S_1 excitation of OC(CH₃)O substituted trans 2,2'-bithiophene

Substitution Position	ADC(2)			CC2		
	Occupied	Virtual	%	Occupied	Virtual	%
3	HOMO	LUMO +3	91.4	HOMO	LUMO +3	90.9
	HOMO	LUMO +6	2.6	HOMO	LUMO +6	2.6
Substitution Position	ADC(2)			CC2		
	Occupied	Virtual	%	Occupied	Virtual	%
4	HOMO	LUMO +2	90.1			
	HOMO -1	LUMO +2	2.8			
	HOMO -2	LUMO +2	1.8			
Substitution Position	ADC(2)			CC2		
	Occupied	Virtual	%	Occupied	Virtual	%
3,3'	HOMO	LUMO +3	65.8			
	HOMO	LUMO +1	18.4			
	HOMO	LUMO +4	3.8			
	HOMO	LUMO +2	1.2			
Substitution Position	ADC(2)			CC2		
	Occupied	Virtual	%	Occupied	Virtual	%
4,4'	HOMO	LUMO	89.7	HOMO	LUMO	90.3
	HOMO -2	LUMO	3.5	HOMO -2	LUMO	2.9
	HOMO -1	LUMO	1.3	HOMO -1	LUMO	1
Substitution Position	ADC(2)			CC2		
	Occupied	Virtual	%	Occupied	Virtual	%
3,4'	HOMO	LUMO	76.9			
	HOMO	LUMO +1	7.5			
	HOMO	LUMO +2	5.7			
	HOMO -1	LUMO	2			

Table 7.6 Contributors to the S_1 excitation of phenyl substituted *trans* 2,2'-bithiophene

Substitution Position	ADC(2)			CC2		
	Occupied	Virtual	%	Occupied	Virtual	%
3	HOMO	LUMO	89.6	HOMO	LUMO	88.9
	HOMO -2	LUMO	2.5	HOMO -2	LUMO	2.3
				HOMO -1	LUMO	1.1
Substitution Position	ADC(2)			CC2		
	Occupied	Virtual	%	Occupied	Virtual	%
4	HOMO	LUMO +2	90.2	HOMO	LUMO +2	90.3
	HOMO	LUMO +9	1.5	HOMO	LUMO +9	1.4
	HOMO -4	LUMO	1			
Substitution Position	ADC(2)			CC2		
	Occupied	Virtual	%	Occupied	Virtual	%
3,3'	HOMO	LUMO	93.3	HOMO	LUMO	93.1
	HOMO -2	LUMO	2.3	HOMO -2	LUMO	2.3
Substitution Position	ADC(2)			CC2		
	Occupied	Virtual	%	Occupied	Virtual	%
4,4'	HOMO	LUMO +2	89.7	HOMO	LUMO +2	88.4
	HOMO -2	LUMO +16	2.3	HOMO -2	LUMO +16	2.3
	HOMO -6	LUMO	1.9	HOMO -6	LUMO	1.6
Substitution Position	ADC(2)			CC2		
	Occupied	Virtual	%	Occupied	Virtual	%
3,4'	HOMO	LUMO	89.1	HOMO	LUMO	88.9
	HOMO -1	LUMO	1.3	HOMO -1	LUMO	1.4
	HOMO	LUMO +1	1.2	HOMO	LUMO +1	1.3

Table 7.7 Contributors to the S_1 excitation of singly dimethylamino substituted *trans* 2,2'-bithiophene

Substitution Position	ADC(2)			CC2		
	Occupied	Virtual	%	Occupied	Virtual	%
3	HOMO	LUMO +5	20.8	HOMO	LUMO +5	23.4
	HOMO	LUMO +6	16.3	HOMO	LUMO +3	15
	HOMO	LUMO +3	13.2	HOMO	LUMO +6	13.7
	HOMO	LUMO +4	12.5	HOMO	LUMO +4	12.9
	HOMO -1	LUMO +5	6.9	HOMO -1	LUMO +5	6.9
	HOMO -1	LUMO +6	5.2	HOMO -1	LUMO +3	4.4
	HOMO -1	LUMO +3	4.5	HOMO -1	LUMO +6	3.8
	HOMO -1	LUMO +4	4.1	HOMO -1	LUMO +4	3.7
	HOMO -4	LUMO +5	2.3	HOMO -4	LUMO +5	2.2
	HOMO -4	LUMO +6	1.7	HOMO -4	LUMO +3	1.5
	HOMO -4	LUMO +3	1.5	HOMO -4	LUMO +6	1.2
	HOMO -4	LUMO +4	1.3	HOMO	LUMO +1	1.2
	HOMO	LUMO +1	1	HOMO -4	LUMO +4	1.1
Substitution Position	ADC(2)			CC2		
	Occupied	Virtual	%	Occupied	Virtual	%
4	HOMO	LUMO +2	71.5	HOMO	LUMO +2	71.9
	HOMO -1	LUMO +2	10.5	HOMO -1	LUMO +2	10.6
	HOMO	LUMO +5	4.1	HOMO	LUMO +5	5
	HOMO	LUMO	4.1	HOMO	LUMO	2.6

Table 7.8 Contributors to the S_1 excitation of doubly dimethylamino substituted *trans* 2,2'-bithiophene

Substitution Position	ADC(2)			CC2		
	Occupied	Virtual	%	Occupied	Virtual	%
3,3'	HOMO	LUMO +8	64.5	HOMO	LUMO +8	65.5
	HOMO	LUMO +9	8	HOMO	LUMO +9	6.9
	HOMO	LUMO +3	5.6	HOMO	LUMO +3	6.1
	HOMO -5	LUMO +8	4.5	HOMO -5	LUMO +8	4.1
	HOMO	LUMO +4	3.4	HOMO	LUMO +4	3.5
	HOMO -2	LUMO +9	3	HOMO	LUMO	2.4
	HOMO	LUMO	2.9	HOMO -2	LUMO +9	2.4
	HOMO	LUMO +5	1	HOMO	LUMO +5	1
Substitution Position	ADC(2)			CC2		
	Occupied	Virtual	%	Occupied	Virtual	%
4,4'	HOMO	LUMO +2	68.4	HOMO	LUMO +2	67.3
	HOMO -1	LUMO +2	8.9	HOMO	LUMO +6	8.6
	HOMO	LUMO +6	6.4	HOMO -1	LUMO +2	8.6
	HOMO -2	LUMO	2.1	HOMO -2	LUMO	2.2
	HOMO	LUMO	1.6	HOMO	LUMO +1	1.2
	HOMO	LUMO +1	1.5	HOMO -1	LUMO +6	1.1
Substitution Position	ADC(2)			CC2		
	Occupied	Virtual	%	Occupied	Virtual	%
3,4'	HOMO	LUMO +3	40.8	HOMO	LUMO +6	37.1
	HOMO	LUMO +6	22.9	HOMO	LUMO +5	16.2
	HOMO	LUMO +5	12.1	HOMO	LUMO +3	15.9
	HOMO -1	LUMO +3	3.8	HOMO	LUMO +4	7.6
	HOMO	LUMO +7	3.4	HOMO	LUMO +7	2.7
	HOMO -1	LUMO +6	2.1	HOMO	LUMO +11	2
	HOMO	LUMO +11	1.3	HOMO -1	LUMO +6	1.9
	HOMO -1	LUMO +5	1.1	HOMO -2	LUMO +6	1.7
	HOMO	LUMO +1	1.1			

Table 7.9 Changes in selected bond lengths and dihedral angle of OC(CH₃)O substituted BP on excitation at the ADC(2) level

Sub. pos.	Bond length change /Å											C2-S-S'-C2' angle change /°
	C2-C2'	C2-C3	C3-C4	C4-C5	C5-S	S-C2	C2'-C3'	C3'-C4'	C4'-C5'	C5'-S'	S'-C2'	
-	-0.07	0.048	-0.025	0.026	0.002	0.047	0.048	-0.025	0.026	0.002	0.047	32.7
C3	-0.065	0.057	-0.02	0.028	0.002	0.048	0.055	-0.026	0.021	0.01	0.04	39.1
C4	-0.067	0.041	-0.019	0.032	-0.001	0.065	0.045	-0.022	0.021	0.004	0.036	0
C3,C3'	-0.056	0.048	-0.028	0.029	0.002	0.039	0.058	-0.018	0.015	0.016	0.027	-10.3
C4,C4'	-0.066	0.044	-0.021	0.023	0.004	0.047	0.042	-0.013	0.034	-0.006	0.057	31.1
C3,C4'	-0.069	0.051	-0.021	0.018	0.007	0.043	0.05	-0.025	0.03	0.001	0.06	35.1

Table 7.10 Changes in selected bond lengths and dihedral angle of OC(CH₃)O substituted BP on excitation at the CC2 level

Sub. pos.	Bond length change /Å											C2-S-S'-C2' angle change /°
	C2-C2'	C2-C3	C3-C4	C4-C5	C5-S	S-C2	C2'-C3'	C3'-C4'	C4'-C5'	C5'-S'	S'-C2'	
-	-0.07	0.048	-0.025	0.026	0.002	0.047	0.048	-0.025	0.026	0.002	0.047	32.7
C3	-0.062	0.056	-0.019	0.026	0.004	0.043	0.053	-0.025	0.022	0.008	0.039	38.1
C4,C4'	-0.065	0.045	-0.021	0.025	0.004	0.045	0.041	-0.015	0.033	-0.007	0.054	29.6

Table 7.11 Selected bond lengths of substituents of phenyl substituted trans 2,2'-bithiophene at ADC(2) level

Sub. pos.	Bond length change/Å													
	C3-C6	C6-C7	C7-C8	C8-C9	C9-C10	C10-C11	C11-C6	C3'-C6'	C6'-C7'	C7'-C8'	C8'-C9'	C9'-C10'	C10'-C11'	C11'-C6'
3	-0.043	0.028	0.006	-0.007	0.017	-0.013	0.021							
3,3'	-0.027	0.012	-0.001	0	0.007	-0.007	0.013	-0.027	0.012	-0.001	0	0.007	-0.007	0.013
Sub. pos.	Bond length change/Å													
	C4-C6	C6-C7	C7-C8	C8-C9	C9-C10	C10-C11	C11-C6	C4'-C6'	C6'-C7'	C7'-C8'	C8'-C9'	C9'-C10'	C10'-C11'	C11'-C6'
4	-0.008	0.005	-0.002	0.002	0	0	0.005							
4,4'	-0.005	0.002	-0.001	0.001	0	0	0.002	-0.005	0.002	-0.001	0.001	0	0	0.002
Sub. pos.	Bond length change/Å													
	C3-C6	C6-C7	C7-C8	C8-C9	C9-C10	C10-C11	C11-C6	C3'-C6'	C6'-C7'	C7'-C8'	C8'-C9'	C9'-C10'	C10'-C11'	C11'-C6'
3,4'	-0.042	0.027	0.008	-0.008	0.017	-0.013	0.02	-0.007	0.003	-0.001	0.001	0	-0.001	0.002

Table 7.12 Selected bond lengths of substituents of phenyl substituted *trans* 2,2'-bithiophene at CC2 level

Sub. pos.	Bond length change/Å													
	C3-C6	C6-C7	C7-C8	C8-C9	C9-C10	C10-C11	C11-C6	C3'-C6'	C6'-C7'	C7'-C8'	C8'-C9'	C9'-C10'	C10'-C11'	C11'-C6'
3	-0.045	0.031	0.008	-0.008	0.019	-0.014	0.022							
3,3'	-0.028	0.012	0	0	0.008	-0.006	0.012	-0.027	0.012	0	0	0.008	-0.006	0.012
Sub. pos.	Bond length change/Å													
	C4-C6	C6-C7	C7-C8	C8-C9	C9-C10	C10-C11	C11-C6	C4'-C6'	C6'-C7'	C7'-C8'	C8'-C9'	C9'-C10'	C10'-C11'	C11'-C6'
4	-0.009	0.006	-0.002	0.002	0.001	-0.001	0.005							
4,4'	-0.006	0.003	-0.002	0.001	0.001	-0.001	0.003	-0.058	-0.01	0.003	0.001	-0.003	0.011	0.055
Sub. pos.	Bond length change/Å													
	C3-C6	C6-C7	C7-C8	C8-C9	C9-C10	C10-C11	C11-C6	C3'-C6'	C6'-C7'	C7'-C8'	C8'-C9'	C9'-C10'	C10'-C11'	C11'-C6'
3,4'	-0.045	0.032	0.01	-0.009	0.019	-0.014	0.021	-0.008	0.004	-0.002	0.002	0	-0.001	0.003

Table 7.13 Selected bond lengths of the OH substituted *cis* BP ground state geometry

Sub. pos.	Method	Bond length /Å										
		C2-C2'	C2-C3	C3-C4	C4-C5	C5-S	S-C2	C2'-C3'	C3'-C4'	C4'-C5'	C5'-S'	S'-C2'
-	MP2	1.455	1.398	1.421	1.392	1.728	1.741	1.398	1.421	1.392	1.728	1.741
	CC2	1.455	1.397	1.425	1.392	1.735	1.749	1.397	1.425	1.392	1.735	1.749
4	MP2	1.454	1.398	1.42	1.391	1.728	1.74	1.4	1.42	1.391	1.73	1.742
	CC2	1.454	1.398	1.424	1.391	1.735	1.747	1.399	1.424	1.391	1.736	1.749
4,4'	MP2	1.452	1.396	1.418	1.392	1.732	1.743	1.399	1.42	1.391	1.729	1.74
	CC2	1.453	1.396	1.422	1.392	1.739	1.75	1.398	1.424	1.391	1.735	1.747
3,4'	MP2	1.45	1.401	1.422	1.388	1.728	1.743	1.397	1.42	1.39	1.732	1.746
	CC2	1.449	1.4	1.425	1.389	1.734	1.751	1.397	1.423	1.391	1.74	1.753

Table 7.14 Selected bond lengths of the OH substituted *cis* BP excited state geometry

Sub. pos.	Method	Bond length /Å										
		C2-C2'	C2-C3	C3-C4	C4-C5	C5-S	S-C2	C2'-C3'	C3'-C4'	C4'-C5'	C5'-S'	S'-C2'
-	ADC(2)	1.386	1.445	1.394	1.42	1.727	1.79	1.445	1.394	1.42	1.727	1.79
	CC2	1.387	1.444	1.397	1.421	1.733	1.797	1.444	1.397	1.421	1.733	1.797
4	ADC(2)	1.388	1.43	1.414	1.422	1.725	1.829	1.437	1.4	1.413	1.73	1.782
	CC2	1.389	1.428	1.416	1.423	1.727	1.829	1.436	1.403	1.414	1.737	1.79
4,4'	ADC(2)	1.388	1.429	1.405	1.418	1.727	1.803	1.429	1.413	1.416	1.725	1.811
	CC2	1.389	1.428	1.408	1.419	1.732	1.809	1.428	1.415	1.417	1.729	1.815
3,4'	ADC(2)	1.381	1.446	1.392	1.423	1.737	1.789	1.435	1.398	1.432	1.725	1.825
	CC2	1.383	1.438	1.398	1.418	1.743	1.808	1.425	1.402	1.429	1.726	1.851

Table 7.15 Selected bond lengths of the OC(H)O substituted cis BP ground state geometry

Sub. pos.	Method	Bond length /Å										
		C2-C2'	C2-C3	C3-C4	C4-C5	C5-S	S-C2	C2'-C3'	C3'-C4'	C4'-C5'	C5'-S'	S'-C2'
-	MP2	1.455	1.398	1.421	1.392	1.728	1.741	1.398	1.421	1.392	1.728	1.741
	CC2	1.455	1.397	1.425	1.392	1.735	1.749	1.397	1.425	1.392	1.735	1.749
3	MP2	1.452	1.396	1.416	1.39	1.73	1.736	1.398	1.42	1.393	1.726	1.738
4	MP2	1.454	1.395	1.417	1.387	1.726	1.744	1.398	1.421	1.392	1.728	1.74
	CC2	1.454	1.394	1.421	1.387	1.733	1.751	1.397	1.424	1.392	1.735	1.748
4,4'	MP2	1.453	1.399	1.421	1.392	1.723	1.74	1.399	1.421	1.392	1.723	1.74
	CC2	1.453	1.398	1.425	1.391	1.73	1.748	1.398	1.425	1.391	1.73	1.748
3,4'	MP2	1.451	1.399	1.421	1.389	1.738	1.746	1.397	1.42	1.392	1.734	1.752
	CC2	1.451	1.399	1.421	1.389	1.738	1.746	1.397	1.42	1.392	1.734	1.752

Table 7.16 Selected bond lengths of the OC(H)O substituted cis BP excited state geometry

Sub. pos.	Method	Bond length /Å										
		C2-C2'	C2-C3	C3-C4	C4-C5	C5-S	S-C2	C2'-C3'	C3'-C4'	C4'-C5'	C5'-S'	S'-C2'
-	ADC(2)	1.386	1.445	1.394	1.42	1.727	1.79	1.445	1.394	1.42	1.727	1.79
	CC2	1.387	1.444	1.397	1.421	1.733	1.797	1.444	1.397	1.421	1.733	1.797
3	ADC(2)	1.385	1.447	1.392	1.413	1.737	1.787	1.446	1.396	1.417	1.728	1.785
4	ADC(2)	1.386	1.44	1.4	1.424	1.722	1.804	1.441	1.396	1.419	1.726	1.789
	CC2	1.387	1.438	1.403	1.424	1.725	1.809	1.44	1.399	1.419	1.732	1.796
4,4'	ADC(2)	1.387	1.436	1.401	1.421	1.72	1.799	1.436	1.401	1.421	1.72	1.799
	CC2	1.388	1.435	1.405	1.422	1.725	1.806	1.435	1.405	1.422	1.725	1.806
3,4'	ADC(2)	1.385	1.44	1.395	1.416	1.739	1.808	1.432	1.4	1.428	1.723	1.838
	CC2	1.385	1.44	1.395	1.416	1.739	1.808	1.432	1.4	1.428	1.723	1.838

Table 7.17 Selected bond lengths of the OC(CH₃)O substituted cis BP ground state geometry

Sub. pos.	Method	Bond length /Å										
		C2-C2'	C2-C3	C3-C4	C4-C5	C5-S	S-C2	C2'-C3'	C3'-C4'	C4'-C5'	C5'-S'	S'-C2'
-	MP2	1.455	1.398	1.421	1.392	1.728	1.741	1.398	1.421	1.392	1.728	1.741
	CC2	1.455	1.397	1.425	1.392	1.735	1.749	1.397	1.425	1.392	1.735	1.749
3	MP2	1.455	1.395	1.416	1.39	1.73	1.737	1.398	1.421	1.393	1.727	1.741
	CC2	1.455	1.394	1.42	1.39	1.737	1.745	1.398	1.425	1.392	1.733	1.749
4	MP2	1.454	1.394	1.418	1.388	1.727	1.744	1.398	1.421	1.392	1.728	1.741
	CC2	1.454	1.394	1.422	1.388	1.734	1.751	1.397	1.425	1.392	1.735	1.748
3,3'	MP2	1.45	1.398	1.42	1.389	1.73	1.742	1.397	1.421	1.387	1.728	1.743
4,4'	MP2	1.453	1.395	1.418	1.388	1.727	1.743	1.395	1.418	1.388	1.727	1.743
	CC2	1.453	1.394	1.422	1.388	1.733	1.751	1.394	1.422	1.388	1.733	1.751
3,4'	MP2	1.449	1.401	1.418	1.389	1.732	1.738	1.399	1.418	1.391	1.727	1.746
	CC2	1.448	1.4	1.422	1.389	1.739	1.745	1.397	1.422	1.391	1.734	1.754

Table 7.18 Selected bond lengths of the OC(CH₃)O substituted cis BP excited state geometry

Sub. pos.	Method	Bond length /Å										
		C2-C2'	C2-C3	C3-C4	C4-C5	C5-S	S-C2	C2'-C3'	C3'-C4'	C4'-C5'	C5'-S'	S'-C2'
-	ADC(2)	1.386	1.445	1.394	1.42	1.727	1.79	1.445	1.394	1.42	1.727	1.79
	CC2	1.387	1.444	1.397	1.421	1.733	1.797	1.444	1.397	1.421	1.733	1.797
3	ADC(2)	1.388	1.454	1.397	1.417	1.731	1.783	1.447	1.394	1.42	1.727	1.795
	CC2	1.387	1.447	1.402	1.416	1.739	1.802	1.442	1.398	1.419	1.733	1.808
4	ADC(2)	1.387	1.438	1.402	1.425	1.721	1.806	1.441	1.397	1.418	1.727	1.788
	CC2	1.388	1.436	1.406	1.426	1.725	1.812	1.439	1.4	1.418	1.734	1.795
3,3'	ADC(2)	1.386	1.45	1.392	1.415	1.731	1.795	1.453	1.392	1.414	1.73	1.808
4,4'	ADC(2)	1.387	1.436	1.403	1.422	1.721	1.799	1.436	1.403	1.422	1.721	1.799
	CC2	1.388	1.434	1.406	1.423	1.726	1.806	1.434	1.406	1.423	1.726	1.806
3,4'	ADC(2)	1.387	1.442	1.395	1.411	1.739	1.778	1.430	1.418	1.425	1.722	1.828
	CC2	1.389	1.438	1.4	1.408	1.746	1.78	1.428	1.423	1.429	1.726	1.838

Table 7.19 Selected bond lengths of the phenyl substituted cis BP ground state geometry

Sub. pos.	Method	Bond length /Å										
		C2-C2'	C2-C3	C3-C4	C4-C5	C5-S	S-C2	C2'-C3'	C3'-C4'	C4'-C5'	C5'-S'	S'-C2'
-	MP2	1.455	1.398	1.421	1.392	1.728	1.741	1.398	1.421	1.392	1.728	1.741
	CC2	1.455	1.397	1.425	1.392	1.735	1.749	1.397	1.425	1.392	1.735	1.749
4	MP2	1.454	1.396	1.426	1.399	1.725	1.742	1.398	1.421	1.392	1.728	1.741
	CC2	1.454	1.396	1.43	1.398	1.733	1.75	1.398	1.424	1.392	1.735	1.749
3,3'	MP2	1.454	1.407	1.425	1.391	1.73	1.739	1.407	1.425	1.391	1.73	1.739
	CC2	1.454	1.406	1.429	1.391	1.737	1.747	1.406	1.429	1.391	1.737	1.747
4,4'	MP2	1.454	1.399	1.425	1.398	1.726	1.743	1.399	1.425	1.398	1.726	1.743

Table 7.20 Selected bond lengths of the phenyl substituted cis BP excited state geometry

Sub. pos.	Method	Bond length /Å										
		C2-C2'	C2-C3	C3-C4	C4-C5	C5-S	S-C2	C2'-C3'	C3'-C4'	C4'-C5'	C5'-S'	S'-C2'
-	ADC(2)	1.386	1.445	1.394	1.42	1.727	1.79	1.445	1.394	1.42	1.727	1.79
	CC2	1.387	1.444	1.397	1.421	1.733	1.797	1.444	1.397	1.421	1.733	1.797
4	ADC(2)	1.389	1.436	1.407	1.433	1.72	1.805	1.441	1.398	1.417	1.729	1.787
	CC2	1.39	1.433	1.411	1.435	1.723	1.812	1.439	1.401	1.417	1.735	1.793
3,3'	ADC(2)	1.397	1.468	1.423	1.388	1.751	1.764	1.468	1.423	1.388	1.751	1.764
	CC2	1.397	1.466	1.427	1.388	1.759	1.77	1.466	1.427	1.388	1.759	1.77
4,4'	ADC(2)	1.39	1.436	1.408	1.428	1.722	1.8	1.435	1.408	1.428	1.722	1.8

Table 7.21 Selected bond lengths of the dimethylamino substituted cis BP ground state geometry

Sub. pos.	Method	Bond length /Å										
		C2-C2'	C2-C3	C3-C4	C4-C5	C5-S	S-C2	C2'-C3'	C3'-C4'	C4'-C5'	C5'-S'	S'-C2'
-	MP2	1.455	1.398	1.421	1.392	1.728	1.741	1.398	1.421	1.392	1.728	1.741
	CC2	1.455	1.397	1.425	1.392	1.735	1.749	1.397	1.425	1.392	1.735	1.749
3	MP2	1.453	1.41	1.428	1.391	1.725	1.738	1.399	1.42	1.393	1.728	1.743
	CC2	1.452	1.409	1.433	1.391	1.731	1.746	1.398	1.423	1.393	1.735	1.751
4	MP2	1.454	1.393	1.43	1.401	1.731	1.74	1.398	1.421	1.392	1.729	1.741
	CC2	1.454	1.393	1.434	1.402	1.738	1.747	1.398	1.425	1.392	1.735	1.749
3,3'	MP2	1.45	1.417	1.432	1.389	1.724	1.747	1.417	1.432	1.389	1.724	1.747
	CC2	1.448	1.416	1.436	1.389	1.731	1.755	1.416	1.436	1.389	1.731	1.755
4,4'	MP2	1.453	1.395	1.428	1.4	1.732	1.742	1.395	1.428	1.4	1.732	1.742
	CC2	1.454	1.394	1.432	1.401	1.739	1.748	1.394	1.432	1.401	1.739	1.748
3,4'	MP2)	1.451	1.41	1.428	1.391	1.726	1.738	1.394	1.427	1.402	1.732	1.742
	CC2	1.45	1.41	1.433	1.391	1.732	1.746	1.394	1.431	1.402	1.74	1.75

Table 7.22 Selected bond lengths of the dimethylamino substituted cis BP excited state geometry

Sub. pos.	Method	Bond length /Å										
		C2-C2'	C2-C3	C3-C4	C4-C5	C5-S	S-C2	C2'-C3'	C3'-C4'	C4'-C5'	C5'-S'	S'-C2'
-	ADC(2)	1.386	1.445	1.394	1.42	1.727	1.79	1.445	1.394	1.42	1.727	1.79
	CC2	1.387	1.444	1.397	1.421	1.733	1.797	1.444	1.397	1.421	1.733	1.797
3	ADC(2)	1.403	1.452	1.412	1.405	1.769	1.766	1.438	1.408	1.401	1.746	1.766
	CC2	1.403	1.452	1.417	1.405	1.771	1.772	1.437	1.411	1.402	1.753	1.772
4	ADC(2)	1.395	1.434	1.434	1.433	1.737	1.829	1.431	1.409	1.402	1.741	1.771
	CC2	1.398	1.429	1.44	1.43	1.74	1.826	1.429	1.411	1.402	1.748	1.777
3,3'	ADC(2)	1.405	1.455	1.418	1.402	1.751	1.782	1.455	1.418	1.402	1.751	1.782
	CC2	1.406	1.453	1.421	1.402	1.755	1.789	1.453	1.421	1.402	1.755	1.789
4,4'	ADC(2)	1.393	1.426	1.425	1.424	1.731	1.796	1.426	1.425	1.424	1.731	1.796
	CC2	1.394	1.425	1.429	1.425	1.736	1.801	1.425	1.429	1.415	1.736	1.801
3,4'	ADC(2)	1.384	1.451	1.41	1.405	1.743	1.779	1.438	1.425	1.439	1.734	1.834
	CC2	1.39	1.446	1.413	1.406	1.75	1.784	1.431	1.433	1.434	1.737	1.831

Table 7.23 OH substituted cis 2,2'-bithiophene selected substituent bond length changes on excitation

Sub. pos.	Method	Bond length change/Å			
		C4-O	O-H	C4'-O	O-H
4	ADC(2)	-0.029	0.005		
	CC2	-0.023	0.005		
4,4'	ADC(2)	-0.014	0.002	-0.019	0.003
	CC2	-0.012	0.001	-0.017	0.004
Sub. pos.	Method	Bond length change/Å			
		C3-O	O-H	C4'-O	O-H
3,4'	ADC(2)	-0.01	0.002	-0.025	0.003
	CC2	-0.007	0.003	-0.1	0

Table 7.24 OC(H)O substituted cis 2,2'-bithiophene selected substituent bond length changes on excitation

Sub. pos.	Method	Bond length change/Å					
		C4-O	O1-C6	C6-O2	C3'-O	O1-C6'	C6'-O2'
3	ADC(2)	-0.013	0.015	0.003			
Sub. pos.	Method	Bond length change/Å					
		C4-O	O1-C6	C6-O2	C4'-O	O1-C6'	C6'-O2'
4	ADC(2)	-0.019	0.109	-0.003			
	CC2	-0.018	0.008	-0.003			
4,4'	ADC(2)	-0.013	0.012	-0.004	-0.013	0.012	-0.004
	CC2	-0.013	0.012	-0.004	-0.013	0.012	-0.004
Sub. pos.	Method	Bond length change/Å					
		C3-O	O1-C6	C6-O2	C4'-O	O1-C6'	C6'-O2'
3,4'	ADC(2)	0	-0.001	0.001	-0.016	0.011	-0.003
	CC2	0	-0.001	0.001	-0.016	0.011	-0.003

Table 7.25 OC(CH₃)O substituted cis 2,2'-bithiophene selected substituent bond length changes on excitation

Sub. pos.	Method	Bond length change/Å					
		C3-O	O1-C6	C6-O2	C3'-O	O1-C6'	C6'-O2'
3	ADC(2)	-0.02	0.006	0			
	CC2	-0.016	0.006	0			
3,3'	ADC(2)	-0.005	0.017	-0.003	-0.015	0.012	0
Sub. pos.	Method	Bond length change/Å					
		C4-O	O1-C6	C6-O2	C4'-O	O1-C6'	C6'-O2'
4	ADC(2)	-0.021	0.014	-0.005			
	CC2	-0.019	0.013	-0.005			
4,4'	ADC(2)	-0.016	0.007	-0.003	-0.016	0.007	-0.003
	CC2	-0.015	0.008	-0.003	-0.015	0.008	-0.003
Sub. pos.	Method	Bond length change/Å					
		C3-O	O1-C6	C6-O2	C4'-O	O1-C6'	C6'-O2'
3,4'	ADC(2)	0.004	-0.007	0.006	-0.041	0.051	-0.909
	CC2	0.003	-0.007	0.008	-0.034	0.047	-0.007

Table 7.26 phenyl substituted cis 2,2'-bithiophene selected substituent bond length changes on excitation at the ADC(2) level

Sub. pos.	Bond length change/Å													
	C3-C6	C6-C7	C7-C8	C8-C9	C9-C10	C10-C11	C11-C6	C3'-C6'	C6'-C7'	C7'-C8'	C8'-C9'	C9'-C10'	C10'-C11'	C11'-C6'
3,3'	-0.033	0.017	0.001	-0.003	0.012	-0.011	0.016	-0.033	0.017	0.001	-0.003	0.012	-0.011	0.016
Sub. pos.	Bond length change/Å													
	C4-C6	C6-C7	C7-C8	C8-C9	C9-C10	C10-C11	C11-C6	C4'-C6'	C6'-C7'	C7'-C8'	C8'-C9'	C9'-C10'	C10'-C11'	C11'-C6'
4	-0.009	0.004	-0.002	0.002	0	-0.001	0.003							
4,4'	-0.006	0.003	-0.002	0.001	0	0	0.002	-0.006	0.003	-0.002	0.001	0	0	0.002

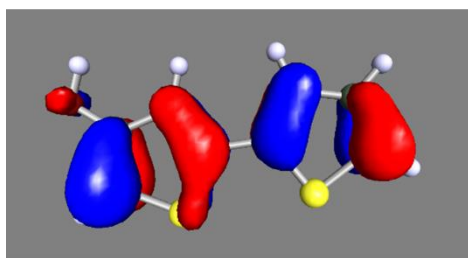
Table 7.27 phenyl substituted cis 2,2'-bithiophene selected substituent bond length changes on excitation at the CC2 level

Sub. pos.	Bond length change/Å													
	C3-C6	C6-C7	C7-C8	C8-C9	C9-C10	C10-C11	C11-C6	C3'-C6'	C6'-C7'	C7'-C8'	C8'-C9'	C9'-C10'	C10'-C11'	C11'-C6'
3,3'	-0.033	0.018	0.001	-0.003	0.012	-0.01	0.016	-0.033	0.018	0.001	-0.003	0.012	-0.01	0.016
Sub. pos.	Bond length change/Å													
	C4-C6	C6-C7	C7-C8	C8-C9	C9-C10	C10-C11	C11-C6	C4'-C6'	C6'-C7'	C7'-C8'	C8'-C9'	C9'-C10'	C10'-C11'	C11'-C6'
4	-0.009	0.005	-0.002	0.002	0.001	-0.001	0.004							

Table 7.28 Dimethylamino substituted *cis* 2,2'-bithiophene selected substituent bond length changes on

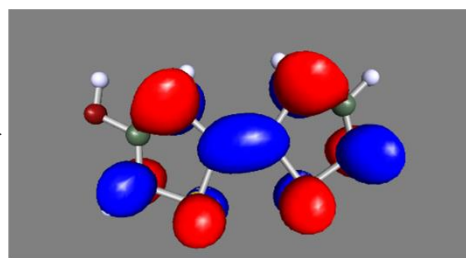
Substitution position	Method	Bond length change/Å					
		C3-N	N-C	N-C	C3'-N'	N'-C'	N'-C'
3	ADC(2)	-0.029	0.002	-0.003			
	CC2	-0.028	0.002	-0.003			
3,3'	ADC(2)	-0.017	-0.004	-0.001	-0.017	-0.004	-0.001
	CC2	-0.015	-0.005	-0.001	-0.015	-0.005	-0.001
Substitution position	Method	Bond length change/Å					
		C4-N	N-C	N-C	C4'-N'	N'-C'	N'-C'
4	ADC(2)	-0.054	-0.003	0.002			
	CC2	-0.047	-0.003	0.002			
4,4'	ADC(2)	-0.035	-0.008	-0.001	-0.035	-0.008	-0.001
	CC2	-0.031	-0.007	-0.001	-0.031	-0.007	-0.001
Substitution position	Method	Bond length change/Å					
		C3-N	N-C	N-C	C4'-N'	N'-C'	N'-C'
3,4'	ADC(2)	-0.007	0.003	-0.001	-0.056	-0.003	0.002
	CC2	-0.004	0.002	-0.001	-0.049	-0.004	0.001

4 OH cis 2,2'-bithiophene



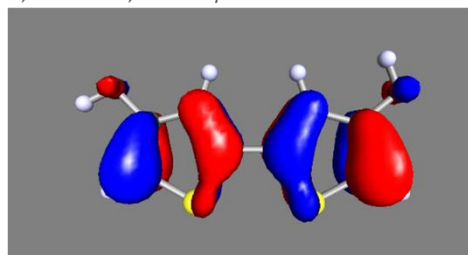
HOMO

83.2%



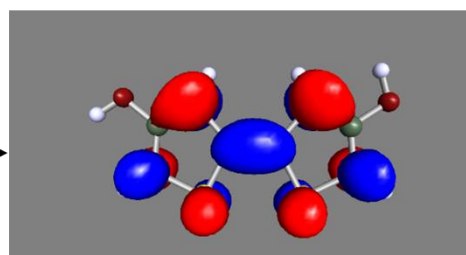
LUMO +1

4,4' OH cis 2,2'-bithiophene



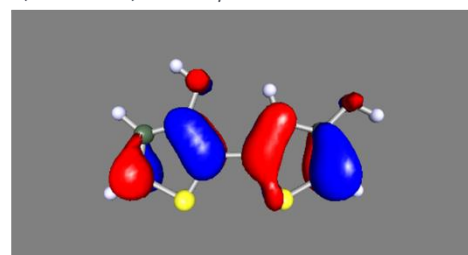
HOMO

85.3%



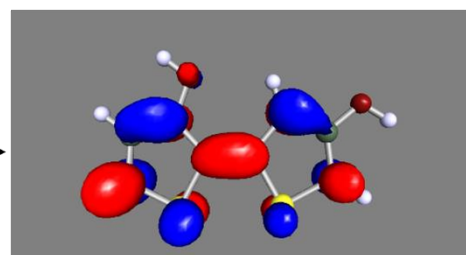
LUMO +1

3,4' OH cis 2,2'-bithiophene



HOMO

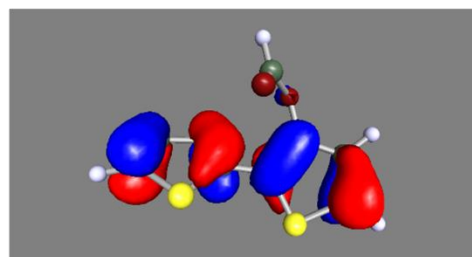
86.7%



LUMO +3

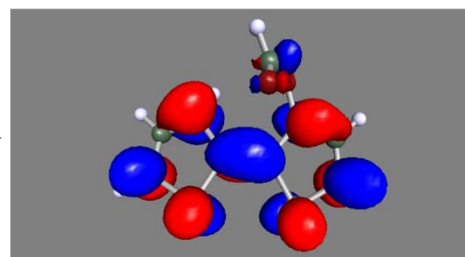
Figure 7.1 MOs involved in S_1 excitation of OH substituted cis 2,2'-bithiophene

3 OC(H)O 2,2-bithiophene



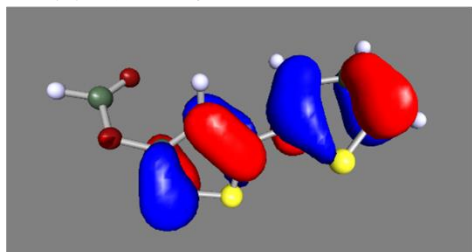
HOMO

71.1%



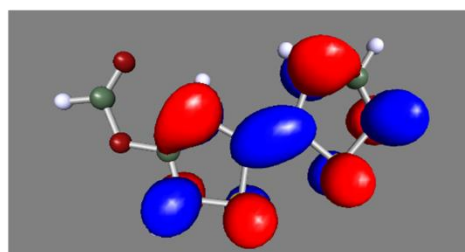
LUMO +2

4 OC(H)O 2,2-bithiophene



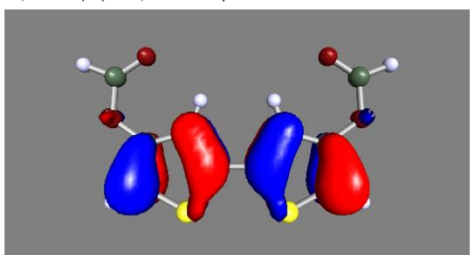
HOMO

88.3%



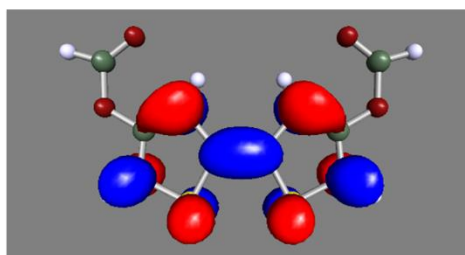
LUMO

4,4' OC(H)O 2,2-bithiophene



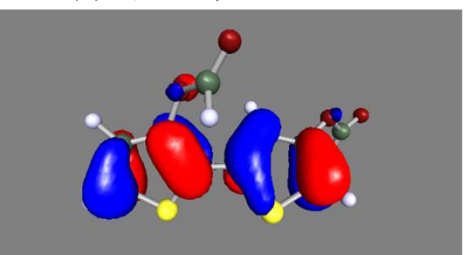
HOMO

87.5%



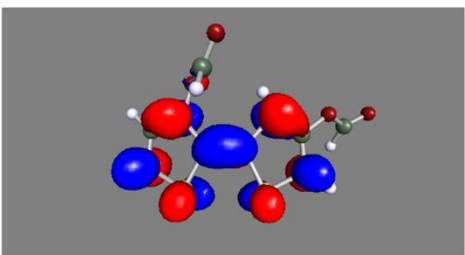
LUMO

3,4' OC(H)O 2,2-bithiophene



HOMO

81.5%



LUMO

Figure 7.2 MOs involved in S_1 excitation of OC(H)O substituted cis 2,2'-bithiophene

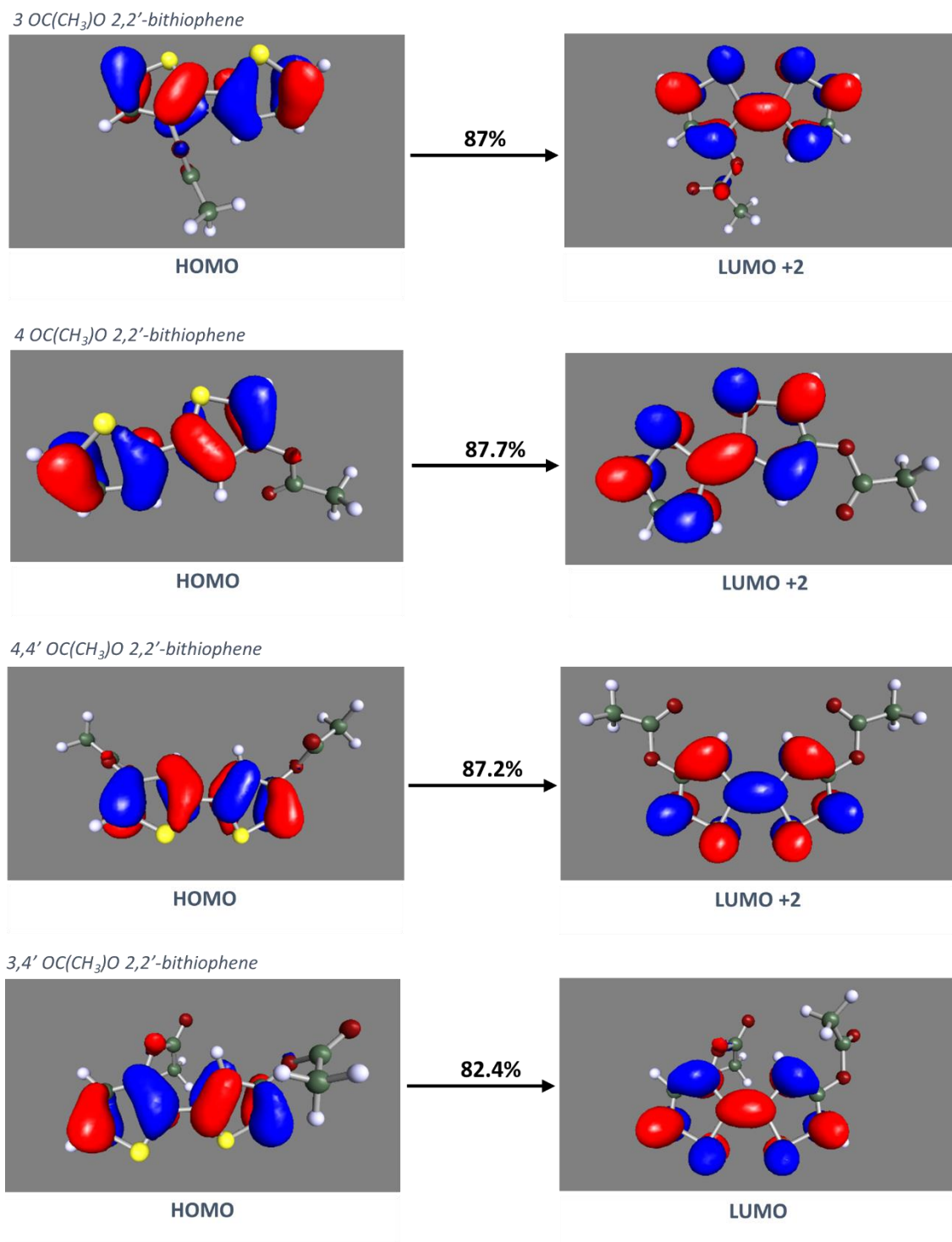
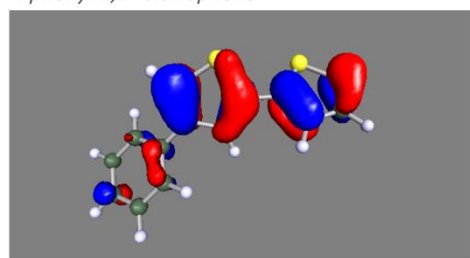


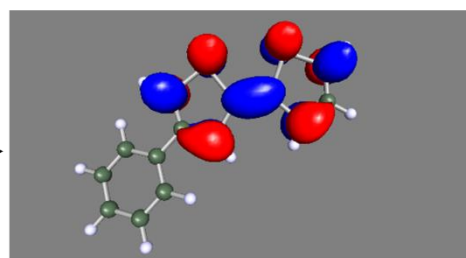
Figure 7.3 MOs involved in S_1 excitation of $OC(CH_3)O$ substituted *cis* 2,2'-bithiophene

4 phenyl 2,2'-bithiophene



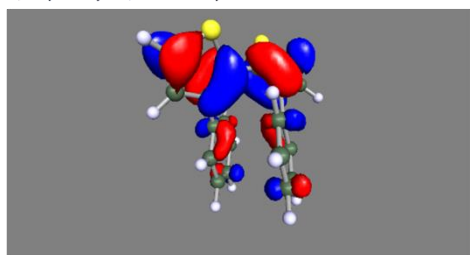
HOMO

85.9%



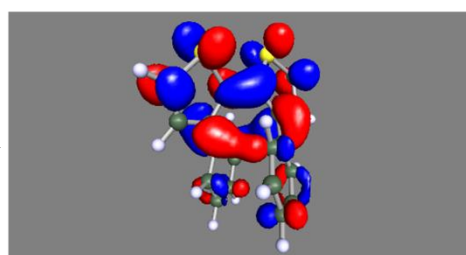
LUMO +2

3,3' phenyl 2,2'-bithiophene



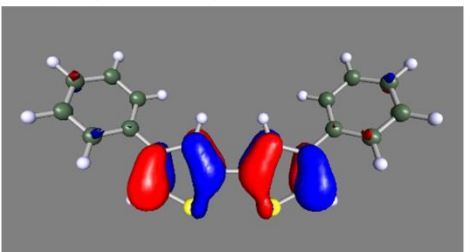
HOMO

94.2%



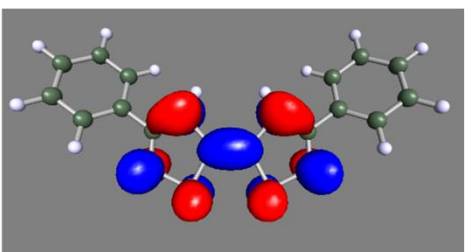
LUMO

4,4' phenyl 2,2'-bithiophene



HOMO

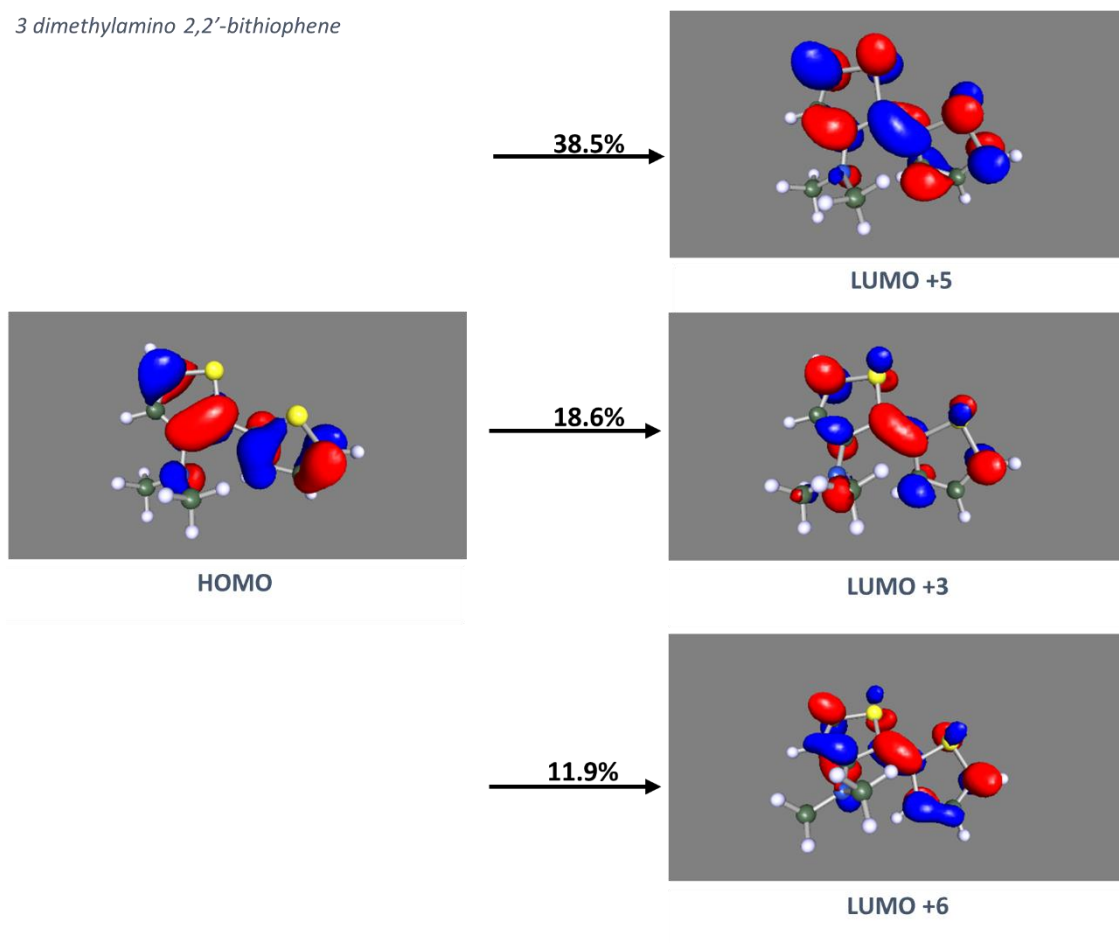
80.7%



LUMO +2

Figure 7.4 MOs involved in S_1 excitation of phenyl substituted *cis* 2,2'-bithiophene

3 dimethylamino 2,2'-bithiophene



4 dimethylamino 2,2'-bithiophene

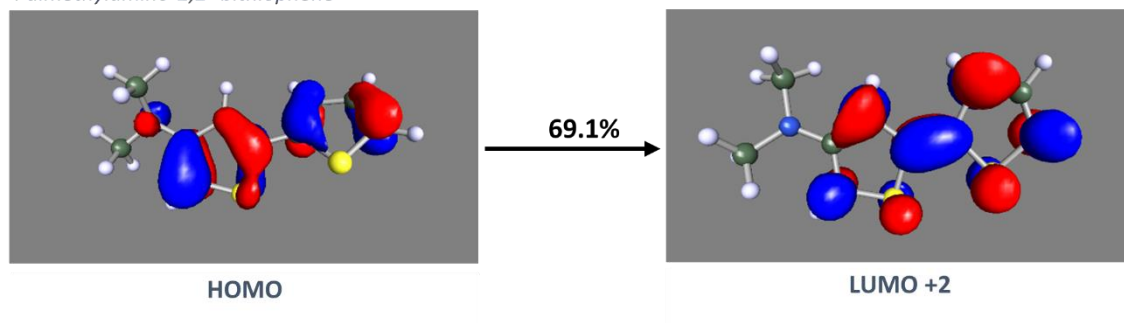
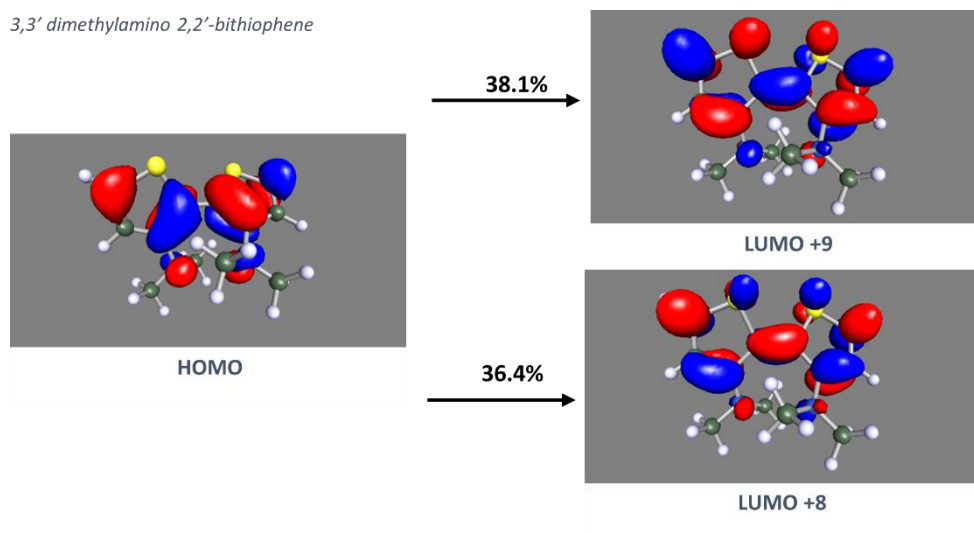
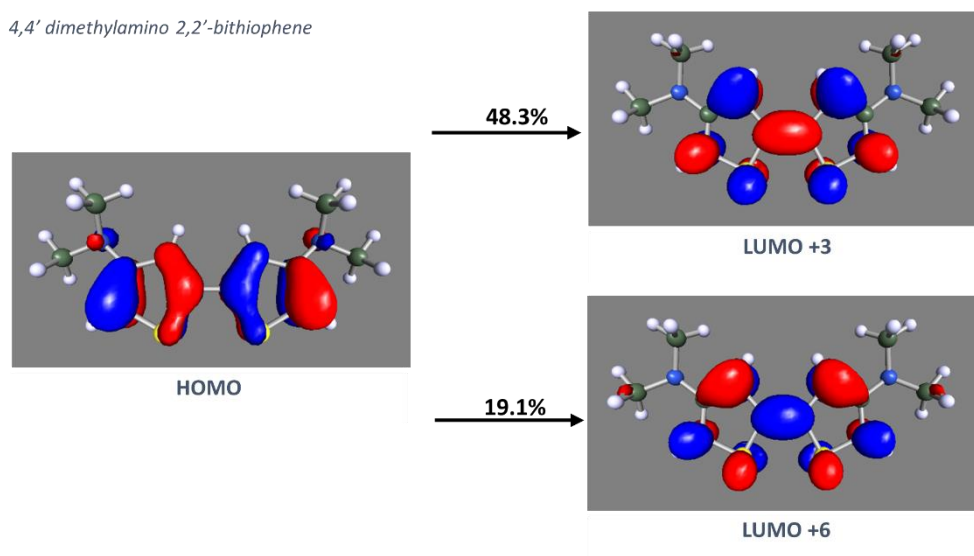


Figure 7.5 MOs involved in S₁ excitation of singly dimethylamino substituted cis 2,2'-bithiophene

3,3' dimethylamino 2,2'-bithiophene



4,4' dimethylamino 2,2'-bithiophene



3,4' dimethylamino 2,2'-bithiophene

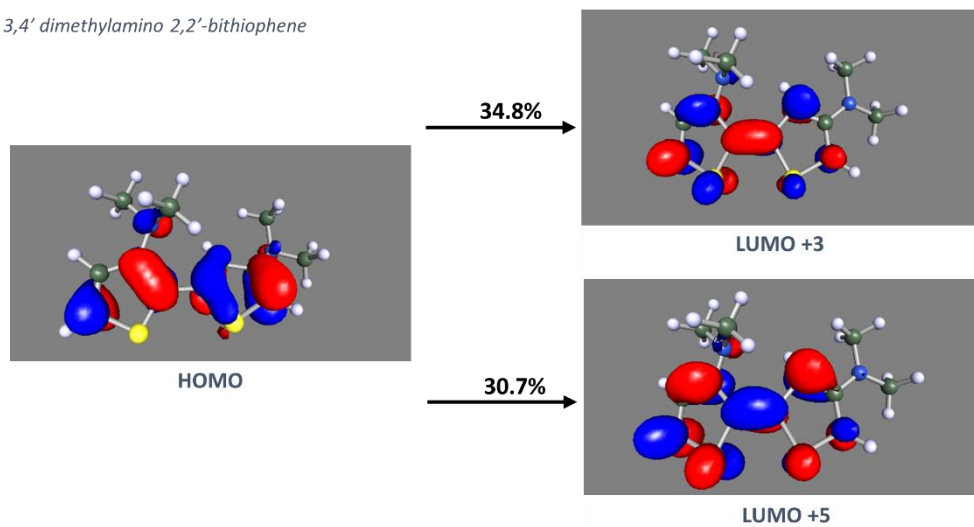


Figure 7.6 MOs involved in S_1 excitation of doubly dimethylamino substituted *cis* 2,2'-bithiophene

Table 7.29 Contributors to the S_1 excitation of OH substituted cis 2,2'-bithiophene

Substitution Position	ADC(2)			CC2		
	Occupied	Virtual	%	Occupied	Virtual	%
4	HOMO	LUMO +1	83.2	HOMO	LUMO +1	85
	HOMO - 1	LUMO +1	10.5	HOMO -1	LUMO +1	8.5
Substitution Position	ADC(2)			CC2		
	Occupied	Virtual	%	Occupied	Virtual	%
4,4'	HOMO	LUMO +2	84.3	HOMO	LUMO +1	85.3
	HOMO -2	LUMO +2	10.3	HOMO -2	LUMO +1	9.1
Substitution Position	ADC(2)			CC2		
	Occupied	Virtual	%	Occupied	Virtual	%
3,4'				HOMO	LUMO +3	64.7
				HOMO	LUMO +2	12.9
				HOMO -1	LUMO +3	4.7
				HOMO	LUMO + 8	2
				HOMO	LUMO +15	1.9
				HOMO	LUMO +10	1
				HOMO	LUMO +13	1

Table 7.30 Contributors to the S_1 excitation of OC(H)O substituted cis 2,2'-bithiophene

Substitution Position	ADC(2)			CC2		
	Occupied	Virtual	%	Occupied	Virtual	%
3	HOMO	LUMO +2	71.1	HOMO	LUMO +2	60
	HOMO	LUMO	10.9	HOMO	LUMO	12.6
	HOMO	LUMO +1	5.6	HOMO	LUMO +1	12.2
	HOMO	LUMO +12	1.8	HOMO	LUMO +12	3.3
	HOMO -1	LUMO +2	1.2			
	HOMO	LUMO +5	1			
Substitution Position	ADC(2)			CC2		
	Occupied	Virtual	%	Occupied	Virtual	%
4	HOMO	LUMO	88.3	HOMO	LUMO	89
	HOMO -2	LUMO	6.2	HOMO -1	LUMO	5.4
Substitution Position	ADC(2)			CC2		
	Occupied	Virtual	%	Occupied	Virtual	%
4,4'	HOMO	LUMO	87.5	HOMO	LUMO	88.1
	HOMO -1	LUMO	7.7	HOMO -1	LUMO	6.4
Substitution Position	ADC(2)			CC2		
	Occupied	Virtual	%	Occupied	Virtual	%
3,4'				HOMO	LUMO	81.5
				HOMO -1	LUMO	6.5
				HOMO	LUMO +12	3.2

Table 7.31 Contributors to the S_1 excitation of $OC(CH_3)O$ substituted *cis* 2,2'-bithiophene

Substitution Position	ADC(2)			CC2		
	Occupied	Virtual	%	Occupied	Virtual	%
3	HOMO	LUMO +2	87	HOMO	LUMO +2	52.8
	HOMO	LUMO +6	5.7	HOMO	LUMO +1	16.8
	HOMO -1	LUMO +2	1.5	HOMO	LUMO +3	10.9
				HOMO	LUMO +5	4
				HOMO	LUMO + 16	3.7
				HOMO -1	LUMO +2	1
Substitution Position	ADC(2)			CC2		
	Occupied	Virtual	%	Occupied	Virtual	%
4	HOMO	LUMO +2	87.7	HOMO	LUMO +2	88.4
	HOMO -1	LUMO +2	6.8	HOMO -1	LUMO +2	5.9
Substitution Position	ADC(2)			CC2		
	Occupied	Virtual	%	Occupied	Virtual	%
4,4'	HOMO	LUMO +2	87.2	HOMO	LUMO +2	87.7
	HOMO -1	LUMO +2	8	HOMO -1	LUMO +2	7.3
Substitution Position	ADC(2)			CC2		
	Occupied	Virtual	%	Occupied	Virtual	%
3,4'	HOMO	LUMO	82.4	HOMO	LUMO	82.7
	HOMO -1	LUMO	11.6	HOMO -1	LUMO	8.2
				HOMO	LUMO +15	1.5

Table 7.32 Contributors to the S_1 excitation of phenyl substituted cis 2,2'-bithiophene

Substitution Position	ADC(2)			CC2		
	Occupied	Virtual	%	Occupied	Virtual	%
4	HOMO	LUMO +2	85.9	HOMO	LUMO +2	86.6
	HOMO -3	LUMO +2	2.4	HOMO -3	LUMO +2	2.2
	HOMO	LUMO +3	1.2	HOMO	LUMO +11	1.7
	HOMO	LUMO +12	1.1	HOMO	LUMO	1.1
	HOMO	LUMO	1.1			
Substitution Position	ADC(2)			CC2		
	Occupied	Virtual	%	Occupied	Virtual	%
3,3'	HOMO	LUMO	94.2	HOMO	LUMO	94.3
	HOMO	LUMO +2	1.8	HOMO	LUMO +2	1.5
Substitution Position	ADC(2)			CC2		
	Occupied	Virtual	%	Occupied	Virtual	%
4,4'	HOMO	LMUO +2	80.7			
	HOMO	LUMO +3	4.4			
	HOMO -5	LUMO +2	2.8			
	HOMO	LUMO	2.4			
	HOMO -2	LUMO +2	1.4			
	HOMO	LUMO +15	1.2			
	HOMO	LUMO +19	1			
	HOMO	LUMO +18	1			

Table 7.33 Contributors to the S_1 excitation of singly dimethylamino substituted *cis* 2,2'-bithiophene

Substitution Position	ADC(2)			CC2		
	Occupied	Virtual	%	Occupied	Virtual	%
3	HOMO	LUMO +5	38.5	HOMO	LUMO +5	40.3
	HOMO	LUMO +3	18.6	HOMO	LUMO +3	20
	HOMO	LUMO +6	11.9	HOMO	LUMO +6	9.9
	HOMO -1	LUMO +5	5.9	HOMO -1	LUMO +5	5.4
	HOMO	LUMO +4	4.4	HOMO	LUMO +4	4.4
	HOMO -1	LUMO +3	3.1	HOMO -1	LUMO +3	2.9
	HOMO -3	LUMO +5	2.7	HOMO -3	LUMO +5	2.5
	HOMO -1	LUMO +6	1.8	HOMO -3	LUMO +3	1.4
	HOMO -3	LUMO +3	1.4	HOMO -1	LUMO +6	1.3
	HOMO	LUMO +1	1.1	HOMO	LUMO	1.3
	HOMO	LUMO	1	HOMO	LUMO +1	1.1
Substitution Position	ADC(2)			CC2		
	Occupied	Virtual	%	Occupied	Virtual	%
4	HOMO	LUMO +2	69.1	HOMO	LUMO +2	68.7
	HOMO -1	LUMO +2	11.2	HOMO -1	LUMO +2	11
	HOMO	LUMO +5	5.5	HOMO	LUMO +5	6.8
	HOMO	LUMO	2.7	HOMO	LUMO	1.9
				HOMO	LUMO +8	1.1
				HOMO -1	LUMO +5	1

Table 7.34 Contributors to the S_1 excitation of doubly dimethylamino substituted *cis* 2,2'-bithiophene

Substitution Position	ADC(2)			CC2		
	Occupied	Virtual	%	Occupied	Virtual	%
3,3'	HOMO	LUMO +9	38.1	HOMO	LUMO +9	40.5
	HOMO	LUMO +8	36.4	HOMO	LUMO +8	34.3
	HOMO	LUMO +3	5.2	HOMO	LUMO +3	5.5
	HOMO	LUMO +4	2.8	HOMO	LUMO +4	2.9
	HOMO -2	LUMO +9	2.2	HOMO -4	LUMO +9	2
	HOMO -2	LUMO +8	2.2	HOMO	LUMO +1	2
	HOMO -4	LUMO +9	2.1	HOMO -2	LUMO +0	1.9
	HOMO -4	LUMO +8	2	HOMO -4	LUMO +8	1.8
	HOMO	LUMO +1	1.8	HOMO -2	LUMO +8	1.7
	HOMO	LUMO +10	1.1	HOMO	LUMO +10	1.1
Substitution Position	ADC(2)			CC2		
	Occupied	Virtual	%	Occupied	Virtual	%
4,4'	HOMO	LUMO +3	48.3	HOMO	LUMO +3	48.8
	HOMO	LUMO +6	19.1	HOMO	LUMO +6	18.1
	HOMO	LUMO +5	8.6	HOMO	LUMO +5	8.3
	HOMO -2	LUMO +3	6.2	HOMO -2	LUMO +3	5.9
	HOMO	LUMO +2	4.1	HOMO	LUMO +2	5.4
	HOMO	LUMO +10	3.1	HOMO	LUMO +10	3
	HOMO -2	LUMO +6	2.6	HOMO -2	LUMO +6	2.4
	HOMO -2	LUMO +5	1.1	HOMO -2	LUMO +5	1.1
Substitution Position	ADC(2)			CC2		
	Occupied	Virtual	%	Occupied	Virtual	%
3,4'	HOMO	LUMO +3	34.8	HOMO	LUMO +5	38
	HOMO	LUMO +5	30.7	HOMO	LUMO +3	31.1
	HOMO -1	LUMO +3	5.6	HOMO -1	LUMO +5	6.1
	HOMO	LUMO +2	5.5	HOMO -1	LUMO +3	4.7
	HOMO -1	LUMO +5	5.1	HOMO	LUMO	3.9
	HOMO	LUMO	3.9	HOMO	LUMO +2	2.7
	HOMO	LUMO +4	3.2	HOMO	LUMO +7	2
	HOMO	LUMO +7	1.1	HOMO	LUMO +4	1.3

7.5 Chapter 5 Supplementary Material

Table 7.35 Selected bond lengths of unsubstituted and substituted terthiophene ground state geometries at the MP2 level

Substituent	Bond length /Å					
	C2-C2'	C2-C3	C3-C4	C4-C5	C5-S	S-C2
-	1.45	1.4	1.421	1.392	1.729	1.742
OH	1.45	1.4	1.422	1.39	1.727	1.75
OC(H)O	1.453	1.403	1.417	1.39	1.732	1.736
Substituent	Bond length /Å					
		C2'-C3'	C3'-C4'	C4'-C5'	C5'-S'	S'-C2'
-		1.4	1.416	1.4	1.744	1.744
OH		1.402	1.412	1.401	1.747	1.741
OC(H)O		1.405	1.412	1.397	1.748	1.74
Substituent	Bond length /Å					
	C5'-C2''	C2''-C3''	C3''-C4''	C4''-C5''	C5''-S''	S''-C2''
-	1.45	1.4	1.421	1.392	1.729	1.742
OH	1.446	1.4	1.421	1.388	1.73	1.744
OC(H)O	1.45	1.402	1.417	1.39	1.73	1.737

Table 7.36 Selected bond lengths of unsubstituted and substituted terthiophene ground state geometries at the CC2 level

Substituent	Bond length /Å					
	C2-C2'	C2-C3	C3-C4	C4-C5	C5-S	S-C2
-	1.45	1.399	1.424	1.391	1.736	1.75
OH	1.449	1.399	1.426	1.39	1.734	1.759
OC(H)O	1.452	1.402	1.42	1.39	1.739	1.744
Substituent	Bond length /Å					
		C2'-C3'	C3'-C4'	C4'-C5'	C5'-S'	S'-C2'
-		1.4	1.419	1.4	1.752	1.752
OH		1.402	1.416	1.401	1.755	1.75
OC(H)O		1.405	1.415	1.397	1.757	1.75
Substituent	Bond length /Å					
	C5'-C2''	C2''-C3''	C3''-C4''	C4''-C5''	C5''-S''	S''-C2''
-	1.45	1.399	1.424	1.391	1.736	1.75
OH	1.445	1.4	1.425	1.389	1.736	1.752
OC(H)O	1.449	1.401	1.421	1.389	1.737	1.745

Table 7.37 Selected bond lengths of unsubstituted and substituted terthiophene excited state geometries at the ADC(2) level

Substituent	Bond length /Å					
	C2-C2'	C2-C3	C3-C4	C4-C5	C5-S	S-C2
-	1.401	1.429	1.405	1.404	1.731	1.767
OH	1.4	1.429	1.409	1.396	1.741	1.774
OC(H)O	1.406	1.433	1.405	1.396	1.734	1.764
Substituent	Bond length /Å					
		C2'-C3'	C3'-C4'	C4'-C5'	C5'-S'	S'-C2'
-		1.442	1.382	1.442	1.768	1.768
OH		1.456	1.381	1.447	1.785	1.79
OC(H)O		1.448	1.38	1.449	1.78	1.78
Substituent	Bond length /Å					
	C5'-C2''	C2''-C3''	C3''-C4''	C4''-C5''	C5''-S''	S''-C2''
-	1.401	1.429	1.405	1.404	1.731	1.767
OH	1.39	1.438	1.4	1.41	1.737	1.777
OC(H)O	1.395	1.435	1.4	1.404	1.735	1.771

Table 7.38 Selected bond lengths of unsubstituted and substituted terthiophene excited state geometries at the CC2 level

Substituent	Bond length /Å					
	C2-C2'	C2-C3	C3-C4	C4-C5	C5-S	S-C2
-	1.402	1.428	1.409	1.404	1.737	1.774
OH	1.404	1.428	1.412	1.398	1.747	1.782
OC(H)O	1.406	1.433	1.409	1.397	1.74	1.773
Substituent	Bond length /Å					
		C2'-C3'	C3'-C4'	C4'-C5'	C5'-S'	S'-C2'
-		1.44	1.387	1.44	1.774	1.774
OH		1.45	1.39	1.436	1.791	1.785
OC(H)O		1.445	1.386	1.443	1.789	1.781
Substituent	Bond length /Å					
	C5'-C2''	C2''-C3''	C3''-C4''	C4''-C5''	C5''-S''	S''-C2''
-	1.402	1.428	1.409	1.404	1.737	1.774
OH	1.397	1.432	1.406	1.407	1.745	1.779
OC(H)O	1.397	1.432	1.404	1.403	1.744	1.776

Table 7.39 Selected bond lengths of unsubstituted and substituted tetrathiophene ground state geometries at the ADC(2) level

Substituent	Bond length /Å					
	C2-C2'	C2-C3	C3-C4	C4-C5	C5-S	S-C2
-	1.449	1.4	1.42	1.392	1.729	1.743
OH	1.442	1.405	1.418	1.391	1.726	1.752
OC(H)O	1.446	1.404	1.415	1.39	1.729	1.744
Substituent	Bond length /Å					
		C2'-C3'	C3'-C4'	C4'-C5'	C5'-S'	S'-C2'
-		1.401	1.414	1.402	1.746	1.745
OH		1.407	1.408	1.404	1.749	1.75
OC(H)O		1.404	1.409	1.399	1.746	1.745
Substituent	Bond length /Å					
	C5'-C2''	C2''-C3''	C3''-C4''	C4''-C5''	C5''-S''	S''-C2''
-	1.445	1.401	1.414	1.402	1.746	1.745
OH	1.44	1.404	1.412	1.401	1.751	1.746
OC(H)O	1.443	1.402	1.409	1.401	1.748	1.738
Substituent	Bond length /Å					
	C5''-C2'''	C2'''-C3'''	C3'''-C4'''	C4'''-C5'''	C5'''-S'''	S'''-C2'''
-	1.449	1.4	1.42	1.392	1.729	1.743
OH	1.443	1.401	1.421	1.388	1.731	1.745
OC(H)O	1.447	1.402	1.417	1.389	1.732	1.74

Table 7.40 Selected bond lengths of unsubstituted and substituted tetrathiophene ground state geometries at the CC2 level

Substituent	Bond length /Å					
	C2-C2'	C2-C3	C3-C4	C4-C5	C5-S	S-C2
-	1.449	1.399	1.424	1.391	1.736	1.75
OH	1.441	1.404	1.422	1.39	1.734	1.759
OC(H)O	1.445	1.402	1.419	1.389	1.737	1.752
Substituent	Bond length /Å					
		C2'-C3'	C3'-C4'	C4'-C5'	C5'-S'	S'-C2'
-		1.4	1.418	1.402	1.754	1.753
OH		1.405	1.413	1.404	1.758	1.76
OC(H)O		1.403	1.413	1.398	1.755	1.754
Substituent	Bond length /Å					
	C5'-C2''	C2''-C3''	C3''-C4''	C4''-C5''	C5''-S''	S''-C2''
-	1.445	1.4	1.418	1.402	1.754	1.753
OH	1.438	1.404	1.416	1.401	1.759	1.756
OC(H)O	1.442	1.401	1.413	1.4	1.757	1.747
Substituent	Bond length /Å					
	C5''-C2'''	C2'''-C3'''	C3'''-C4'''	C4'''-C5'''	C5'''-S'''	S'''-C2'''
-	1.449	1.399	1.424	1.391	1.736	1.75
OH	1.441	1.401	1.425	1.389	1.737	1.753
OC(H)O	1.446	1.401	1.421	1.389	1.739	1.748

Table 7.41 Selected bond lengths of unsubstituted and substituted tetrathiophene excited state geometries at the ADC(2) level

Substituent	Bond length /Å					
	C2-C2'	C2-C3	C3-C4	C4-C5	C5-S	S-C2
-	1.416	1.419	1.41	1.399	1.73	1.758
OH	1.412	1.423	1.411	1.392	1.73	1.761
Substituent	Bond length /Å					
		C2'-C3'	C3'-C4'	C4'-C5'	C5'-S'	S'-C2'
-		1.431	1.386	1.44	1.771	1.76
OH		1.434	1.387	1.443	1.778	1.779
Substituent	Bond length /Å					
	C5'-C2''	C2''-C3''	C3''-C4''	C4''-C5''	C5''-S''	S''-C2''
-	1.393	1.431	1.386	1.44	1.771	1.76
OH	1.379	1.442	1.382	1.452	1.771	1.794
Substituent	Bond length /Å					
	C5''-C2'''	C2'''-C3'''	C3'''-C4'''	C4'''-C5'''	C5'''-S'''	S'''-C2'''
-	1.449	1.419	1.41	1.399	1.73	1.758
OH	1.4	1.428	1.406	1.402	1.739	1.769

Table 7.42 Selected bond lengths of unsubstituted and substituted tetrathiophene excited state geometries at the CC2 level

Substituent	Bond length /Å					
	C2-C2'	C2-C3	C3-C4	C4-C5	C5-S	S-C2
-	1.416	1.418	1.414	1.399	1.737	1.765
OH	1.414	1.422	1.415	1.393	1.736	1.768
OC(H)O	1.412	1.423	1.411	1.394	1.739	1.767
Substituent	Bond length /Å					
		C2'-C3'	C3'-C4'	C4'-C5'	C5'-S'	S'-C2'
-		1.429	1.391	1.437	1.777	1.767
OH		1.431	1.395	1.435	1.782	1.779
OC(H)O		1.429	1.392	1.441	1.782	1.775
Substituent	Bond length /Å					
	C5'-C2''	C2''-C3''	C3''-C4''	C4''-C5''	C5''-S''	S''-C2''
-	1.396	1.429	1.391	1.437	1.777	1.767
OH	1.39	1.434	1.392	1.441	1.778	1.791
OC(H)O	1.391	1.442	1.391	1.434	1.775	1.779
Substituent	Bond length /Å					
	C5'''-C2'''	C2'''-C3'''	C3'''-C4'''	C4'''-C5'''	C5'''-S'''	S'''-C2'''
-	1.416	1.418	1.414	1.399	1.737	1.765
OH	1.405	1.424	1.41	1.402	1.747	1.773
OC(H)O	1.412	1.421	1.411	1.396	1.744	1.766

Table 7.43 Selected bond length changes on excitation of oligomer substituents

Method	Bond length change /Å											
	C3-O	O-H	C3'-O'	O'-H'	C3''-O''	O''-H''	C3'''-O'''	O'''-H'''				
ADC(2)	-0.003	0.001	-0.022	0.003	-0.007	0.001						
CC2	-0.005	0.002	-0.016	0.003	-0.002	0.002						
ADC(2)	-0.008	0.001	-0.02	0.003	-0.019	0.003	-0.002	0				
CC2	-0.01	0.002	-0.016	0.002	-0.011	0.002	0.004	0.001				
Method	Bond length change /Å											
	C3-O1	O1-C6	C6-O2	C3'-O1'	O1'-C6'	C6'-O2'	C3''-O1''	O1''-C6''	C6''-O2''	C3'''-O1'''	O1'''-C6'''	C6'''-O2'''
ADC(2)	-0.004	0.007	-0.005	-0.008	0.009	-0.003	0.001	0.003	-0.002			
CC2	-0.006	0.01	-0.006	-0.004	0.008	-0.003	0.003	0.003	-0.002			
CC2	-0.003	0.009	-0.002	-0.011	0.008	-0.002	-0.013	-0.005	-0.002	0.002	-0.001	0.001

References

1. A. M. Bagher, *Sustainable Energy*, 2014, **2**, 85-90.
2. H. Spanggaard and F. C. Krebs, *Solar Energy Materials and Solar Cells*, 2004, **83**, 125-146.
3. S. Emma, Organic Photovoltaics: An Introduction, <https://www.ossila.com/pages/organic-photovoltaics-introduction>, (accessed 19 December, 2021).
4. C. W. Tang, *Applied physics letters*, 1986, **48**, 183-185.
5. J. J. M. Halls, C. A. Walsh, N. C. Greenham, E. A. Marseglia, R. H. Friend, S. C. Moratti and A. B. Holmes, *Nature*, 1995, **376**, 498-500.
6. A. Goetzberger, C. Hebling and H.-W. Schock, *Materials Science and Engineering: R: Reports*, 2003, **40**, 1-46.
7. L. Ye, S. Zhang, D. Qian, Q. Wang and J. Hou, *The Journal of Physical Chemistry C*, 2013, **117**, 25360-25366.
8. X. Li, C. Li, L. Ye, K. Weng, H. Fu, H. S. Ryu, D. Wei, X. Sun, H. Y. Woo and Y. Sun, *Journal of Materials Chemistry A*, 2019, **7**, 19348-19354.
9. P. Meredith, W. Li and A. Armin, *Advanced Energy Materials*, 2020, **10**, 2001788.
10. G. Yu, J. Gao, J. C. Hummelen, F. Wudl and A. J. Heeger, *Science*, 1995, **270**, 1789-1791.
11. L. A. A. Pettersson, L. S. Roman and O. Inganäs, *Journal of Applied Physics*, 1999, **86**, 487-496.
12. O. Andersson and M. Kemerink, *Solar RRL*, 2020, **4**, 2000400.
13. A. Andicsová-Eckstein, K. Tokár, E. Kozma and Z. Tokárová, *New Journal of Chemistry*, 2017, **41**, 14871-14875.
14. H. Sun, Y. Tang, H. Guo, M. A. Uddin, S. Ling, R. Wang, Y. Wang, X. Zhou, H. Y. Woo and X. Guo, *Solar RRL*, 2019, **3**, 1800265.
15. T.-J. Lin and S.-T. Lin, *Physical Chemistry Chemical Physics*, 2015, **17**, 4127-4136.
16. J. Casanovas, D. Zanuy and C. Alemán, *Polymer*, 2005, **46**, 9452-9460.
17. K. Burke, J. Werschnik and E. K. U. Gross, *The Journal of chemical physics*, 2005, **123**, 062206.
18. T. R. Swaroop, Z. A. Tabasi, Y. Zhao and P. E. Georghiou, *ChemistrySelect*, 2018, **3**, 9700-9707.
19. I. Imae, N. Tada and Y. Harima, *Journal of Photopolymer Science and Technology*, 2019, **32**, 585-592.
20. J. R. W. McLay, J. J. Sutton, G. E. Shillito, C. B. Larsen, G. S. Huff, N. T. Lucas and K. C. Gordon, *Inorganic Chemistry*, 2020, **60**, 130-139.
21. M. Pomerantz, *Tetrahedron letters*, 2003, **44**, 1563-1565.
22. M. Pomerantz and Y. Cheng, *Tetrahedron letters*, 1999, **40**, 3317-3320.
23. M. A. De Oliveira, H. A. Duarte, J.-M. Pernaut and W. B. De Almeida, *The Journal of Physical Chemistry A*, 2000, **104**, 8256-8262.
24. R. O. Ramabhadran and K. Raghavachari, *Journal of chemical theory and computation*, 2013, **9**, 3986-3994.
25. F. Della Sala, H. H. Heinze and A. Görling, *Chemical physics letters*, 2001, **339**, 343-350.
26. M. Rubio, M. Merchán and E. Ortí, *ChemPhysChem*, 2005, **6**, 1357-1368.
27. J. P. Coe and M. J. Paterson, *Journal of chemical theory and computation*, 2015, **11**, 4189-4196.
28. A. P. W, Oxford University Press, Walton Street, Oxford OX2 6DP, Third Edition edn., 1987, p. 301.

29. B. Andrew, H. John, P. Andrew, P. Gwen and P. Gareth, Oxford University Press, Great Clarendon Street, Oxford, OX2 6DP, United Kingdom, Third edn., 2017, p. 134.
30. H. D, H. E, S. R and Z. TK, The Born-Oppenheimer Approximation, <https://chem.libretexts.org@go/page/1973>, (accessed 26th October, 2021).
31. C. D. Sherrill, *Journal*.
32. D. Cremer, *Wiley Interdisciplinary Reviews: Computational Molecular Science*, 2011, **1**, 509-530.
33. A. Dreuw and M. Wormit, *Wiley Interdisciplinary Reviews: Computational Molecular Science*, 2015, **5**, 82-95.
34. O. Christiansen, H. Koch and P. Jørgensen, *Chemical Physics Letters*, 1995, **243**, 409-418.
35. J. Toulouse, *Journal*, 2019.
36. Lab #2: Basis sets, <https://www.yumpu.com/en/document/read/26313197/basis-sets-lab>, (accessed 18/04/2022).
37. *Journal*.
38. F. Weigend and M. Häser, *Theoretical Chemistry Accounts*, 1997, **97**, 331-340.
39. C. Hättig, A. Hellweg and A. Köhn, *Physical Chemistry Chemical Physics*, 2006, **8**, 1159-1169.
40. F. Weigend, M. Häser, H. Patzelt and R. Ahlrichs, *Chemical physics letters*, 1998, **294**, 143-152.
41. C. Hättig, *The Journal of chemical physics*, 2003, **118**, 7751-7761.
42. R. A. Kendall, T. H. Dunning Jr and R. J. Harrison, *The Journal of chemical physics*, 1992, **96**, 6796-6806.
43. T. H. Dunning Jr, *The Journal of chemical physics*, 1989, **90**, 1007-1023.
44. C. Hättig and F. Weigend, *The Journal of Chemical Physics*, 2000, **113**, 5154-5161.
45. A. Köhn and C. Hättig, *The Journal of chemical physics*, 2003, **119**, 5021-5036.
46. C. Hättig, *Advances in quantum chemistry*, 2005, **50**, 37-60.
47. C. Steffen, K. Thomas, U. Huniar, A. Hellweg, O. Rubner and A. Schroer, *Journal of computational chemistry*, 2010, **31**, 2967-2970.
48. M. D. Hanwell, D. E. Curtis, D. C. Lonie, T. Vandermeersch, E. Zurek and G. R. Hutchison, *Journal of cheminformatics*, 2012, **4**, 1-17.
49. J. E. Chadwick and B. E. Kohler, *The Journal of Physical Chemistry*, 1994, **98**, 3631-3637.
50. C. L. Janssen and I. M. B. Nielsen, *Chemical physics letters*, 1998, **290**, 423-430.
51. S. S. Zade and M. Bendikov, *Organic letters*, 2006, **8**, 5243-5246.
52. J. Torras, J. Casanovas and C. Alemán, *The Journal of Physical Chemistry A*, 2012, **116**, 7571-7583.
53. S. S. Zade, N. Zamoshchik and M. Bendikov, *Accounts of Chemical Research*, 2011, **44**, 14-24.
54. V. Hernandez and J. T. Lopez Navarrete, *The Journal of chemical physics*, 1994, **101**, 1369-1377.